# Ralf Klessen

Deutsche Forschungsgemeinschaft
DFG

ECOGAL
ERC Synergy Grant

erc European Research Council

STRUCTURES
CLUSTER OF EXCELLENCE

UNIVERSITÄT HEIDELBERG
ZUKUNFT SEIT 1386

# The First Stars:
## Formation, Properties, and Impact

Ralf Klessen

Deutsche Forschungsgemeinschaft
DFG

ECOGAL
ERC Synergy Grant

erc European Research Council

STRUCTURES CLUSTER OF EXCELLENCE

UNIVERSITÄT HEIDELBERG ZUKUNFT SEIT 1386

# The First Stars:
## Formation, Properties, and Impact

some theory
Pop III stars
Pop II stars
supermassive stars
constraints

Ralf Klessen

Deutsche Forschungsgemeinschaft
DFG
ECOGAL
ERC Synergy Grant
erc European Research Council
STRUCTURES CLUSTER OF EXCELLENCE
UNIVERSITÄT HEIDELBERG ZUKUNFT SEIT 1386

ANNUAL REVIEWS

*Annual Review of Astronomy and Astrophysics*

# The First Stars: Formation, Properties, and Impact

Ralf S. Klessen[1,2] and Simon C.O. Glover[1]

[1]Universität Heidelberg, Zentrum für Astronomie, Institut für Theoretische Astrophysik, Heidelberg, Germany; email: klessen@uni-heidelberg.de, glover@uni-heidelberg.de

[2]Universität Heidelberg, Interdisziplinäres Zentrum für Wissenschaftliches Rechnen, Heidelberg, Germany

Annu. Rev. Astron. Astrophys. 2023. 61:65–130

The *Annual Review of Astronomy and Astrophysics* is online at astro.annualreviews.org

https://doi.org/10.1146/annurev-astro-071221-053453



## Keywords

cosmology, first and second stellar population, galactic archeology, high-redshift Universe, Population III and II, star formation

## Abstract

The first generation of stars, often called Population III (or Pop III), form from metal-free primordial gas at redshifts $z \sim 30$ and below. They dominate the cosmic star-formation history until $z \sim 15$–$20$, at which point the formation of metal-enriched Population II stars takes over. We review current theoretical models for the formation, properties, and impact of Pop III stars and discuss existing and future observational constraints. Key takeaways from this review include the following:

- Primordial gas is highly susceptible to fragmentation and Pop III stars form as members of small clusters with a logarithmically flat mass function.
- Feedback from massive Pop III stars plays a central role in regulating subsequent star formation, but major uncertainties remain regarding its imm

Screenshot

# some theory

Deutsche Forschungsgemeinschaft
DFG
ECOGAL
ERC Synergy Grant
erc European Research Council
STRUCTURES CLUSTER OF EXCELLENCE
UNIVERSITÄT HEIDELBERG ZUKUNFT SEIT 1386

# cosmic timeline

UNIVERSITÄT HEIDELBERG
ZUKUNFT SEIT 1386

cover onset of primordial star formation to early reionization

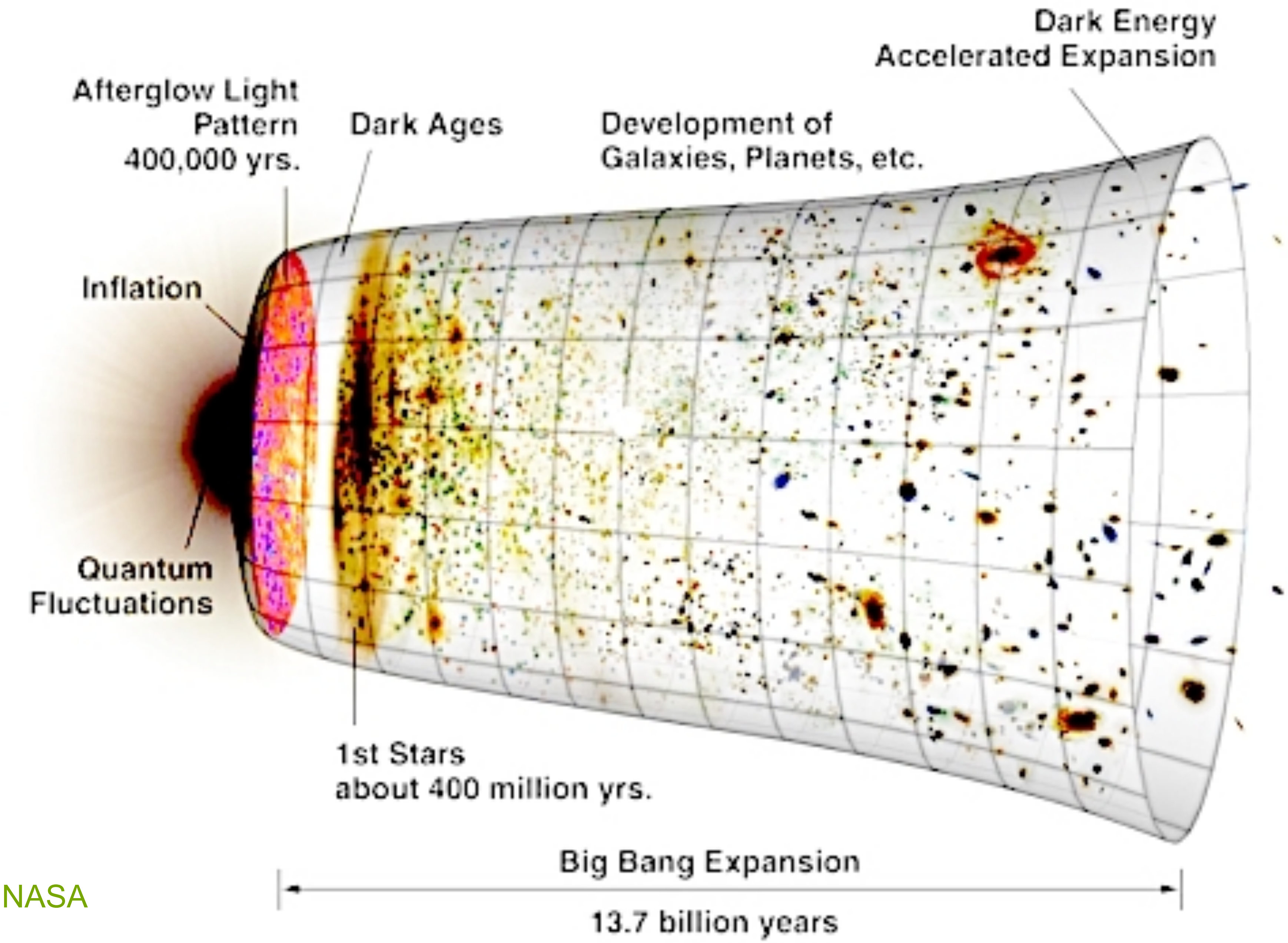


image credit: NASA

# criteria for onset of star formation

criteria for primordial star formation

- DM halos need to decouple from cosmic expansion and start to contract
- gas needs to decouple and go into run-away collapse
  —> **Jeans criterion**: $\tau_{\rm grav} < \tau_{\rm sound}$
- in addition, gas needs to cool away compression heat
  —> **Rees-Ostriker criterion**: $\tau_{\rm cool} < \tau_{\rm dyn}$
- both depend on thermodynamic response of the gas
  —> competition between heating and cooling processes
  —> importance of chemistry
- collapse needs to proceed to stellar densities

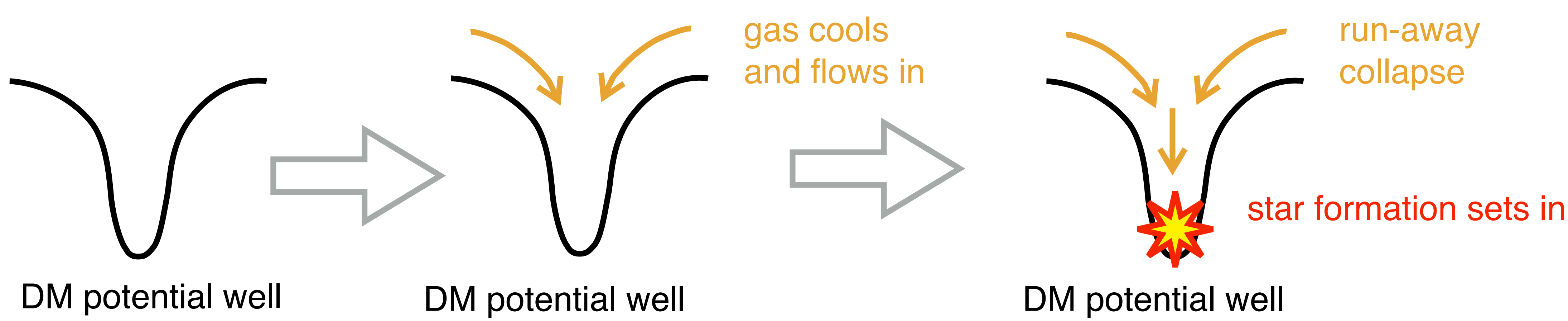


Jeans (1902, PTRS A, 199,1), Rees & Ostriker (1977, MNRAS,179, 541), Silk (1977, ApJ, 211, 638)

some theory

# critical halo mass for star formation 1

UNIVERSITÄT HEIDELBERG
ZUKUNFT SEIT 1386

criteria for collapse and star formation

- look at competition between gravity (density $\rho$) and gas pressure (sound speed $c_\mathrm{s}$ or temperature $T$): **Jeans mass**
- critical mass:

$$M_\mathrm{J} = \frac{\pi^{5/2}}{6}\left(\frac{1}{G}\right)^{3/2}\rho^{-1/2}c_\mathrm{s}^3 = \frac{\pi^{5/2}}{6}\left(\frac{k}{G}\right)^{3/2}\left(\frac{1}{\mu m_\mathrm{H}}\right)^2 n^{-1/2}T^{3/2}$$

- can be extended by considering effective sound speed $c_\mathrm{s,eff}^2 = c_\mathrm{s}^2 + \sigma^2$ with $\sigma = \sigma_\mathrm{turb}$ or $\sigma = v_\mathrm{Alfven}$
- in standard LCDM a low redshift this translates to

$$M_\mathrm{J} \approx 5\times 10^3\,\mathrm{M}_\odot \left(\frac{\Omega_\mathrm{m}h^2}{0.14}\right)^{-1/2}\left(\frac{\Omega_\mathrm{b}h^2}{0.022}\right)^{-3/5}\left(\frac{z+1}{10}\right)^{3/2}$$

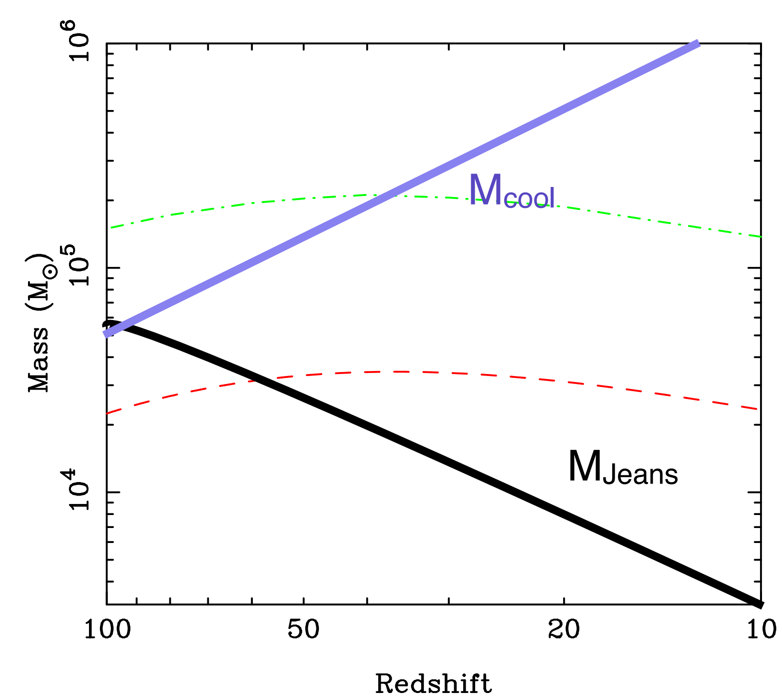


Jeans (1902, PTRS A, 199,1), Barkana & Loeb (2001, Phys. Rep. 349, 125), Glover (2013, ASSL, 396, 103)

some theory

# critical halo mass for star formation 1

UNIVERSITÄT HEIDELBERG ZUKUNFT SEIT 1386

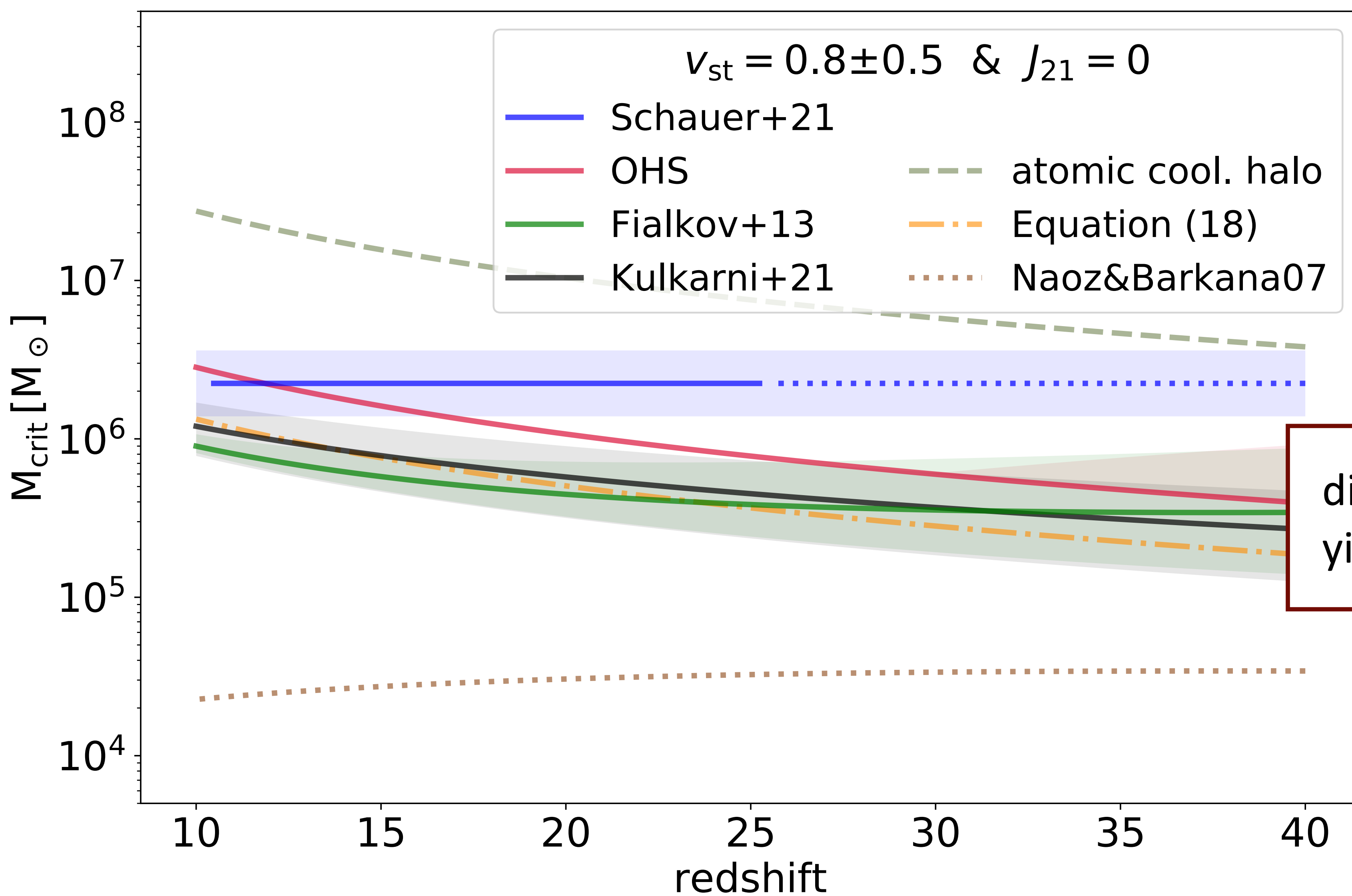


different models yield different $M_{crit}$

Klessen & Glover (2023, ARAA, 61, 65 -- arXiv.2303.12500)

some theory

# critical halo mass for star formation 1

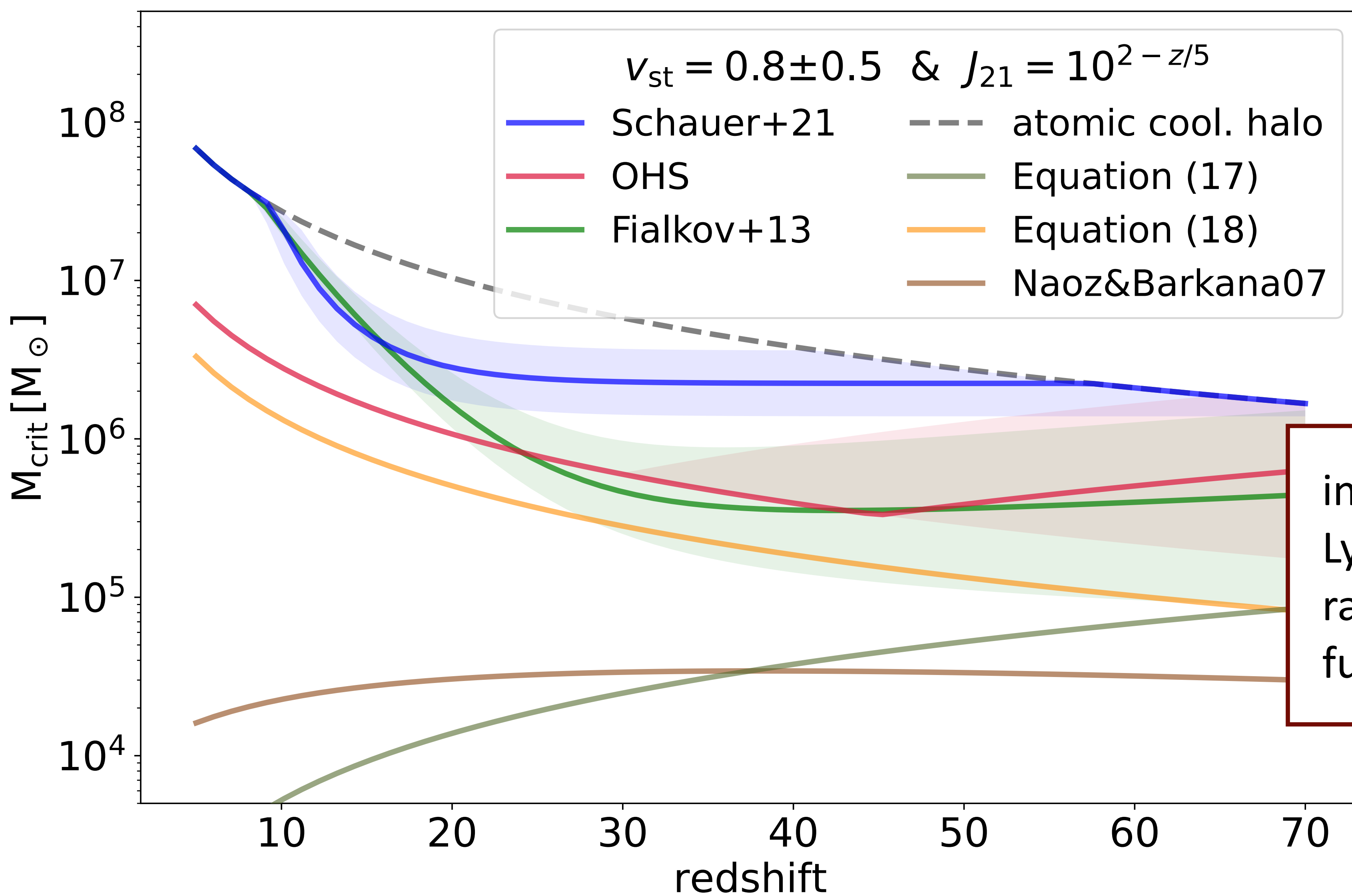


including cosmic Lyman-Werner radiation adds further complexity

Klessen & Glover (2023, ARAA, 61, 65 -- arXiv.2303.12500)

# critical halo mass for star formation 2

UNIVERSITÄT HEIDELBERG ZUKUNFT SEIT 1386

some theory

criteria for collapse and star formation

- this is not sufficient, gas als needs to cool away access heat: **cooling mass**
- efficient cooling requires molecular hydrogen; with $H_2$ we reach T ~ 500 K and with HD down to T ~ 100 K (but typically not important)

- $H_2$ typically needs free electrons as catalyst:
  $\mathrm{H} + \mathrm{e}^- \rightarrow \mathrm{H}^- + \gamma$ and $\mathrm{H}^- + \mathrm{H} \rightarrow \mathrm{H}_2 + \mathrm{e}^-$
- less important: $\mathrm{H} + \mathrm{H}^+ \rightarrow \mathrm{H}_2^+ + \gamma$ and $\mathrm{H}_2^+ + \mathrm{H} \rightarrow \mathrm{H}_2 + \mathrm{H}^+$
- and at high densities ($n \lesssim 10^9 \mathrm{cm}^{-3}$) via the 3-body path:
  $\mathrm{H} + \mathrm{H} + \mathrm{H} \rightarrow \mathrm{H}_2 + \mathrm{H}$

- as result:

$$M_{\mathrm{cool}} \approx 6 \times 10^5 \mathrm{M}_\odot h^{-1} \Omega_{\mathrm{m}}^{-1/2} \left(\frac{\mu}{1.22}\right)^{-3/2} \left(\frac{z+1}{10}\right)^{-3/2}$$

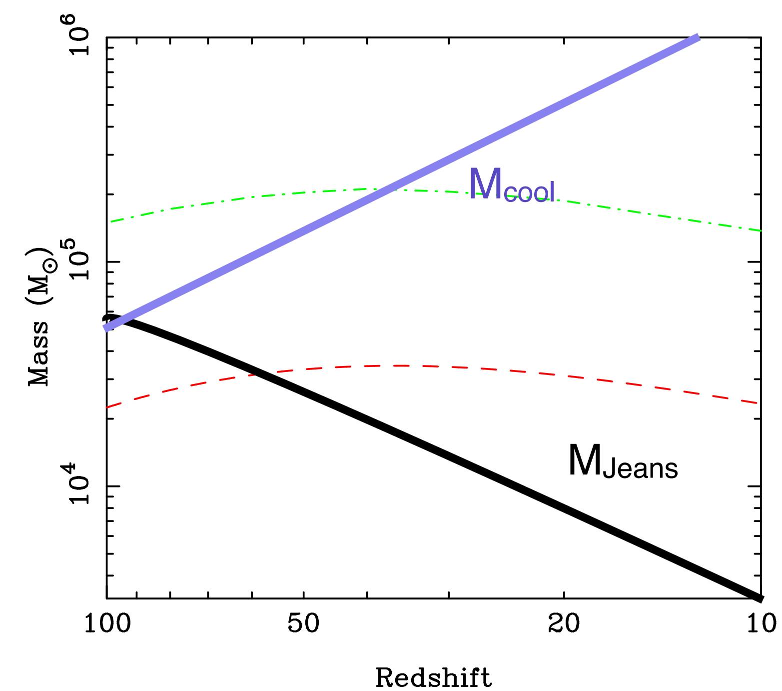


Glover (2005, SSRv.,117, 445), Glover (2013, ASSL, 396, 103)

some theory

# primordial chemistry

primordial chemistry networks largely focus on $H_2$ as primary coolants

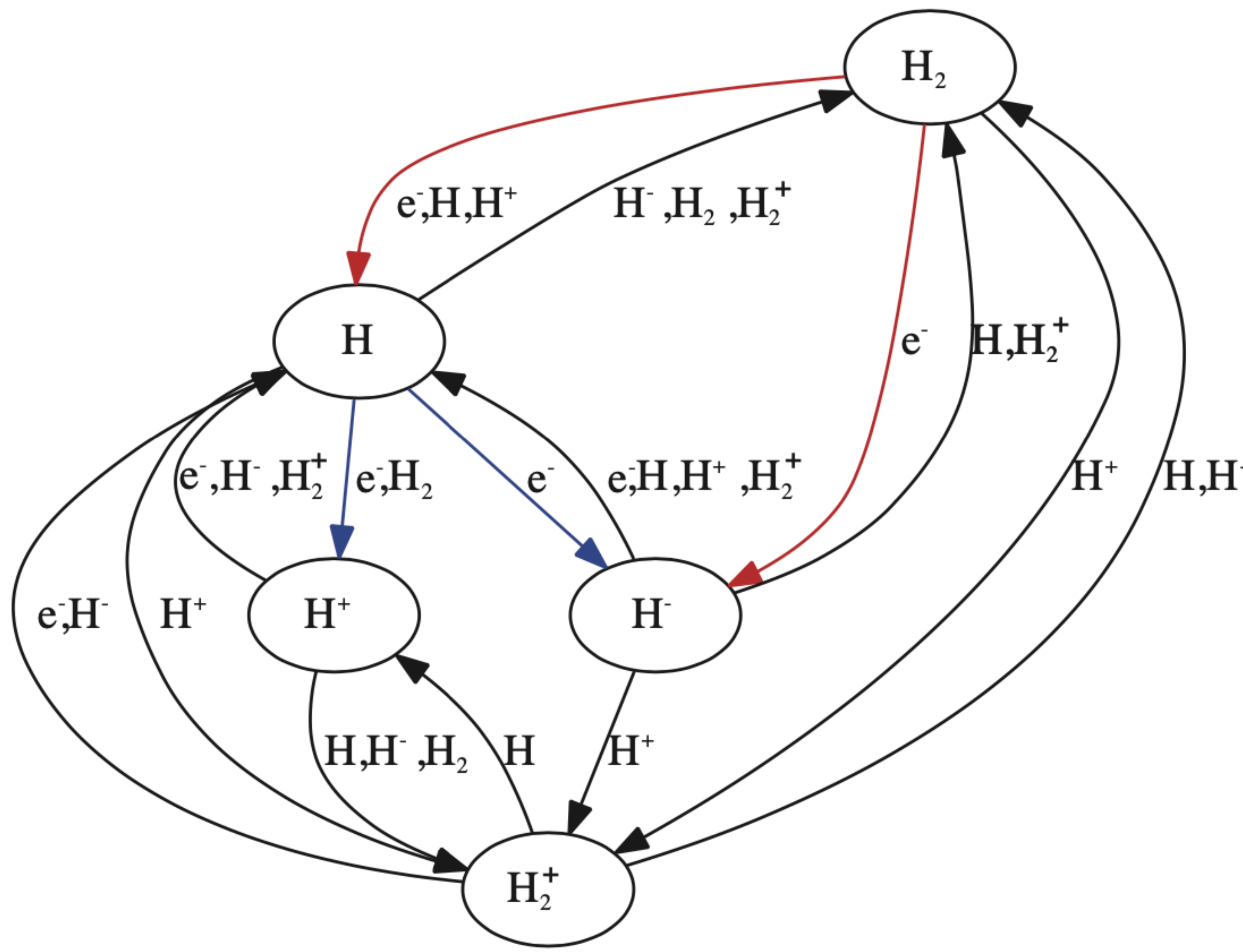


Bovino & Galli (2019, in Formation of the First Black Holes, eds. Latif M. and Schleicher D.R.G), using KROME, see Grassi et al. (2014, MNRAS, 439, 2386)

some theory

# effective equation of state

effective EOS constitutes a relation between temperature and density

(A) gas flows into potential well and is compressionally heated
(B) $H_2$ formation and run-away cooling
(C) gas accumulates and collapse resumes
(D) 3-body $H_2$ formation sets in and gas becomes fully molecular
(E) gas becomes optically thick and temperature rises further
(F) collision-induced emission (CIE) becomes important coolant
(G) at T ~ 2000 K $H_2$ dissociation sets in

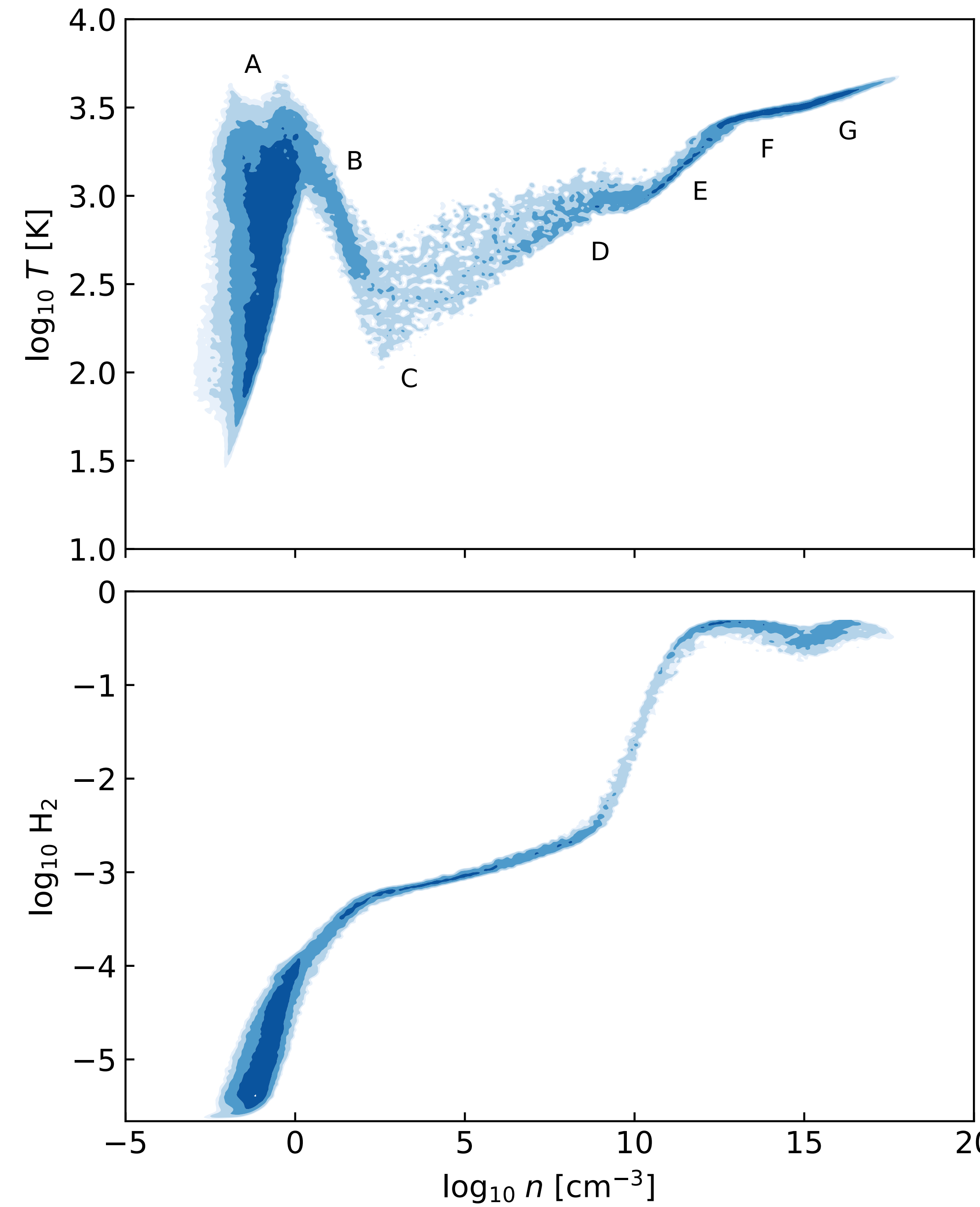


Klessen & Glover (2023, ARAA, 61, 65 -- arXiv.2303.12500)
inspired by Yoshida et al. (2006, ApJ, 652, 6)
using data of Lewis Prole and Anna Schauer

some theory

# heating and cooling processes at $Z \sim Z_{sun}$

overview of main heating and cooling processes
as function of hydrogen nuclei number density n

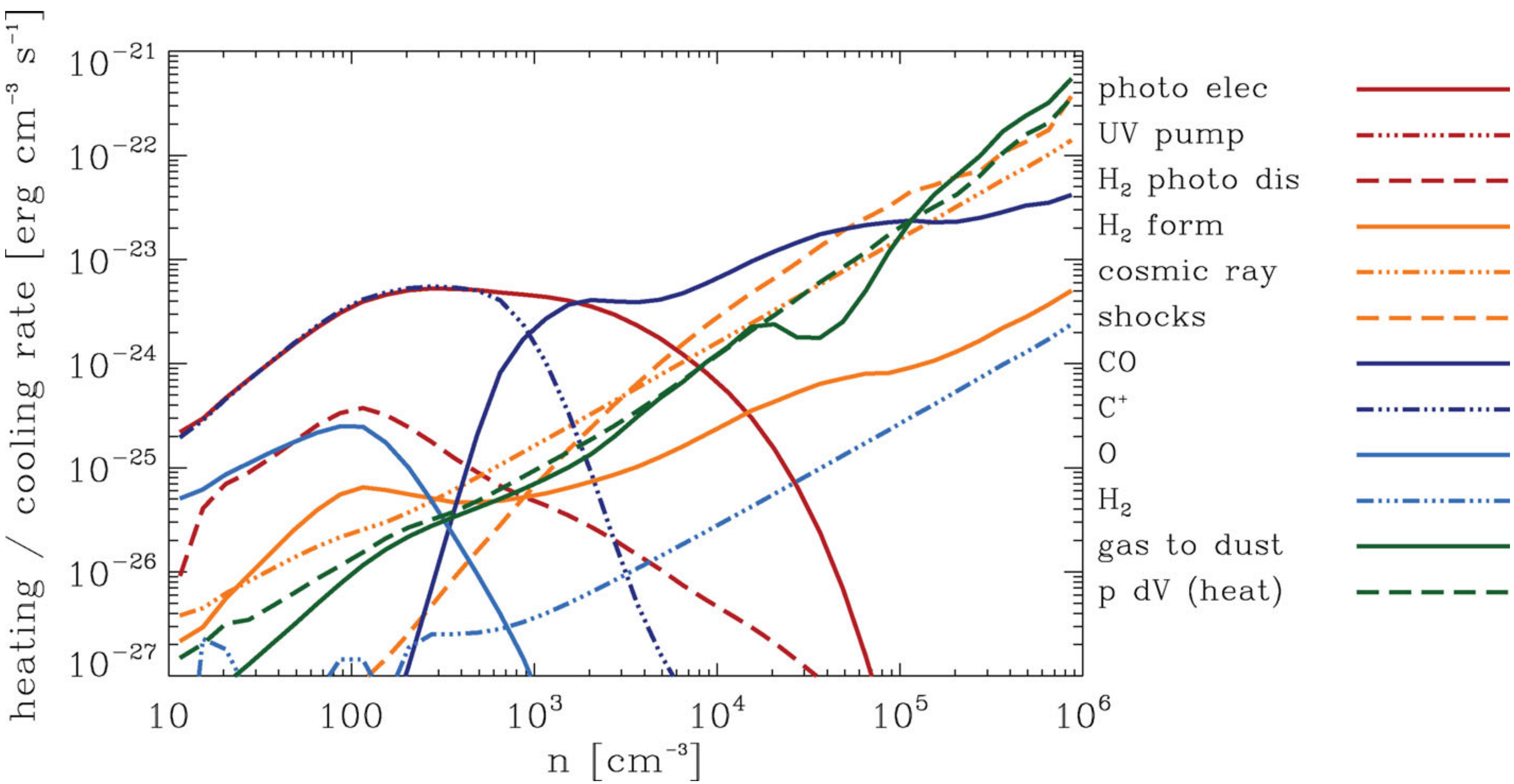


(Klessen, & Glover (2016, SAAS, 43, 85), figure from Glover & Clark (2012, MNRAS, 421, 9 )

# heating and cooling processes at Z ~ 0

UNIVERSITÄT HEIDELBERG
ZUKUNFT SEIT 1386

overview of main heating and cooling processes
as function of hydrogen nuclei number density n

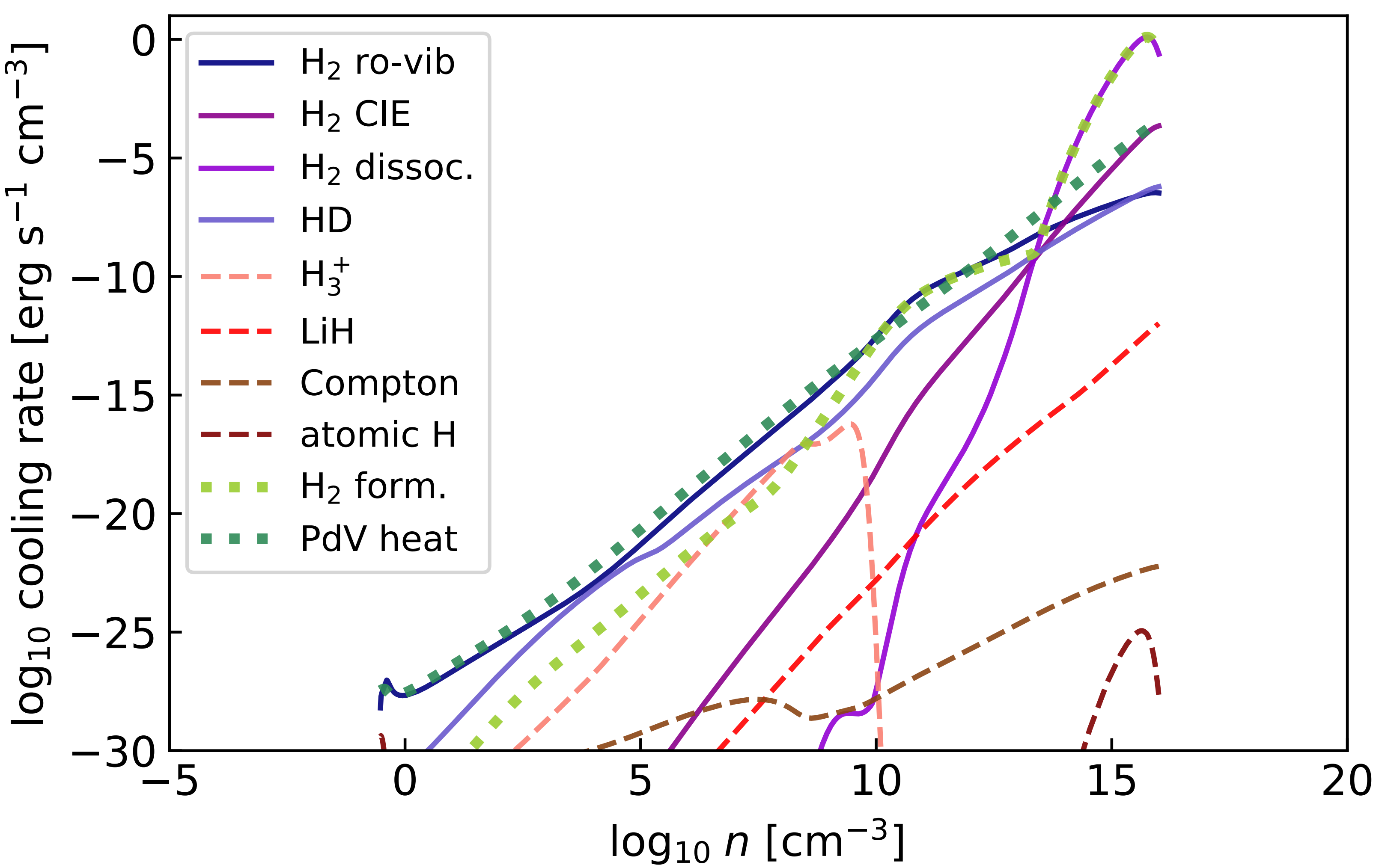


Klessen, & Glover (2023, ARAA, 61, 65 -- arXiv.2303.12500)

some theory

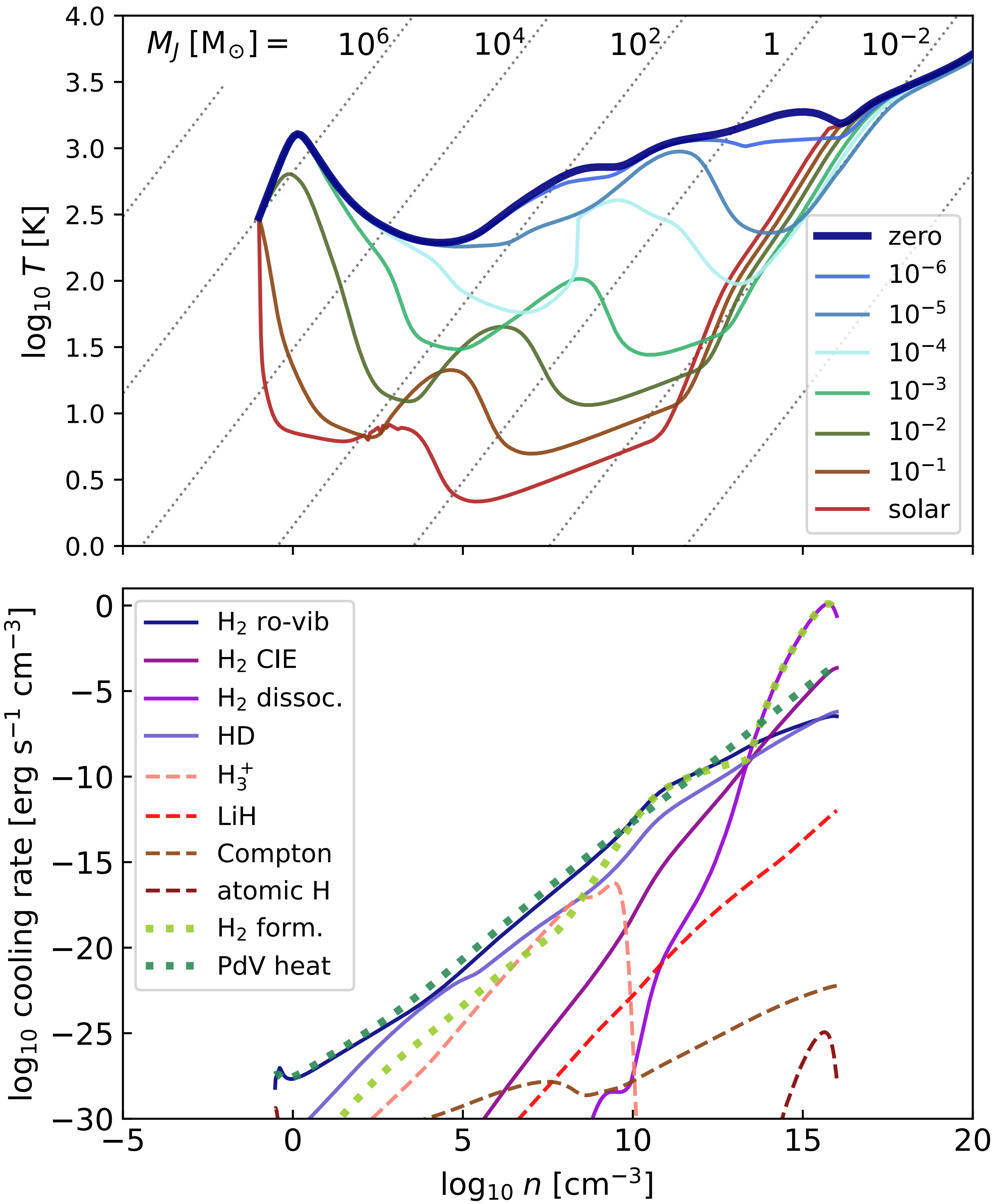


Klessen, & Glover (2023, ARAA, 61, 65 -- arXiv.2303.12500)

UNIVERSITÄT HEIDELBERG
ZUKUNFT SEIT 1386

this can be combined with simple 1D collapse calculations and looking at the density and temperature in the central core

# EOS as function of metallicity

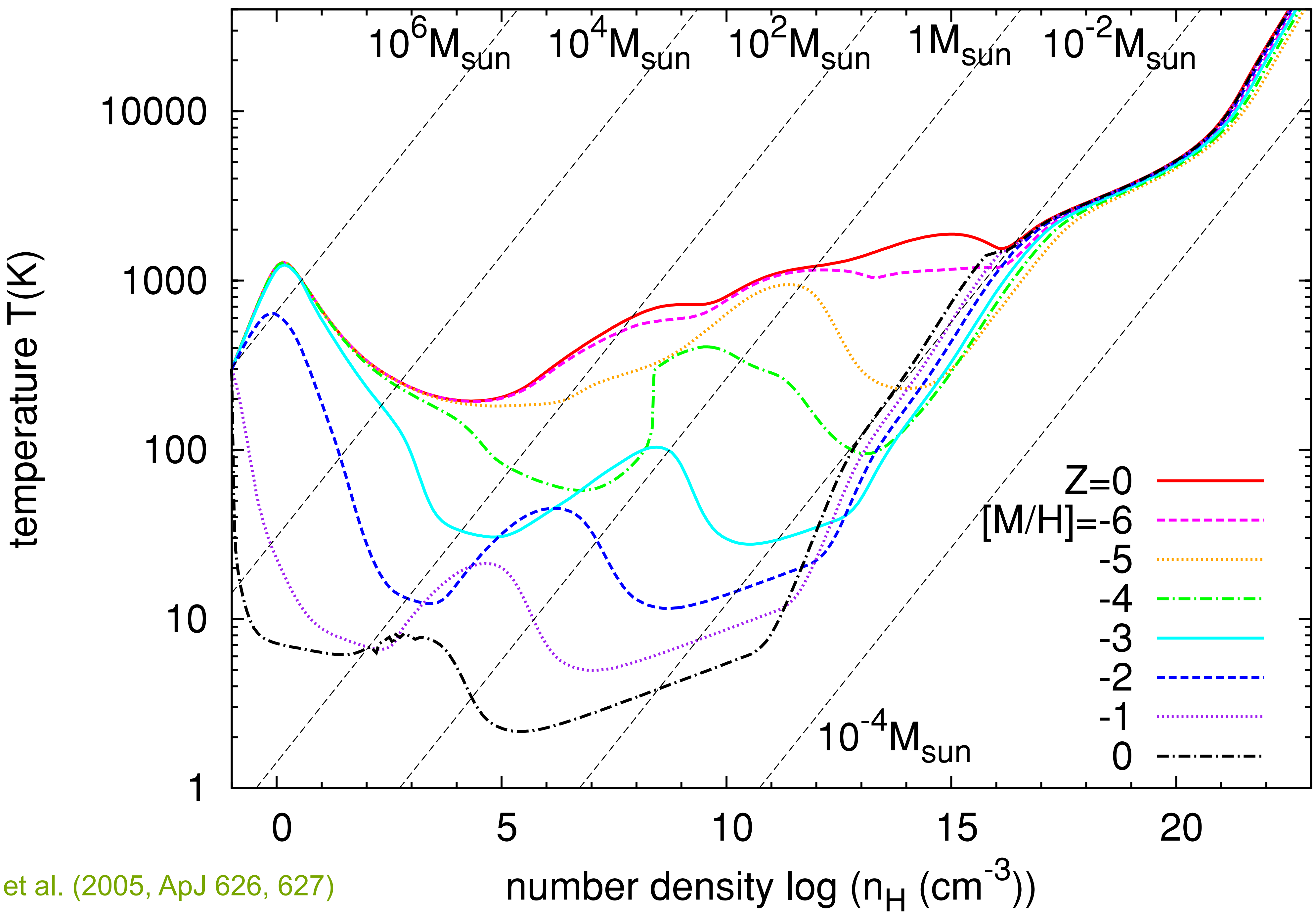


Omukai et al. (2005, ApJ 626, 627)

equation of state

# EOS as function of metallicity

equation of state

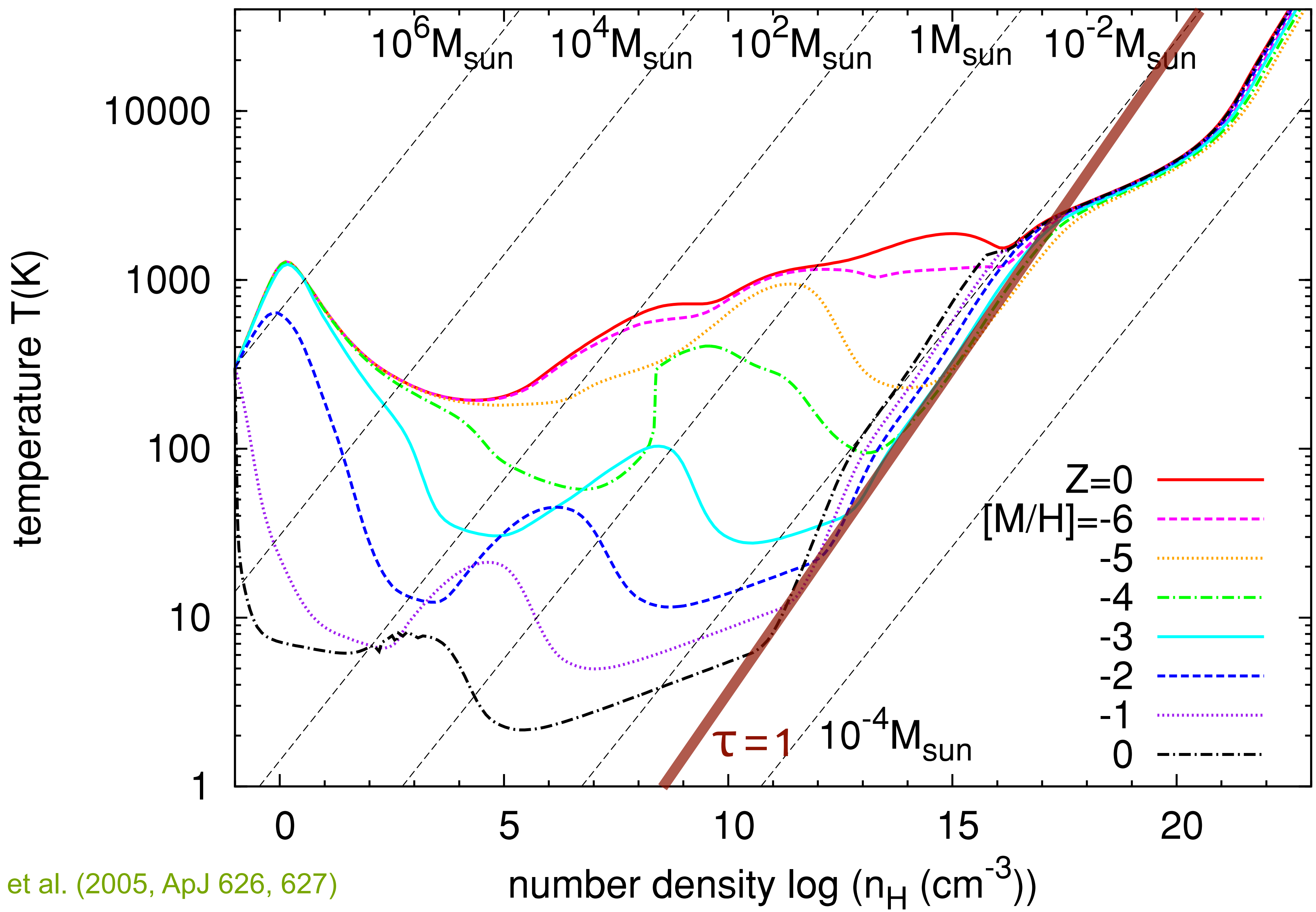


Omukai et al. (2005, ApJ 626, 627)

# EOS as function of metallicity

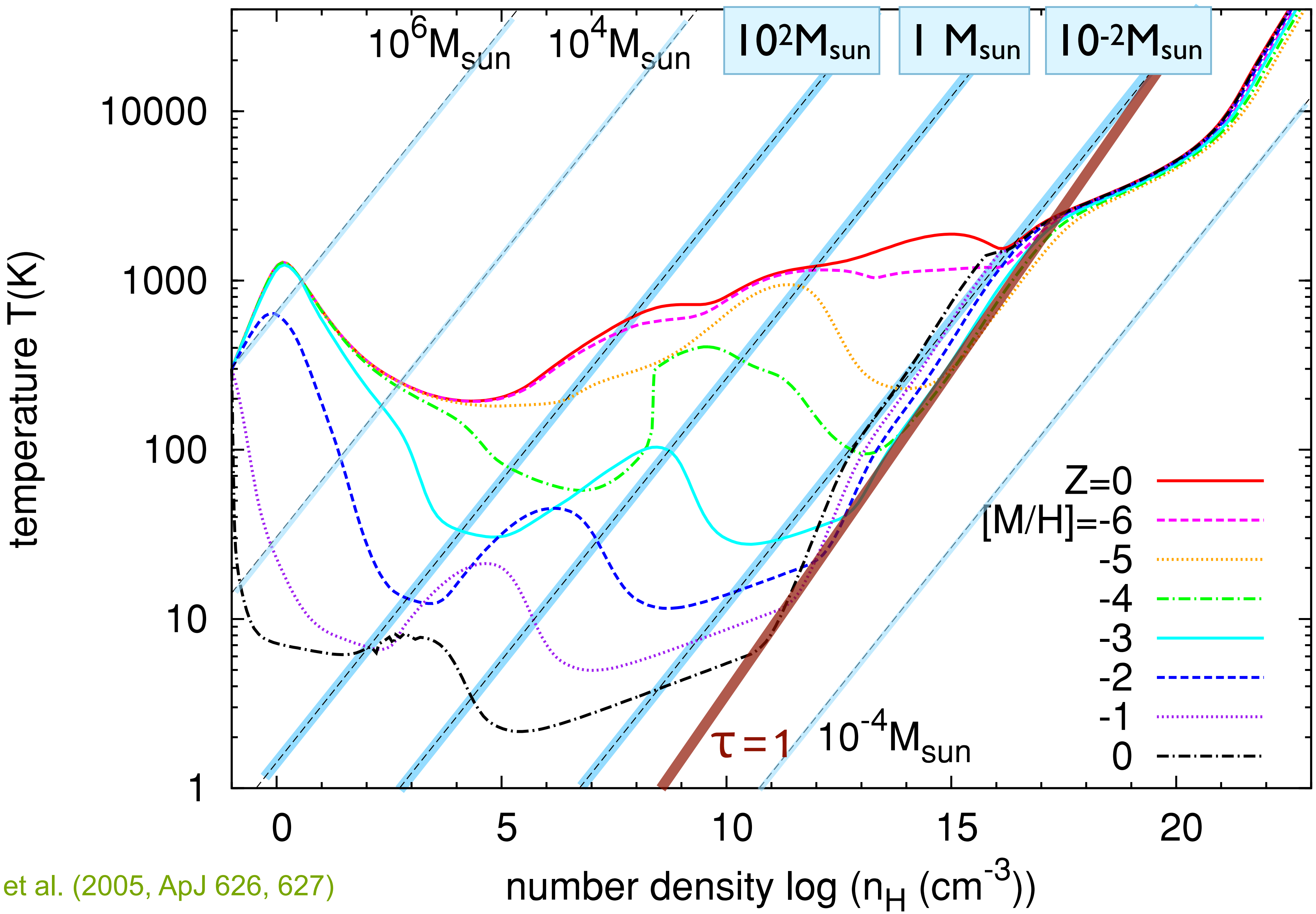


Omukai et al. (2005, ApJ 626, 627)

equation of state

UNIVERSITÄT HEIDELBERG
ZUKUNFT SEIT 1386

# EOS at present days

at present days ($Z \sim Z_{sun}$)
line-cooling and dust cooling
overlap in (n-T space)

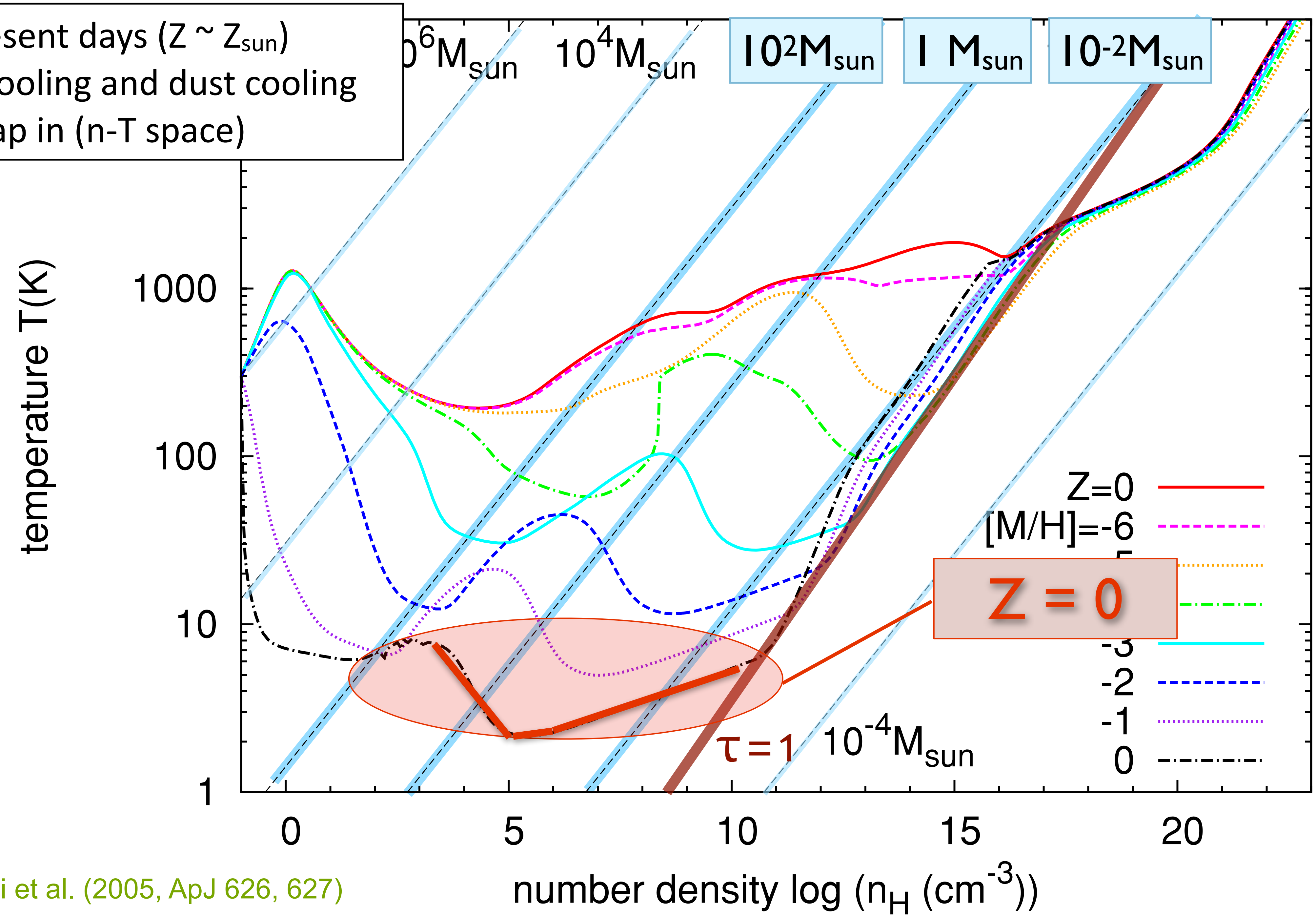


Omukai et al. (2005, ApJ 626, 627)

present-day SF

# characteristic mass from 'kink' in EOS

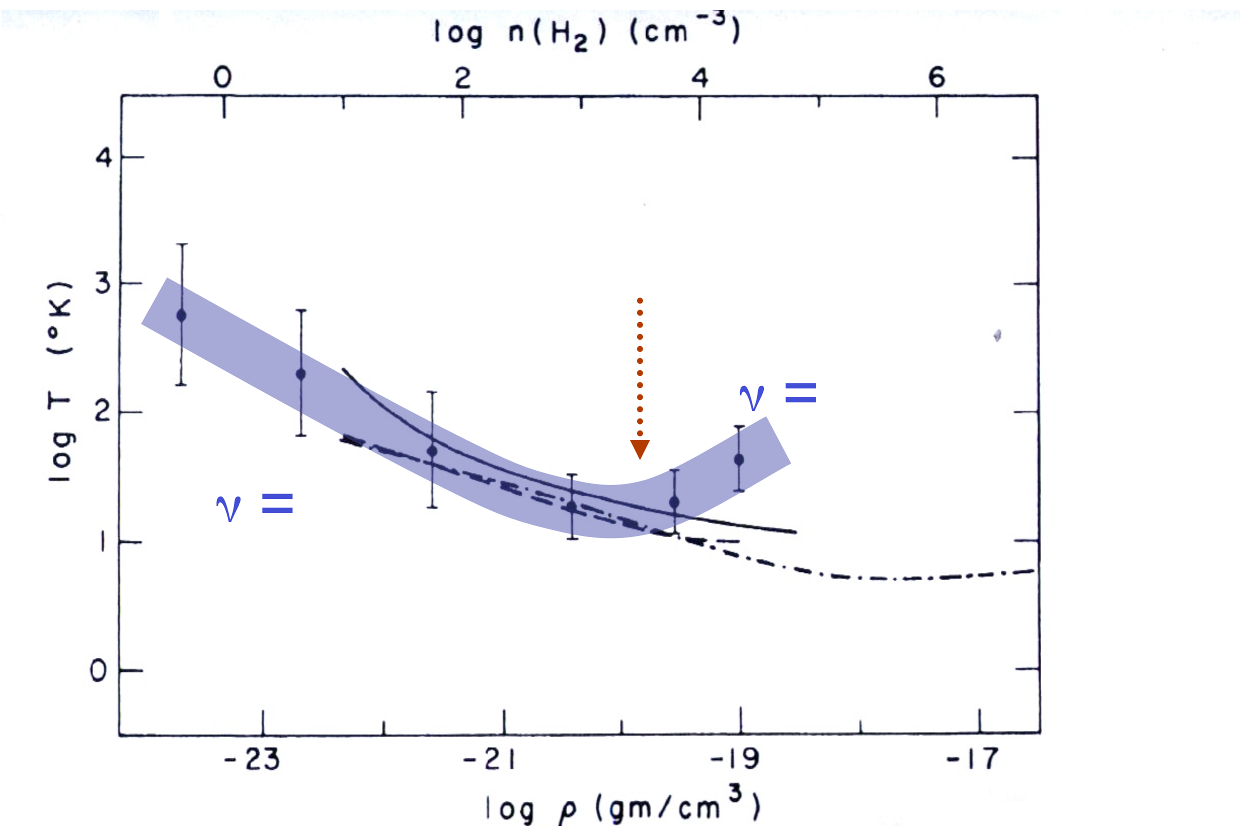


it has been proposed almost 40 years ago, that this kink sets the characteristic mass of the stellar IMF

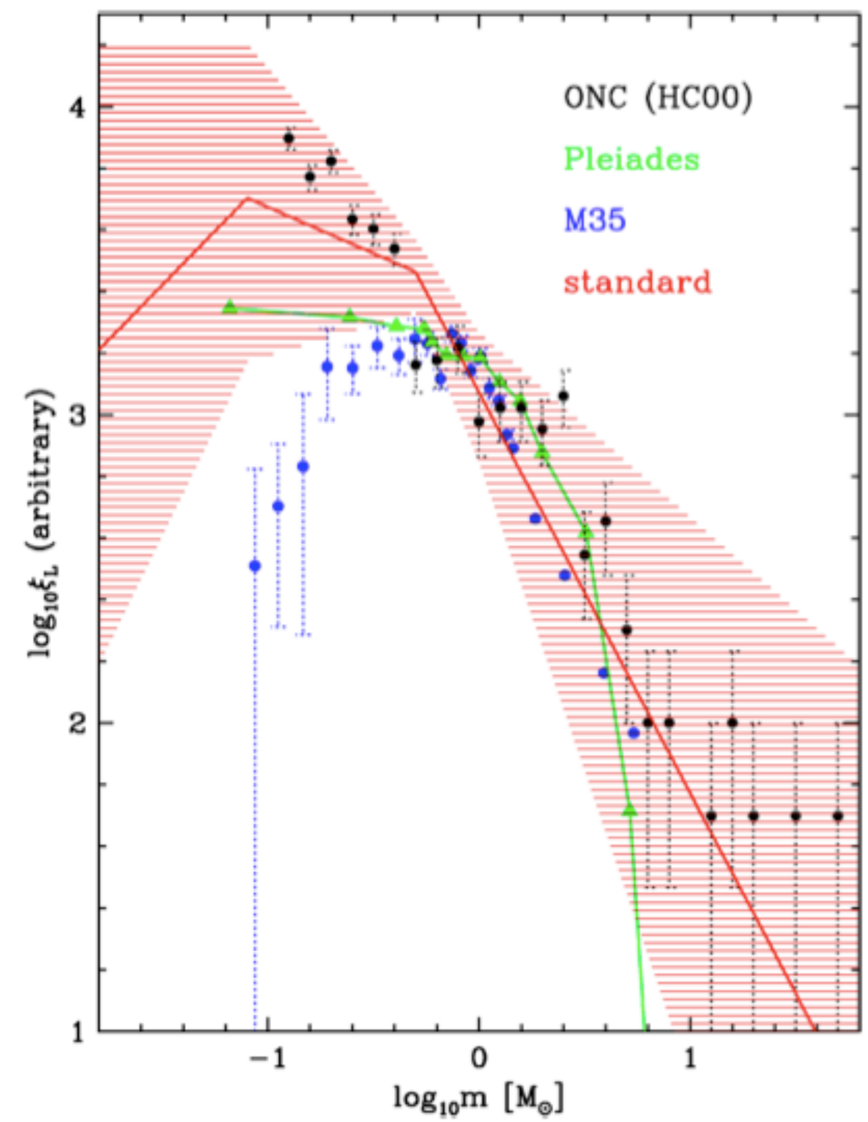


Larson (1985, MNRAS, 214, 379),
Larson (2005, MNRAS, 359, 211),

Kroupa (2002, Science, 295, 82)

present-day SF

UNIVERSITÄT
HEIDELBERG
ZUKUNFT
SEIT 1386

# characteristic mass from 'kink' in EOS

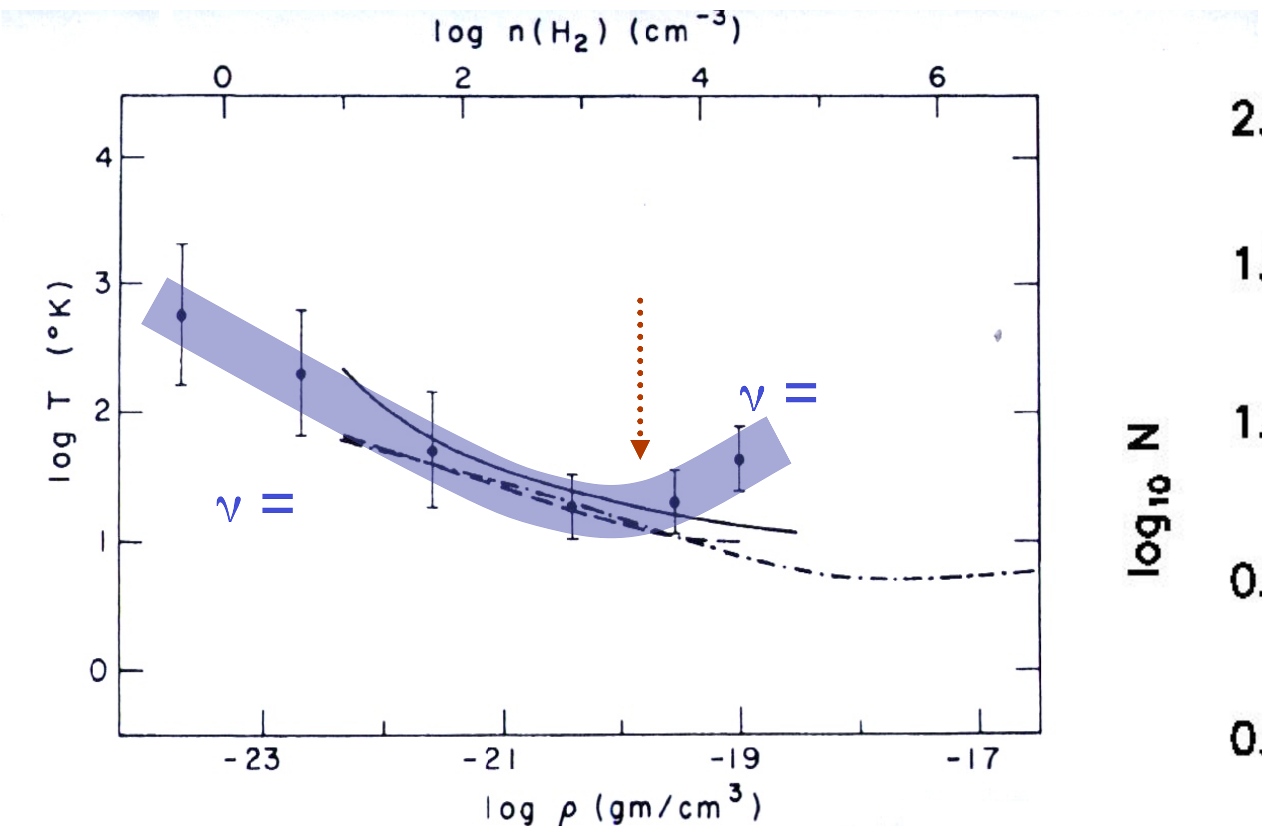


it has been proposed almost 40 years ago, that this kink sets the characteristic mass of the stellar IMF

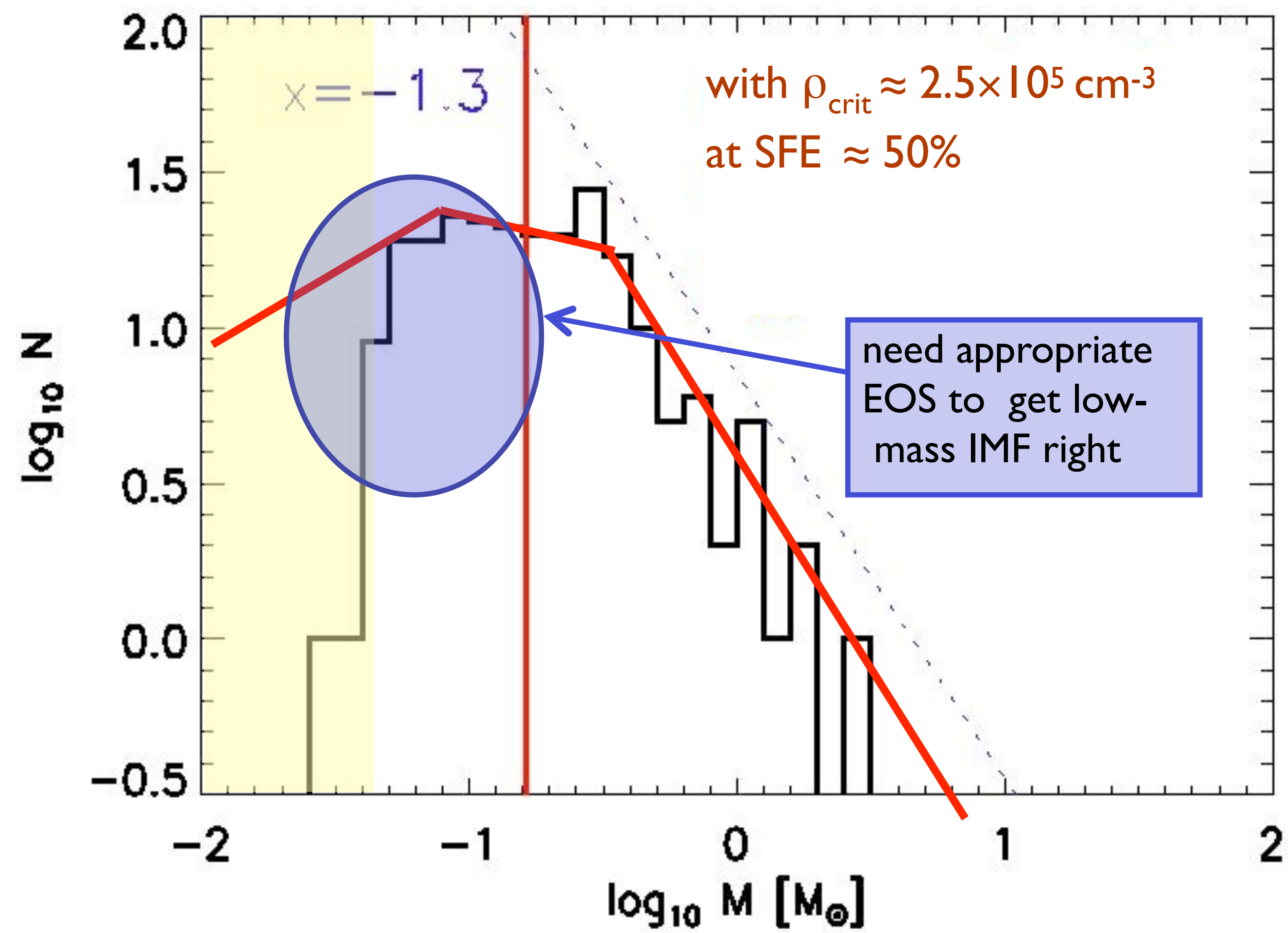


this is supported by numerical simulations

Larson (1985, MNRAS, 214, 379),
Larson (2005, MNRAS, 359, 211),

Jappsen et al. (2005, A&A, 435, 611)

equation of state

# EOS as function of metallicity

UNIVERSITÄT HEIDELBERG ZUKUNFT SEIT 1386

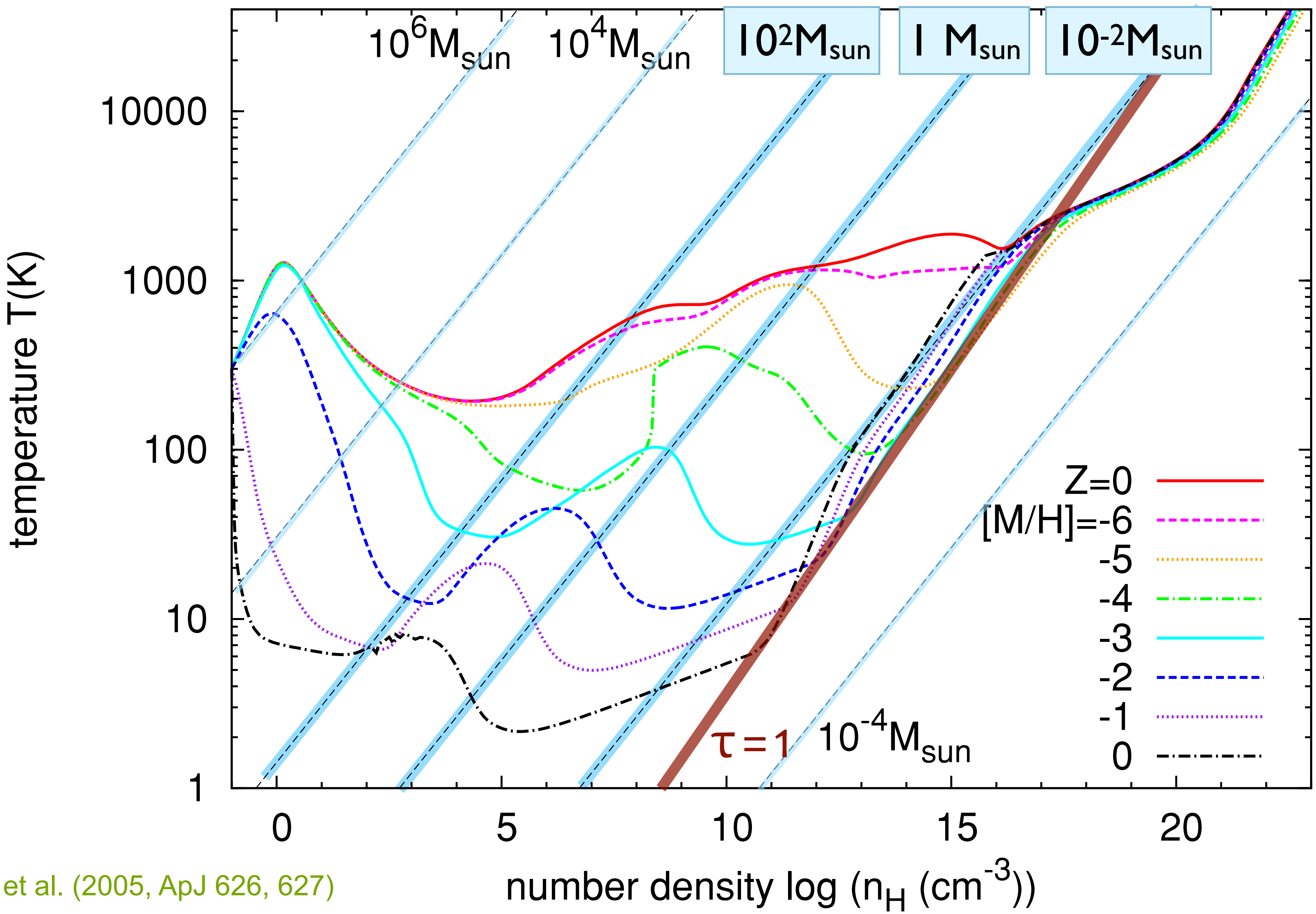


Omukai et al. (2005, ApJ 626, 627)

# Pop III stars

Deutsche Forschungsgemeinschaft DFG
ECOGAL ERC Synergy Grant
European Research Council
STRUCTURES CLUSTER OF EXCELLENCE
UNIVERSITÄT HEIDELBERG ZUKUNFT SEIT 1386

# Pop III stars

UNIVERSITÄT HEIDELBERG ZUKUNFT SEIT 1386

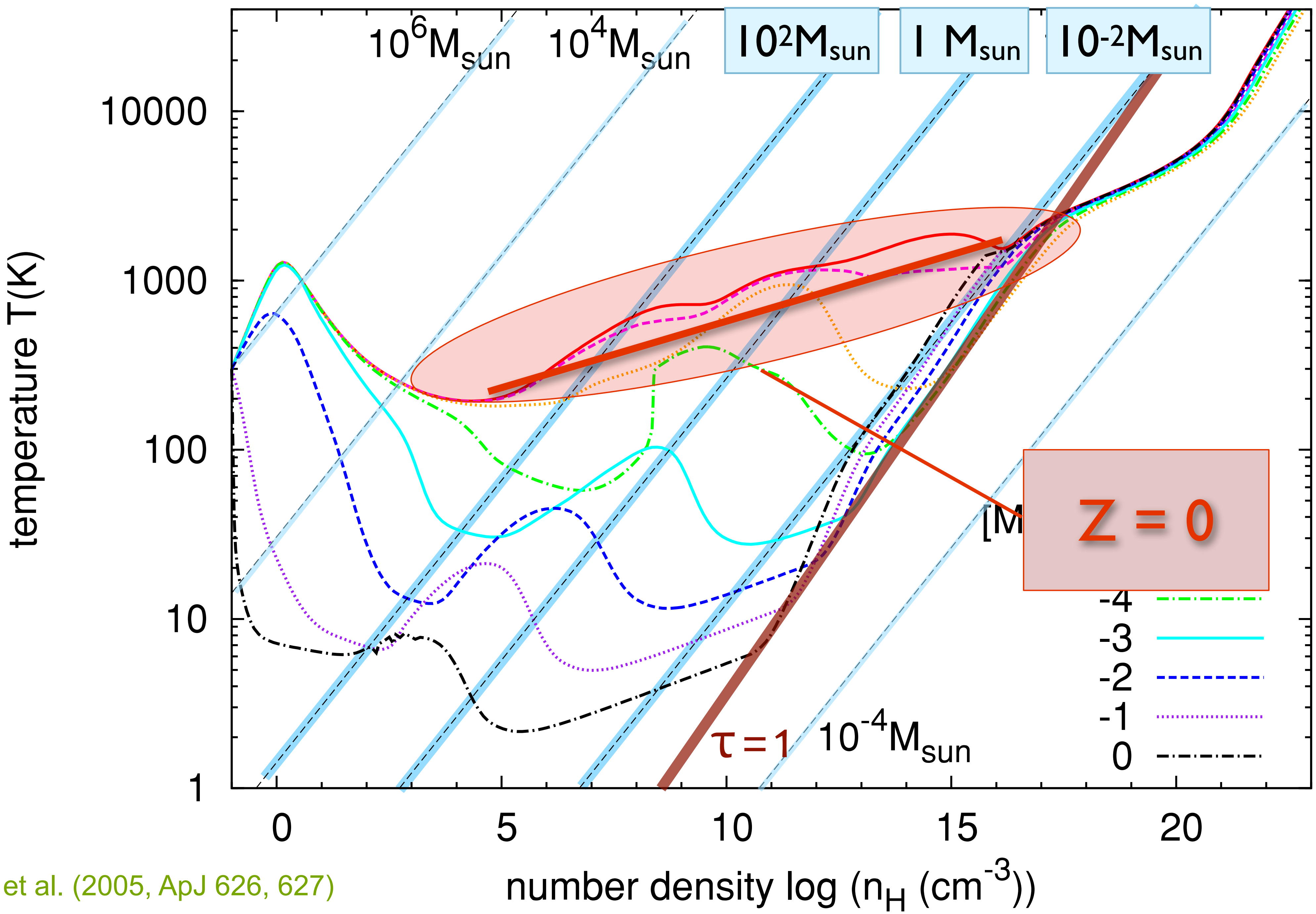


Omukai et al. (2005, ApJ 626, 627)

equation of state

equation of state

# Pop III stars

UNIVERSITÄT
HEIDELBERG
ZUKUNFT
SEIT 1386

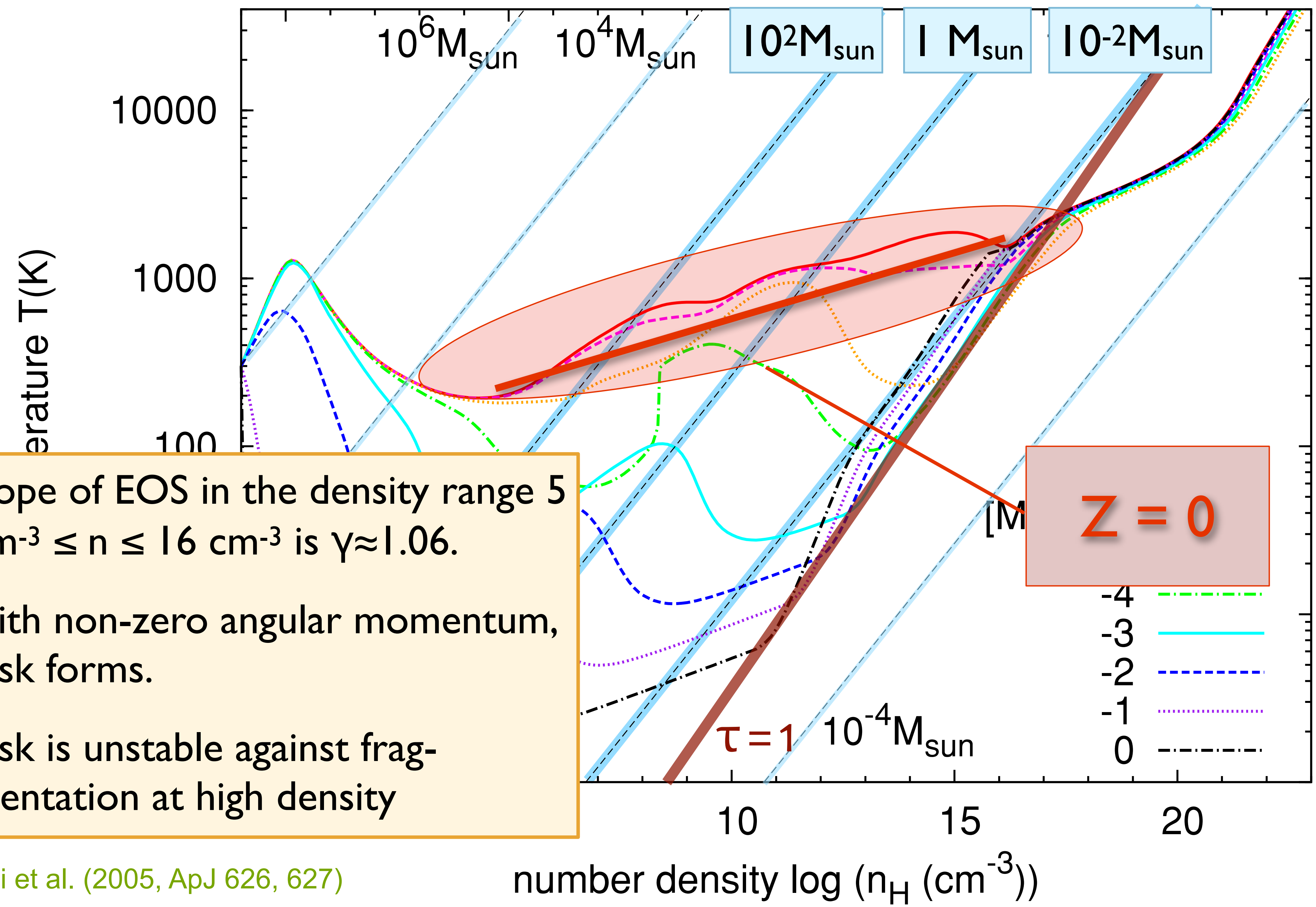


- slope of EOS in the density range 5 $cm^{-3} \le n \le 16\ cm^{-3}$ is $\gamma \approx 1.06$.
- with non-zero angular momentum, disk forms.
- disk is unstable against fragmentation at high density

Omukai et al. (2005, ApJ 626, 627)

disk fragmentation

# Pop III stars

UNIVERSITÄT HEIDELBERG ZUKUNFT SEIT 1386

multiple Pop III stars form by disk fragmentation

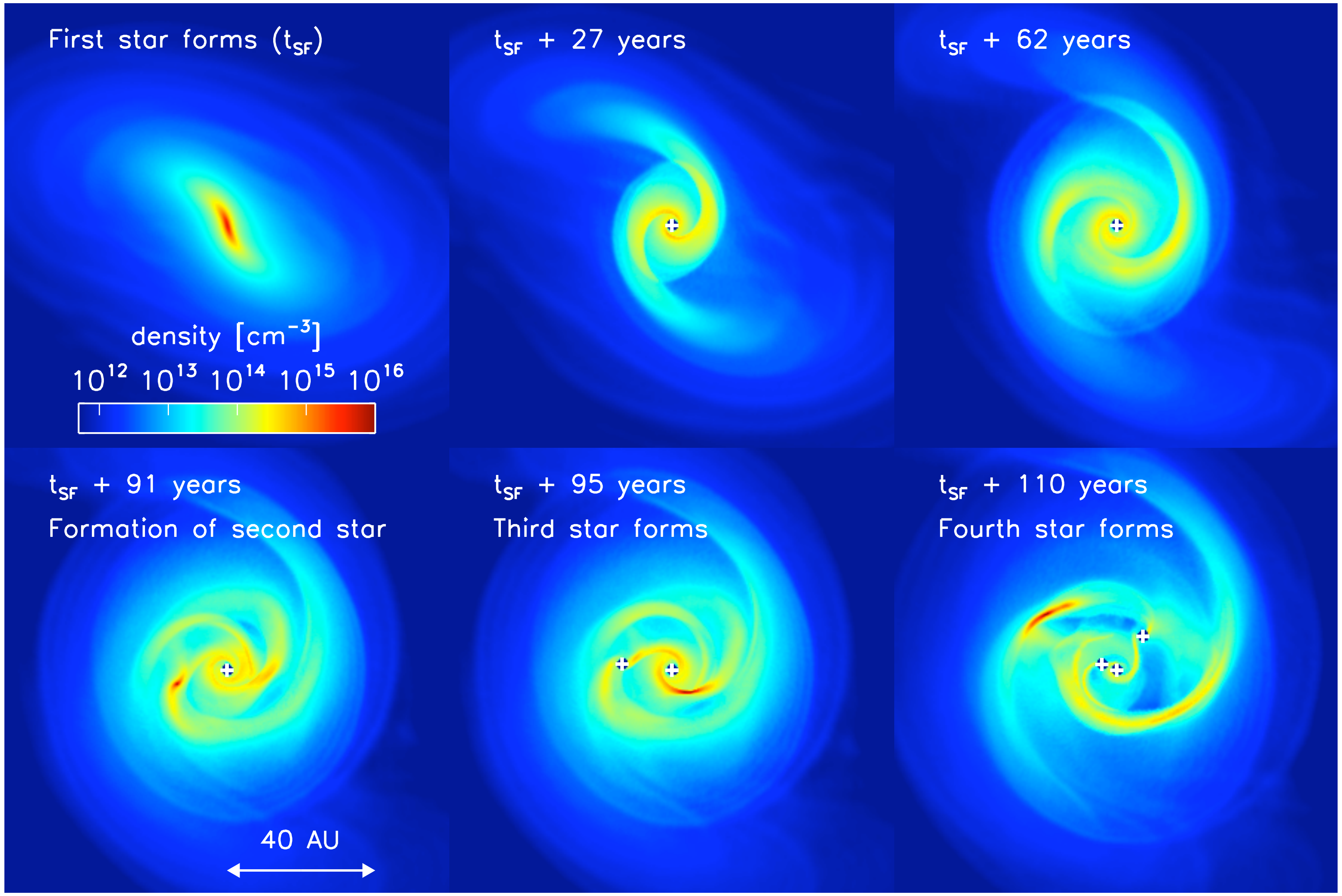


Clark et la. (2011, Science, 331, 1040)

disk fragmentation

# Pop III stars

multiple Pop III stars form by disk fragmentation

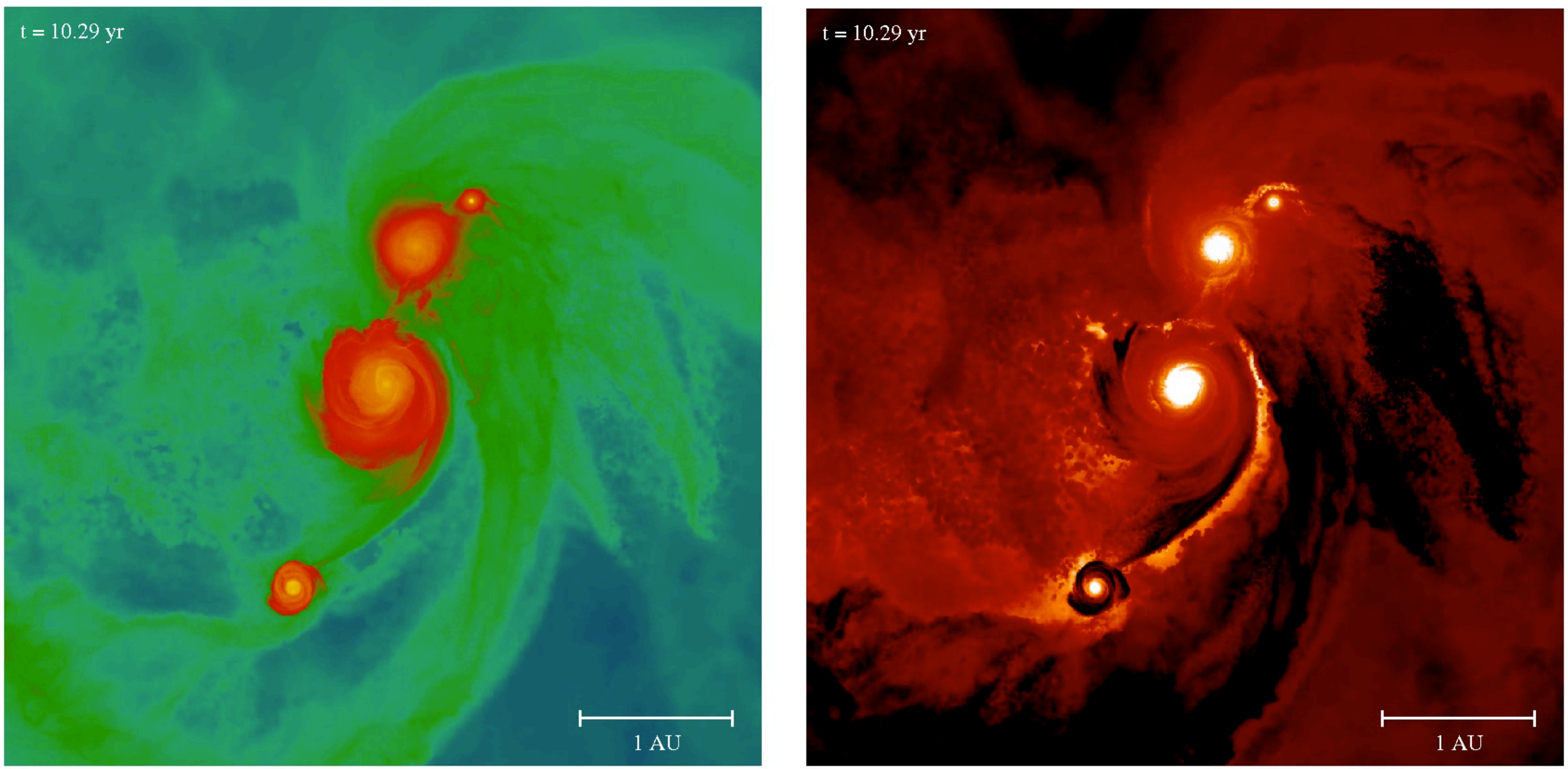


density

temperatur

Greif et al. (2012, MNRAS, 424, 399)

# IMF of Pop III stars



simulations suggest IMF of metal-free stars is log flat (with hint for top-heaviness)

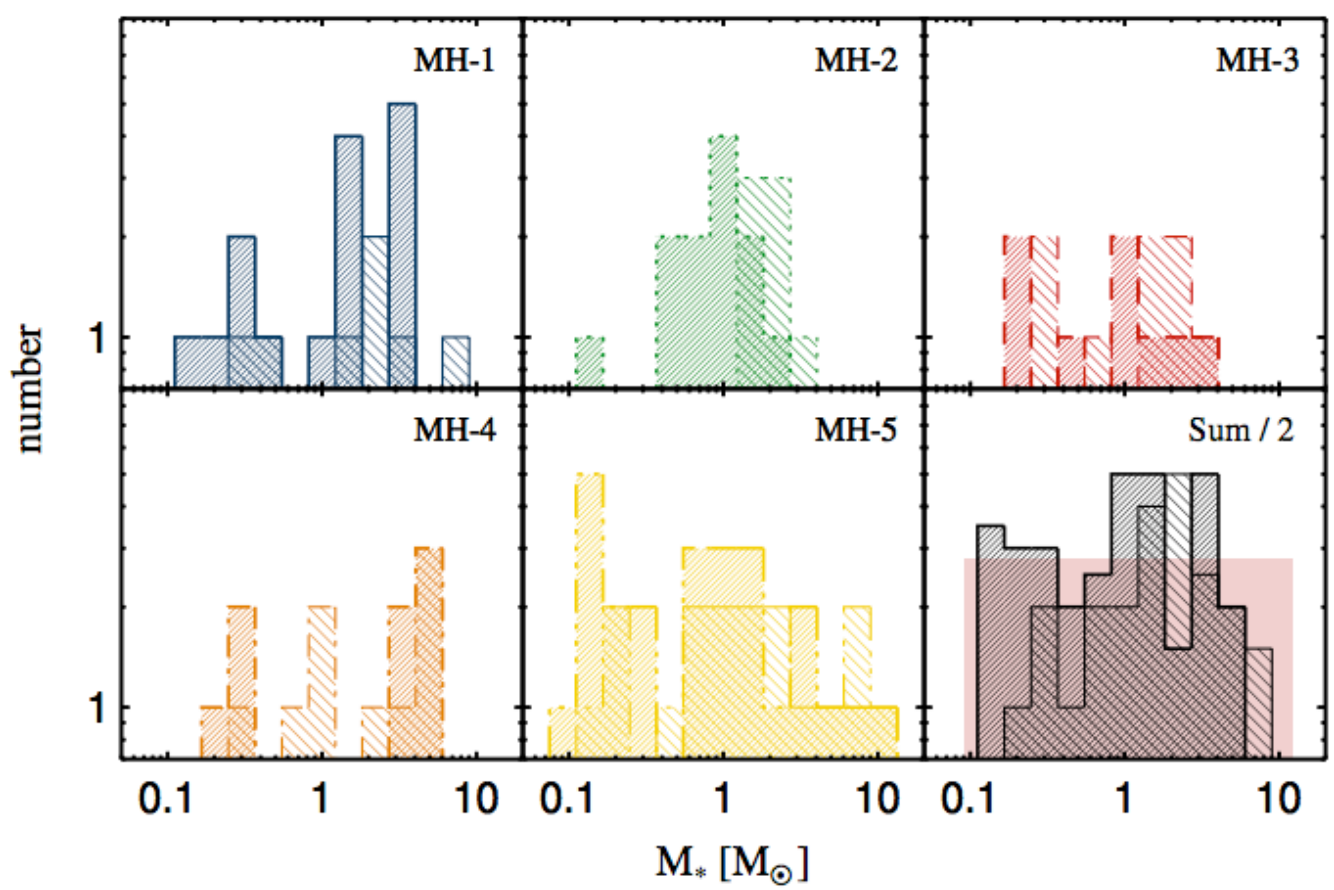


we see "flat" mass spectrum

Greif et al. (2011, ApJ, 737, 75), Clark et al. (2011, Science, 331, 1040), Smith et al. (2011, MNRAS, 414, 3633), Dopcke et al. (2013, ApJ, 766, 103), Hirano et al. (2014, ApJ, 781, 60), Tanaka & Omukai (2014, MNRAS, 439, 1884), Nakauchi et al. (2014, MNRAS, 442, 2667), Wollenberg et al. (2020, MNRAS, 494, 1871), Prole et al. (2022, MNRAS, 510, 4019), Prole et al. (2022, MNRAS, 516, 2223), and many more

UNIVERSITÄT
HEIDELBERG
ZUKUNFT
SEIT 1386

# IMF of Pop III stars

simulations suggest IMF of metal-free stars is log flat
(with hint for top-heaviness)

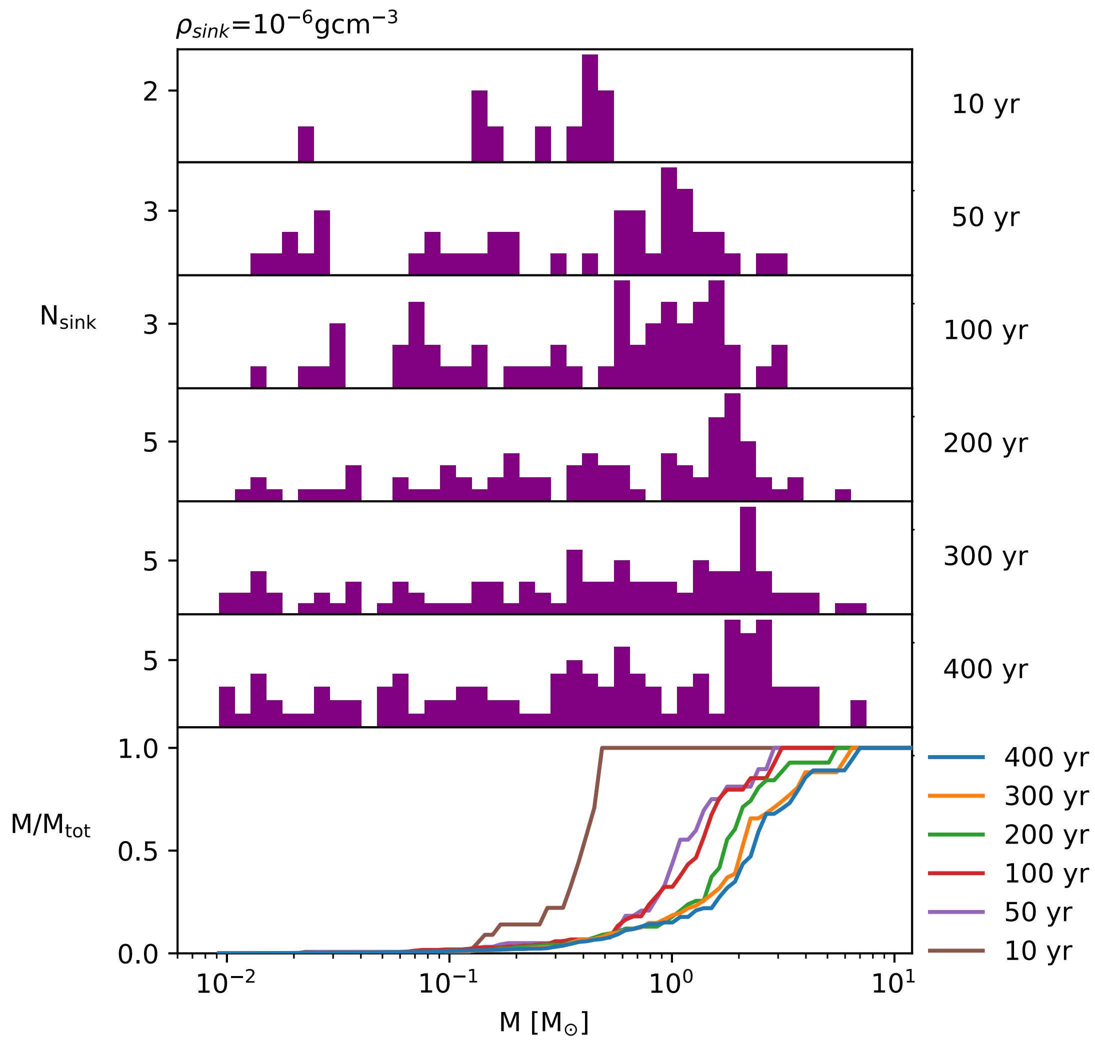


Prole et al. (2022, MNRAS, 510, 4019)

stellar mass spectrum

UNIVERSITÄT
HEIDELBERG
ZUKUNFT
SEIT 1386

# IMF of Pop III stars

simulations suggest IMF of metal-free stars is log flat
(with hint for top-heaviness)

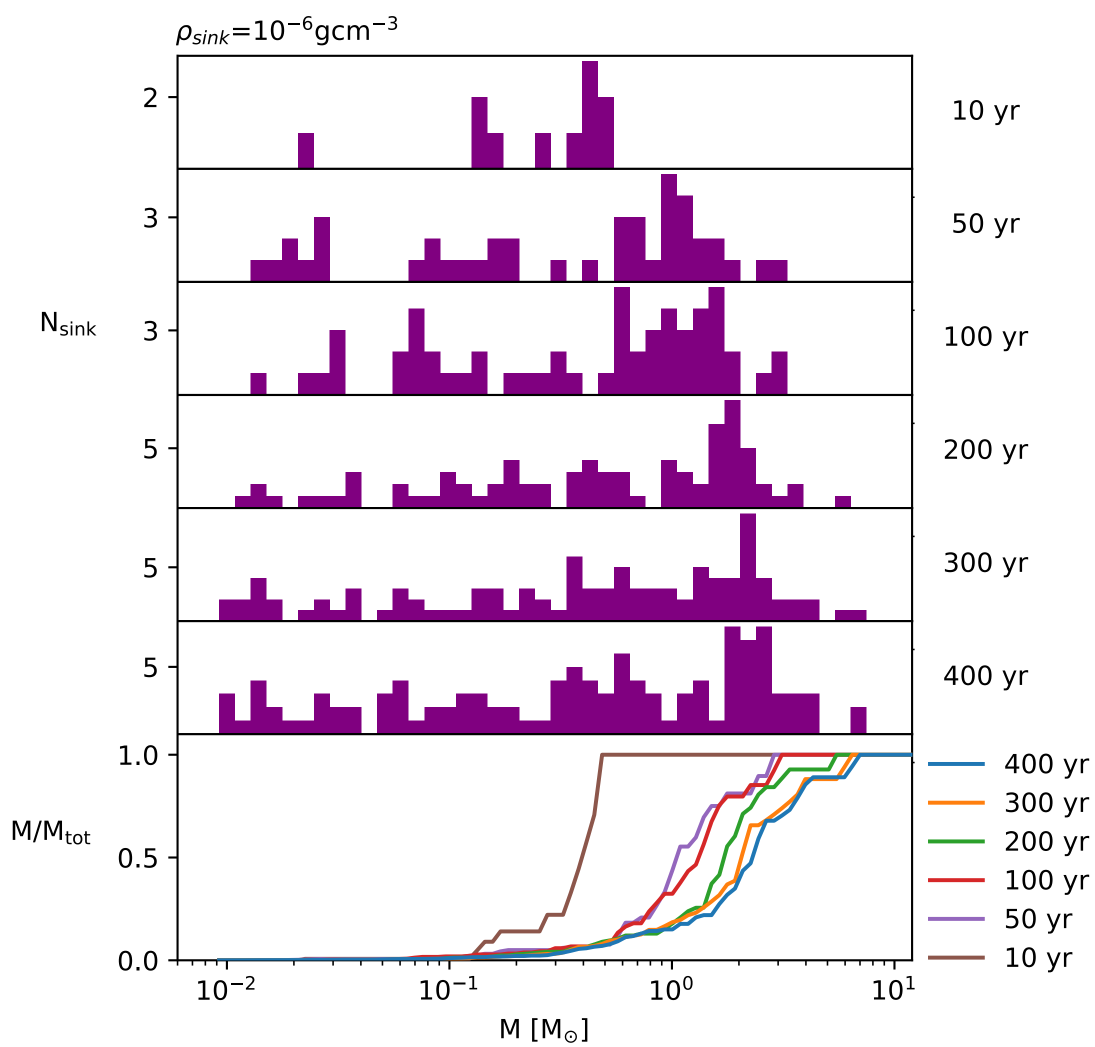


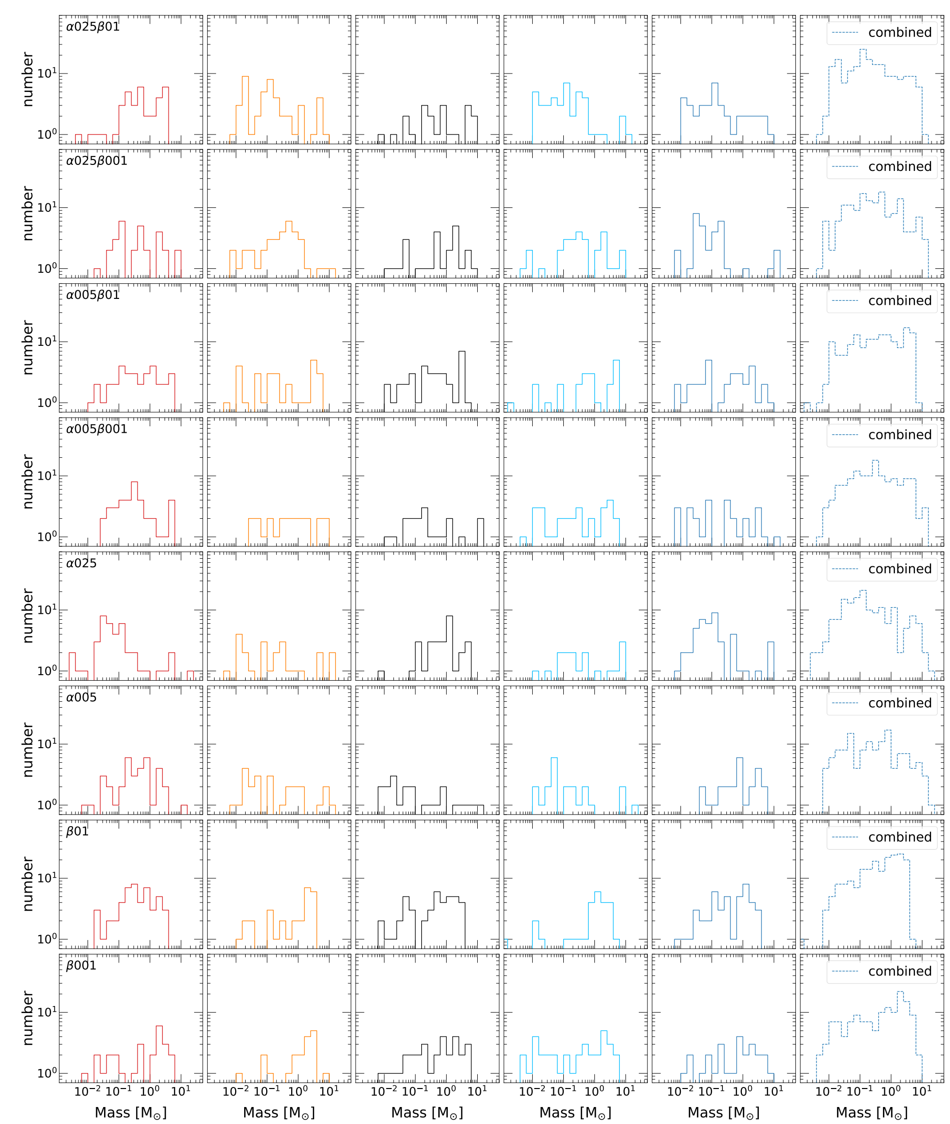


Prole et al. (2022, MNRAS, 510, 4019)

Wollenberg et al. (2020, MNRAS, 494, 1871)

stellar mass spectrum

UNIVERSITÄT HEIDELBERG
ZUKUNFT SEIT 1386

# IMF of Pop III stars

simulations suggest IMF of metal-free stars is log flat (with hint for top-heaviness)

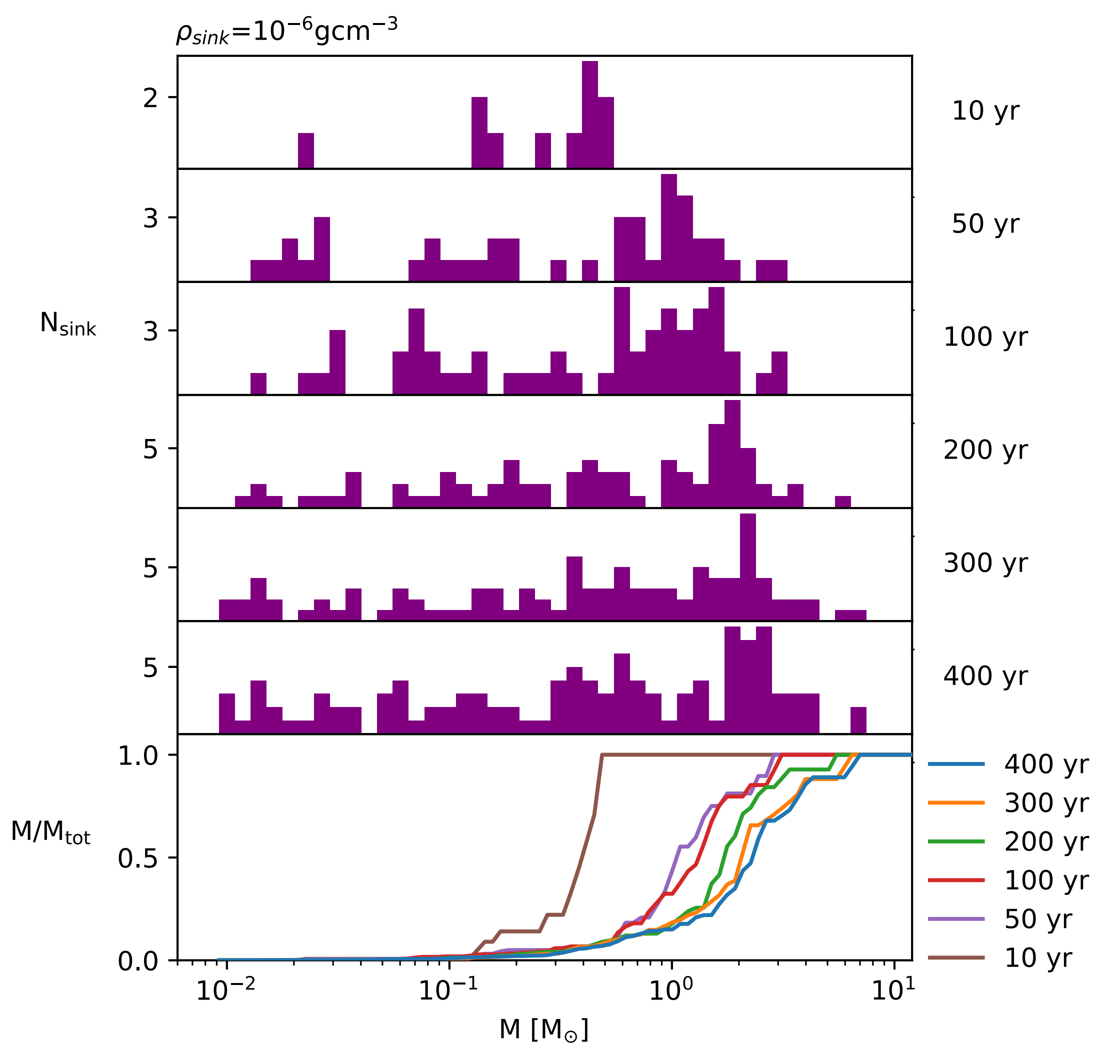


Prole et al. (2022, MNRAS, 510, 4019)

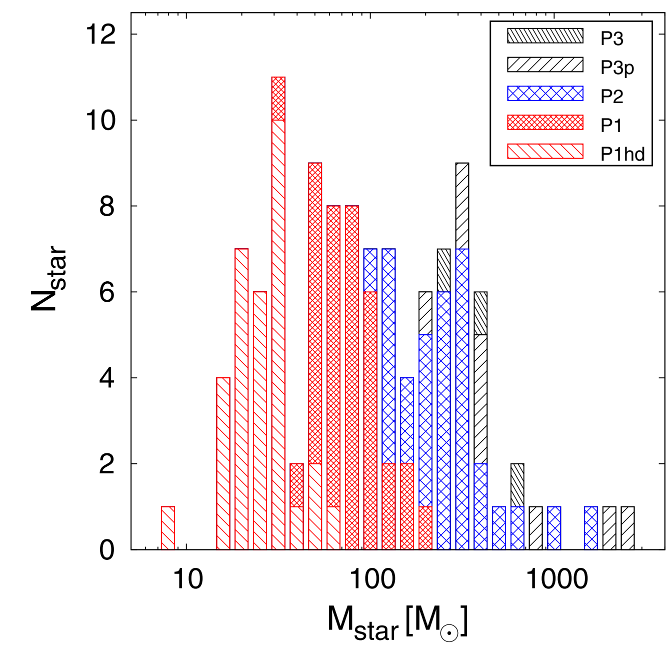


Hirano et al. (2014, ApJ, 781, 60)

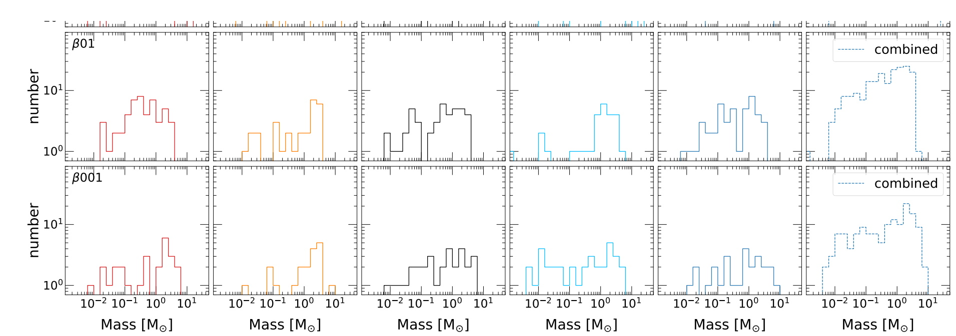


Wollenberg et al. (2020, MNRAS, 494, 1871)

stellar mass spectrum

# IMF of Pop III stars

UNIVERSITÄT
HEIDELBERG
ZUKUNFT
SEIT 1386

simulations suggest IMF of metal-free stars is log flat (meaning it is top heavy)

BUT: result depends strongly on *numerical resolution*, and on the *physics* involved, and on the way *feedback* is taken into account.

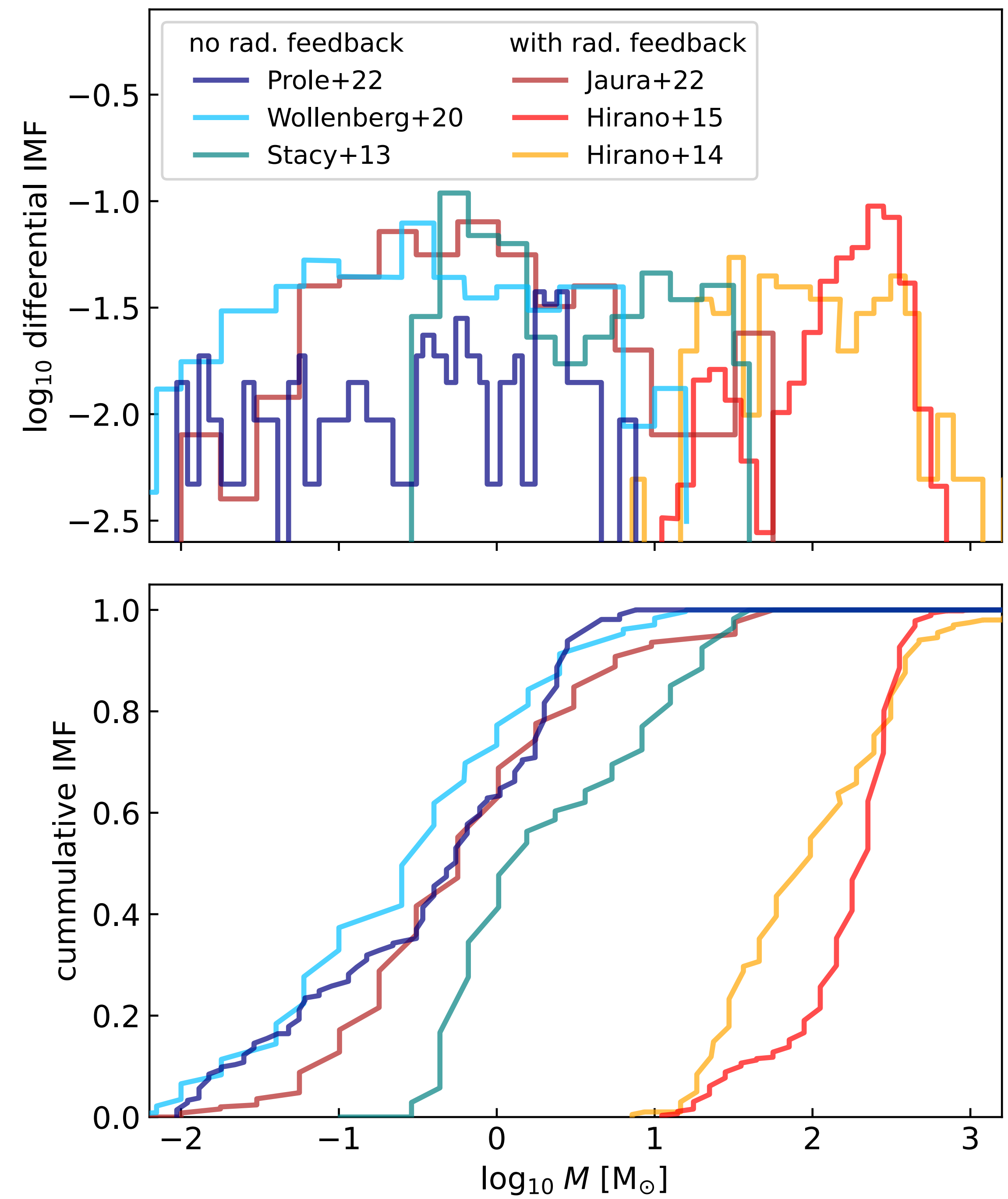


(Klessen, & Glover (2023, ARAA, 61, 65 -- arXiv.2303.12500)

Pop III stars

# some properties of Pop III stars

UNIVERSITÄT HEIDELBERG
ZUKUNFT SEIT 1386

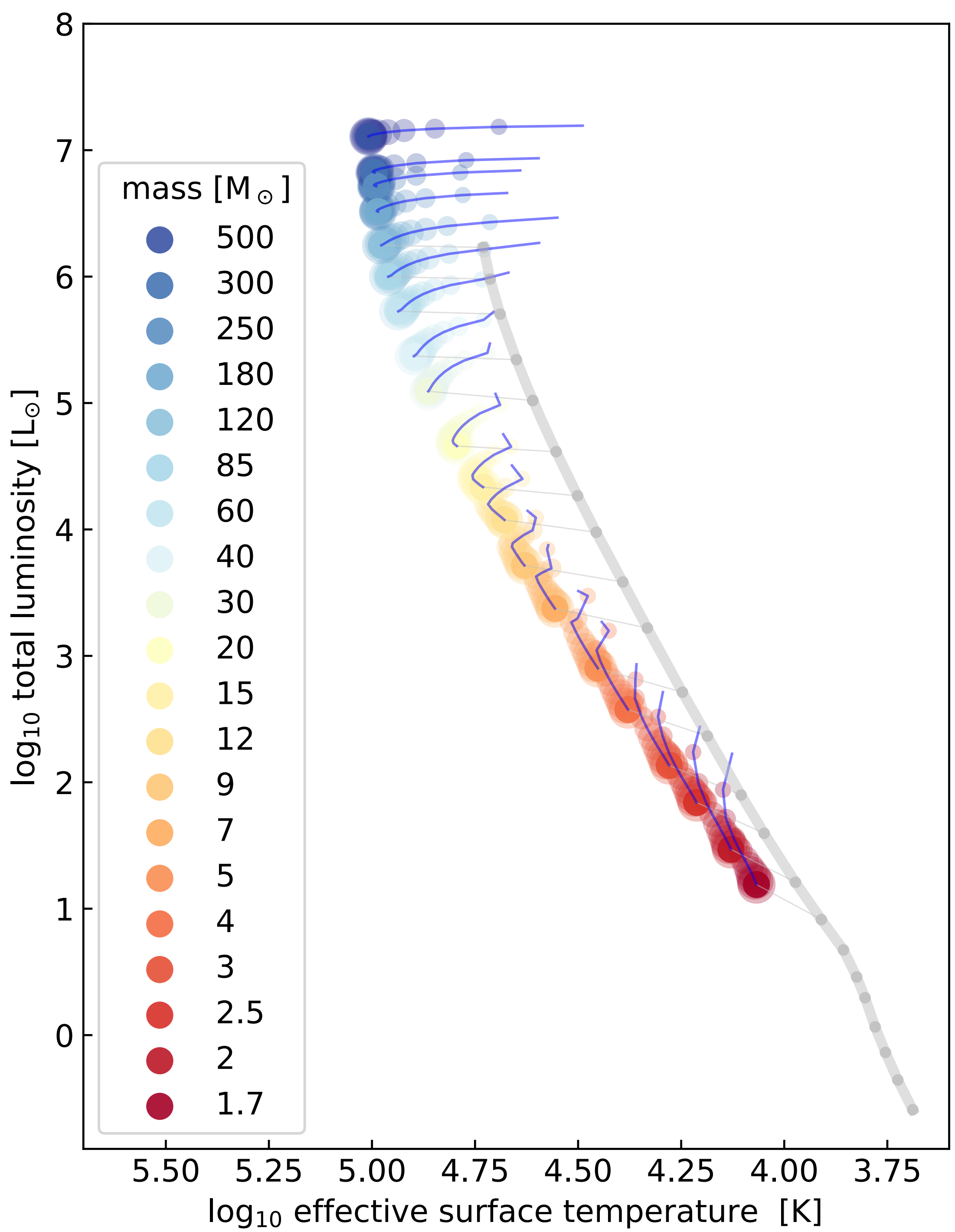


Pop III stars are typically more compact and hotter than their Pop II/I counterparts. But they have similar bolometric luminosity.

Klessen, & Glover (2023, ARAA, 61, 65 -- arXiv.2303.12500)

Pop III stars

# some properties of Pop III stars

UNIVERSITÄT
HEIDELBERG
ZUKUNFT
SEIT 1386

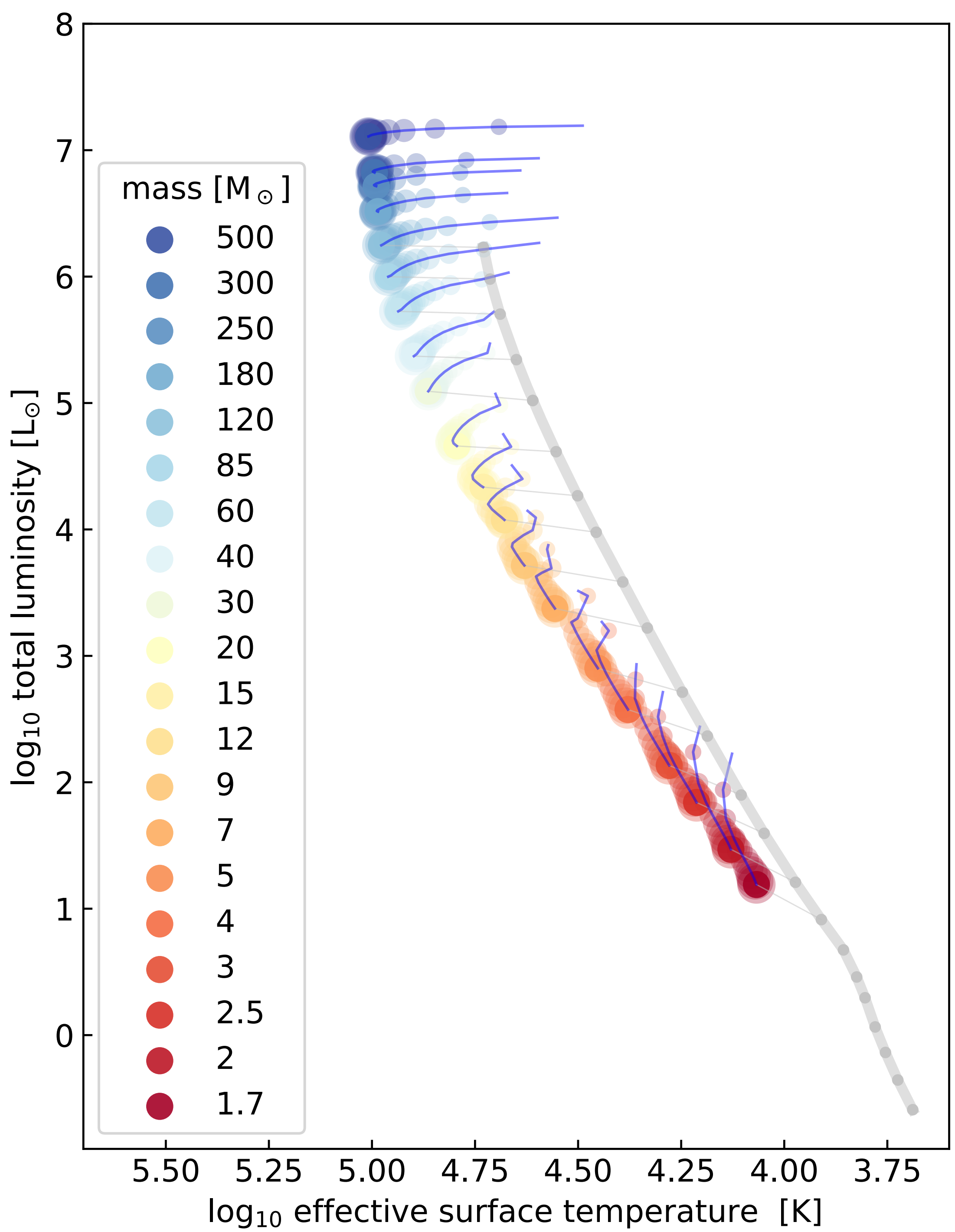


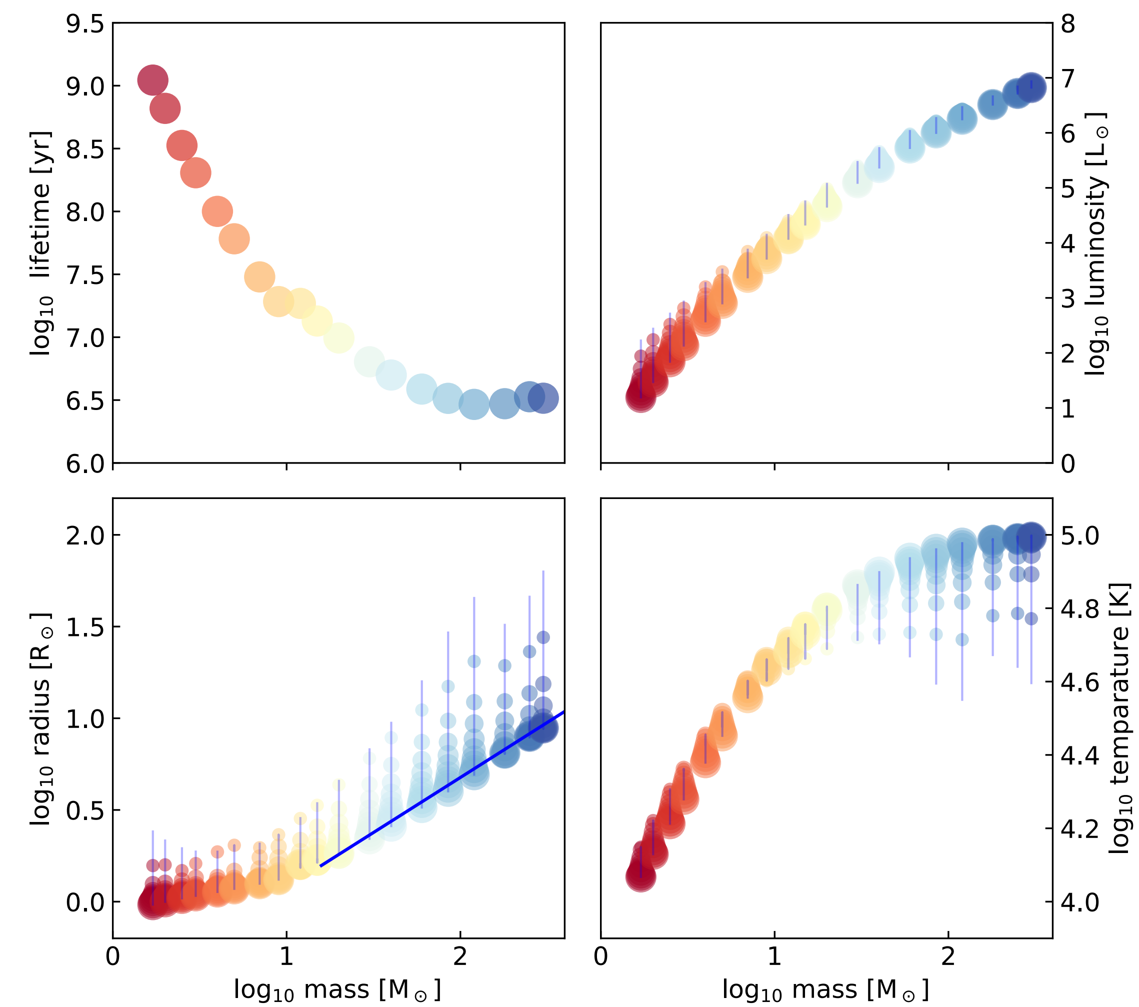


Pop III stars are typically more compact and hotter than their Pop II/I counterparts. But they have similar bolometric luminosity.

Klessen, & Glover (2023, ARAA, 61, 65 -- arXiv.2303.12500)

# some properties of Pop III stars

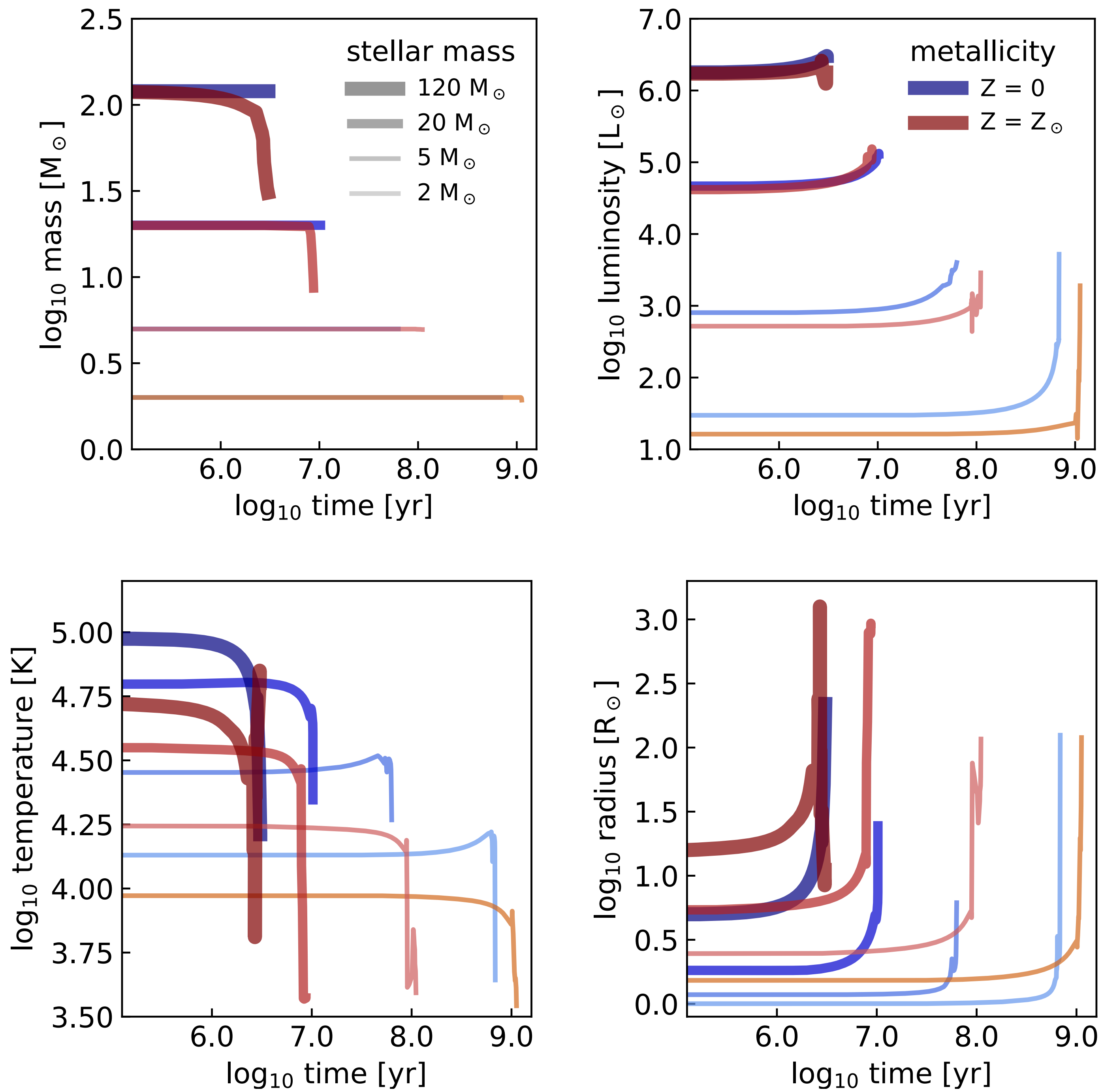


Klessen, & Glover (2023, ARAA, 61,65 -- arXiv.2303.12500)
based on data by Murphy et al. (2021, MNRAS 501, 2745, 2021, MNRAS, 506, 5731) and Ekström et al. (2012, A&A, 537, A146)

UNIVERSITÄT HEIDELBERG
ZUKUNFT SEIT 1386

Pop III stars

# Pop III stars

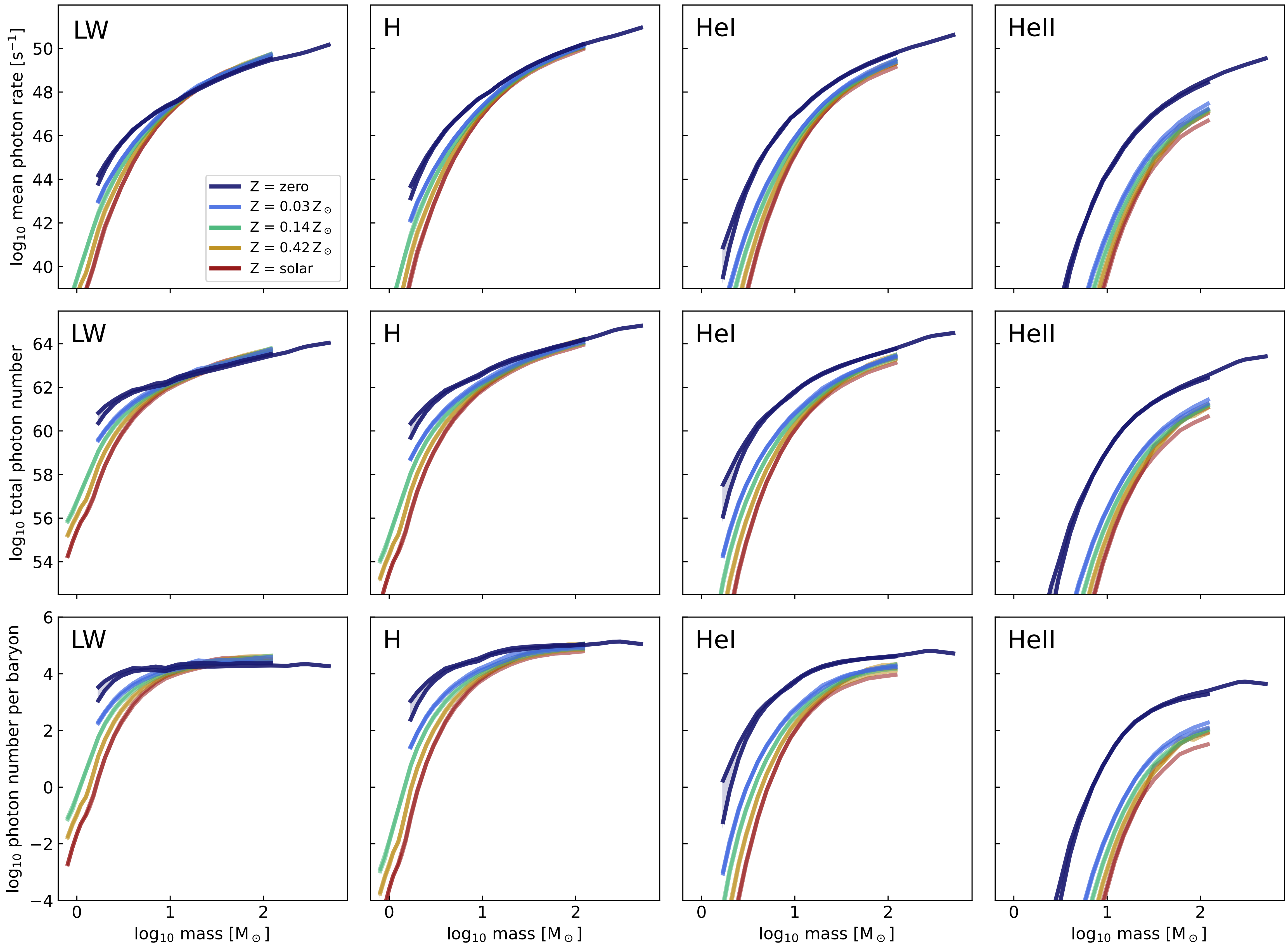


Klessen, & Glover (2023, ARAA, 61, 65 -- arXiv.2303.12500)

Pop III stars

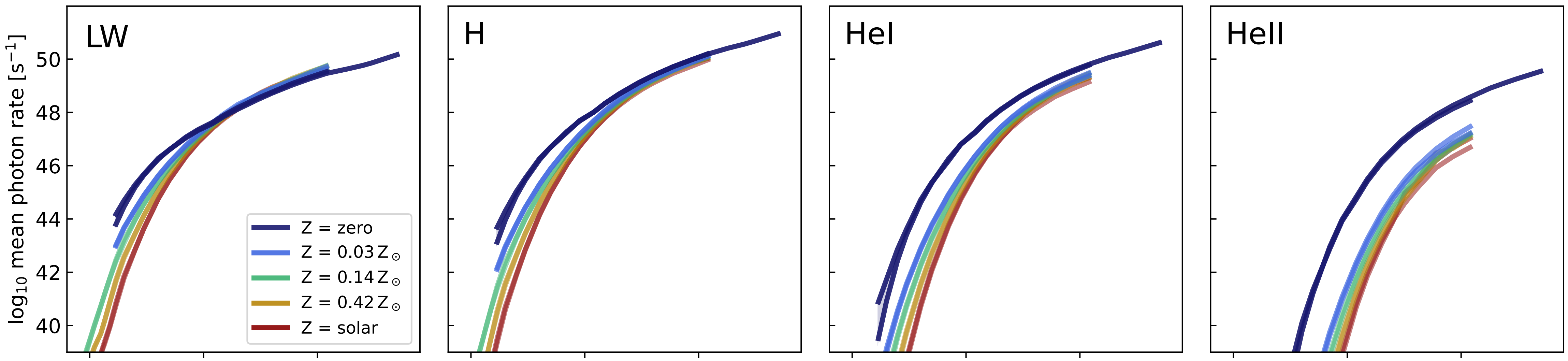


## Table A1: Key stellar properties and production rates of ionizing and non-ionizing photons as function of stellar mass and metallicity

| $Z$ [$Z_\odot$] | rot [$v_{\max}$] | $M$ [$M_\odot$] | age [yr] | $T_*$ [K] | $L_*$ [$L_\odot$] | $R_*$ [$R_\odot$] | $Q_{\rm tot}$ [$s^{-1}$] | $Q_{\rm LW}$ [$s^{-1}$] | $Q_{\rm H}$ [$s^{-1}$] | $Q_{\rm HeI}$ [$s^{-1}$] | $Q_{\rm HeII}$ [$s^{-1}$] | $N_{\rm tot}$ – | $N_{\rm LW}$ – | $N_{\rm H}$ – | $N_{\rm HeI}$ – | $N_{\rm HeII}$ – | $N^b$ – | $N^b_{\rm LW}$ – | $N^b_{\rm H}$ – | $N^b_{\rm HeI}$ – | $N^b_{\rm HeII}$ – |
|---|---|---|---|---|---|---|---|---|---|---|---|---|---|---|---|---|---|---|---|---|---|
| 0.0 | 0.0 | 1.7 | 9.06 | 4.10 | 1.48 | 1.16 | 46.51 | 43.80 | 43.13 | 39.51 | 29.26 | 63.07 | 60.36 | 59.69 | 56.07 | 45.82 | 5.76 | 3.06 | 2.39 | 0 | 0 |
| 0.0 | 0.0 | 2.0 | 8.84 | 4.17 | 1.76 | 1.18 | 46.70 | 44.46 | 43.95 | 40.90 | 32.19 | 63.04 | 60.80 | 60.28 | 57.24 | 48.53 | 5.66 | 3.42 | 2.91 | 0 | 0 |
| 0.0 | 0.0 | 2.5 | 8.54 | 4.25 | 2.13 | 1.20 | 46.96 | 45.19 | 44.86 | 42.43 | 35.37 | 63.00 | 61.23 | 60.90 | 58.47 | 51.41 | 5.53 | 3.76 | 3.43 | 1.0 | 0 |
| 0.0 | 0.0 | 3.0 | 8.33 | 4.32 | 2.41 | 1.23 | 47.17 | 45.65 | 45.46 | 43.40 | 37.36 | 62.99 | 61.48 | 61.28 | 59.23 | 53.19 | 5.44 | 3.93 | 3.73 | 1.68 | 0 |
| 0.0 | 0.0 | 4.0 | 8.02 | 4.42 | 2.84 | 1.29 | 47.49 | 46.24 | 46.22 | 44.61 | 39.78 | 63.00 | 61.76 | 61.73 | 60.13 | 55.29 | 5.33 | 4.08 | 4.06 | 2.45 | 0 |
| 0.0 | 0.0 | 5.0 | 7.80 | 4.48 | 3.15 | 1.34 | 47.71 | 46.60 | 46.69 | 45.35 | 41.21 | 63.01 | 61.90 | 61.99 | 60.65 | 56.51 | 5.24 | 4.13 | 4.22 | 2.87 | 0 |
| 0.0 | 0.0 | 7.0 | 7.50 | 4.58 | 3.59 | 1.45 | 48.04 | 47.05 | 47.29 | 46.25 | 42.94 | 63.04 | 62.04 | 62.29 | 61.25 | 57.94 | 5.12 | 4.12 | 4.37 | 3.33 | 0.02 |
| 0.0 | 0.0 | 9.0 | 7.30 | 4.64 | 3.90 | 1.58 | 48.29 | 47.33 | 47.67 | 46.80 | 43.98 | 63.09 | 62.13 | 62.47 | 61.60 | 58.78 | 5.06 | 4.10 | 4.44 | 3.57 | 0.75 |
| 0.0 | 0.0 | 12.0 | 7.29 | 4.69 | 4.24 | 1.84 | 48.53 | 47.58 | 48.01 | 47.27 | 44.83 | 63.31 | 62.37 | 62.80 | 62.06 | 59.62 | 5.16 | 4.21 | 4.65 | 3.90 | 1.46 |
| 0.0 | 0.0 | 15.0 | 7.15 | 4.73 | 4.48 | 2.03 | 48.79 | 47.84 | 48.34 | 47.68 | 45.49 | 63.43 | 62.49 | 62.98 | 62.32 | 60.14 | 5.18 | 4.23 | 4.73 | 4.07 | 1.89 |
| 0.0 | 0.0 | 20.0 | 7.01 | 4.77 | 4.81 | 2.43 | 49.08 | 48.12 | 48.68 | 48.10 | 46.18 | 63.59 | 62.63 | 63.19 | 62.61 | 60.69 | 5.21 | 4.26 | 4.82 | 4.24 | 2.32 |
| 0.0 | 0.0 | 30.0 | 6.82 | 4.82 | 5.23 | 3.22 | 49.46 | 48.49 | 49.12 | 48.61 | 46.95 | 63.78 | 62.81 | 63.44 | 62.93 | 61.27 | 5.23 | 4.26 | 4.88 | 4.38 | 2.72 |
| 0.0 | 0.0 | 40.0 | 6.72 | 4.84 | 5.50 | 3.96 | 49.71 | 48.73 | 49.39 | 48.92 | 47.39 | 63.92 | 62.94 | 63.60 | 63.14 | 61.60 | 5.25 | 4.26 | 4.93 | 4.46 | 2.93 |
| 0.0 | 0.0 | 60.0 | 6.61 | 4.86 | 5.85 | 5.26 | 50.03 | 49.03 | 49.72 | 49.29 | 47.90 | 64.13 | 63.13 | 63.82 | 63.40 | 62.01 | 5.28 | 4.28 | 4.97 | 4.54 | 3.15 |
| 0.0 | 0.0 | 85.0 | 6.53 | 4.87 | 6.10 | 6.77 | 50.29 | 49.26 | 49.97 | 49.56 | 48.26 | 64.32 | 63.29 | 64.00 | 63.59 | 62.30 | 5.31 | 4.28 | 4.99 | 4.59 | 3.29 |
| 0.0 | 0.0 | 120.0 | 6.48 | 4.88 | 6.34 | 8.55 | 50.51 | 49.47 | 50.19 | 49.80 | 48.57 | 64.50 | 63.45 | 64.17 | 63.79 | 62.55 | 5.34 | 4.29 | 5.02 | 4.63 | 3.40 |
| 0.0 | 0.0 | 180.0 | 6.49 | 4.92 | 6.57 | 9.44 | 50.66 | 49.62 | 50.41 | 50.06 | 48.91 | 64.65 | 63.61 | 64.40 | 64.05 | 62.90 | 5.32 | 4.28 | 5.07 | 4.72 | 3.57 |
| 0.0 | 0.0 | 250.0 | 6.54 | 4.92 | 6.76 | 11.37 | 50.83 | 49.76 | 50.56 | 50.23 | 49.13 | 64.87 | 63.81 | 64.60 | 64.27 | 63.17 | 5.40 | 4.33 | 5.13 | 4.80 | 3.70 |
| 0.0 | 0.0 | 300.0 | 6.53 | 4.92 | 6.86 | 13.06 | 50.95 | 49.86 | 50.66 | 50.33 | 49.24 | 64.98 | 63.89 | 64.69 | 64.36 | 63.28 | 5.43 | 4.34 | 5.14 | 4.81 | 3.72 |
| 0.0 | 0.0 | 500.0 | 6.38 | 4.90 | 7.14 | 19.61 | 51.29 | 50.17 | 50.95 | 50.62 | 49.54 | 65.17 | 64.04 | 64.82 | 64.49 | 63.42 | 5.39 | 4.27 | 5.05 | 4.72 | 3.64 |

*General comment:* Note that the part of the table depicted here only covers models of non-rotating zero-metallicity Pop III stars. The complete table is available electronically in space-separated ASCII format from ARAA or from the authors at heibox.uni-heidelberg.de/f/6b5b3fcbd3974fb98d50/. It can be easily read, for example, using the `astropy.io.ascii.read` command.

Klessen, & Glover (2023, ARAA, 61, 65 -- arXiv.2303.12500)

Pop III stars

## Table A2: Population averaged number of photons per baryon (in log units)

| population | IMF | $\langle N^b \rangle$ | $\langle N^b_{\mathrm{LW}} \rangle$ | $\langle N^b_{\mathrm{H}} \rangle$ | $\langle N^b_{\mathrm{HeI}} \rangle$ | $\langle N^b_{\mathrm{HeII}} \rangle$ |
|---|---|---|---|---|---|---|
| Pop III | log-flat | 5.31 | 4.11 | 4.72 | 4.29 | 3.05 |
| Pop I | Kroupa | 6.11 | 2.67 | 2.69 | 1.50 | 0 |

*Column description:* population = metal-free Pop III or solar-metallicity Pop I stars ■ IMF = stellar initial mass function, either logarithmically flat or (Kroupa 2002) multi-component power-law model ■ $\langle N^b \rangle$ = decadic logarithm of the population averaged total number of photons emitted per stellar baryon ■ $\langle N^b_{\mathrm{LW}} \rangle$ = decadic logarithm of the population averaged number of LW photons emitted per stellar baryon ■ $\langle N^b_{\mathrm{H}} \rangle$ = decadic logarithm of the population averaged number of H ionizing photons emitted per stellar baryon ■ $\langle N^b_{\mathrm{HeI}} \rangle$ = decadic logarithm of the population averaged number of He ionizing photons emitted per stellar baryon ■ $\langle N^b_{\mathrm{HeII}} \rangle$ = decadic logarithm of the population averaged number of $He^+$ ionizing photons emitted per stellar baryon

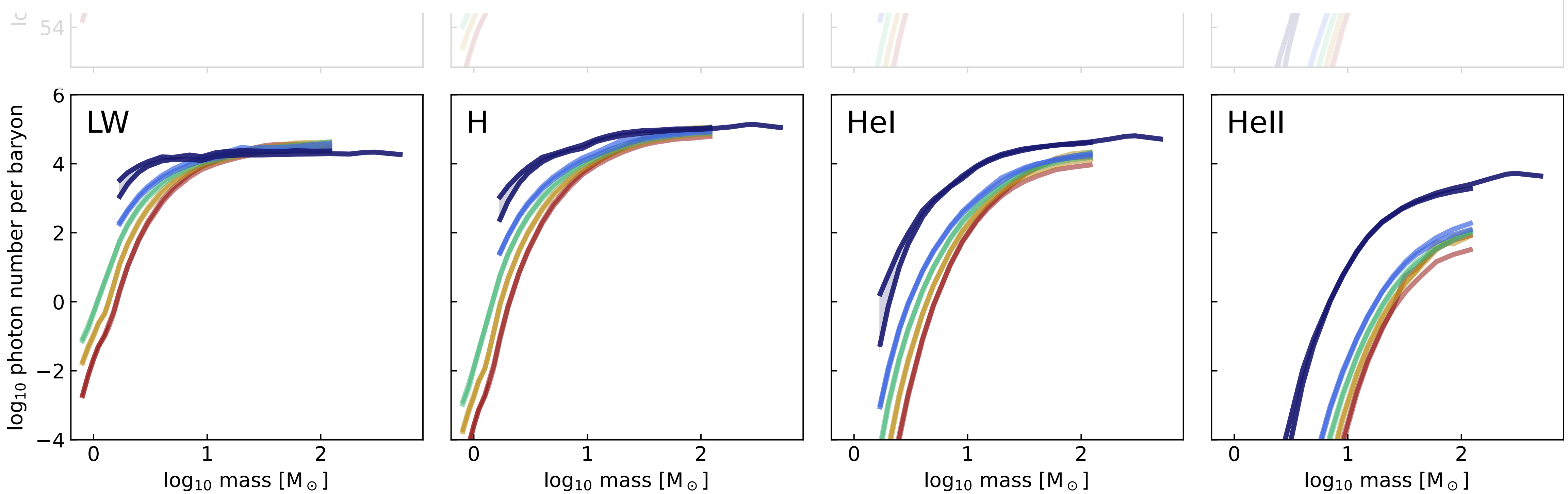


Klessen, & Glover (2023, ARAA, 61, 65 -- arXiv.2303.12500)

# Pop III stars

BUT: note that the spectra are more complex that simply blackbodies, and so this consideration may be wrong by a factor of a few

UNIVERSITÄT
HEIDELBERG
ZUKUNFT
SEIT 1386

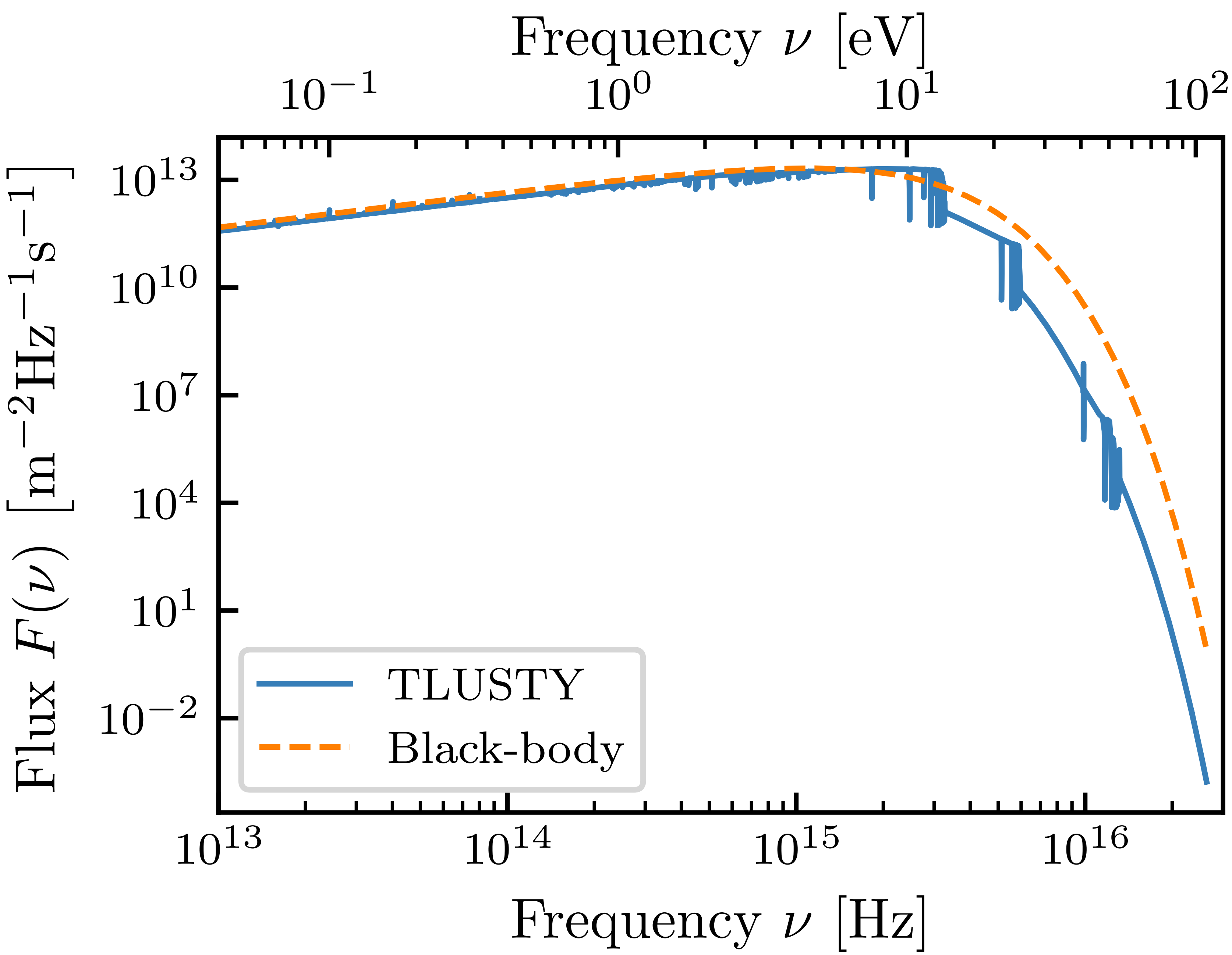


6 solar mass Pop III star, at ~90% of its main sequence lifetime

Gessey-Jones et al. (2022, MNRAS, 516, 841)

# Pop III stars

BUT: note that the spectra are more complex that simply blackbodies, and so this consideration may be wrong by a factor of a few

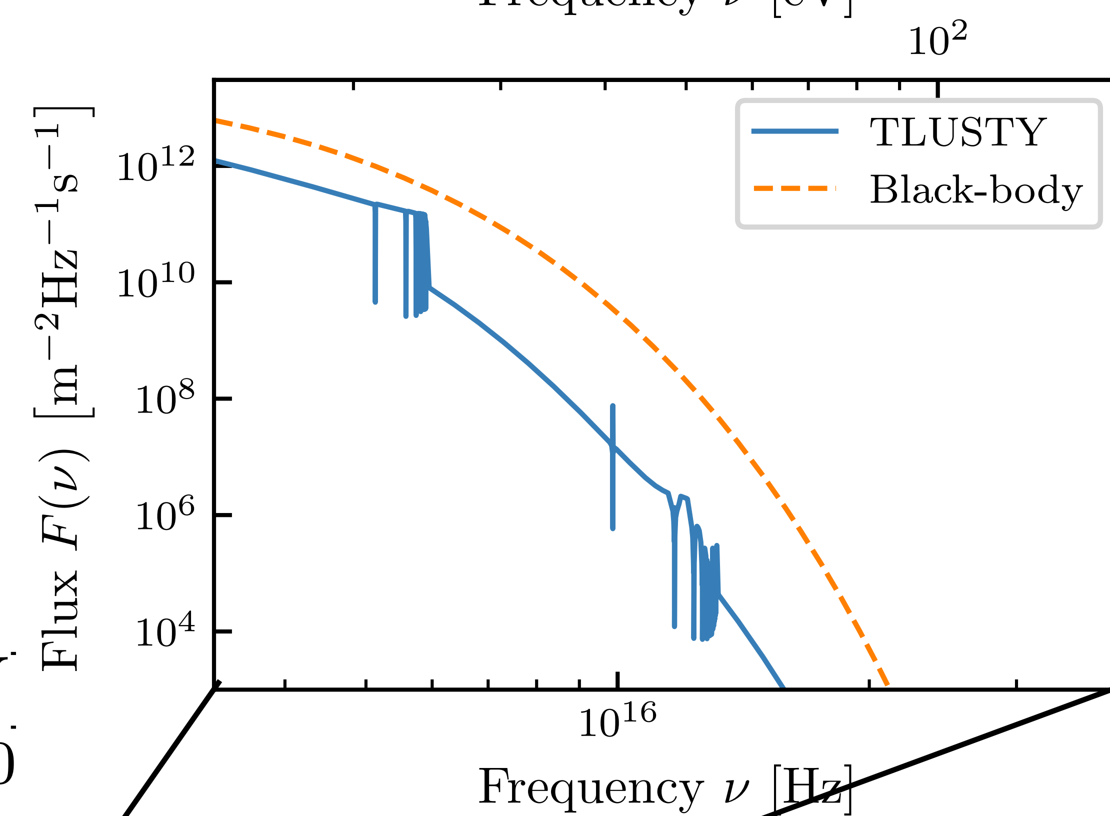


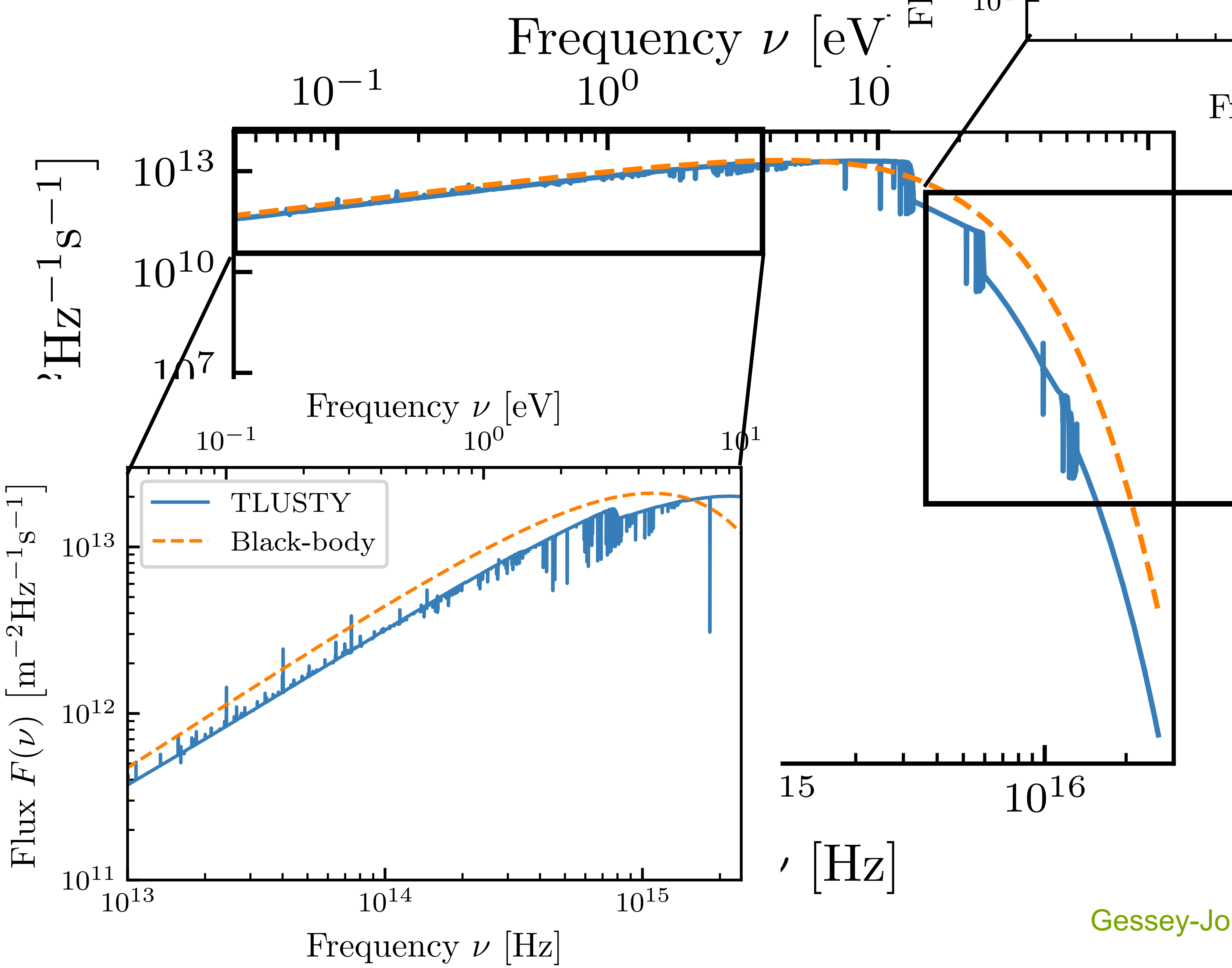


6 solar mass Pop III star, at ~90% of its main sequence lifetime

Gessey-Jones et al. (2022, MNRAS, 516, 841)

# Pop II stars


Deutsche Forschungsgemeinschaft
DFG
ECOGAL
ERC Synergy Grant
European Research Council
STRUCTURES
CLUSTER OF EXCELLENCE
UNIVERSITÄT HEIDELBERG
ZUKUNFT SEIT 1386

Pop II stars

# transition from Pop III to Pop II star formation

UNIVERSITÄT HEIDELBERG
ZUKUNFT SEIT 1386

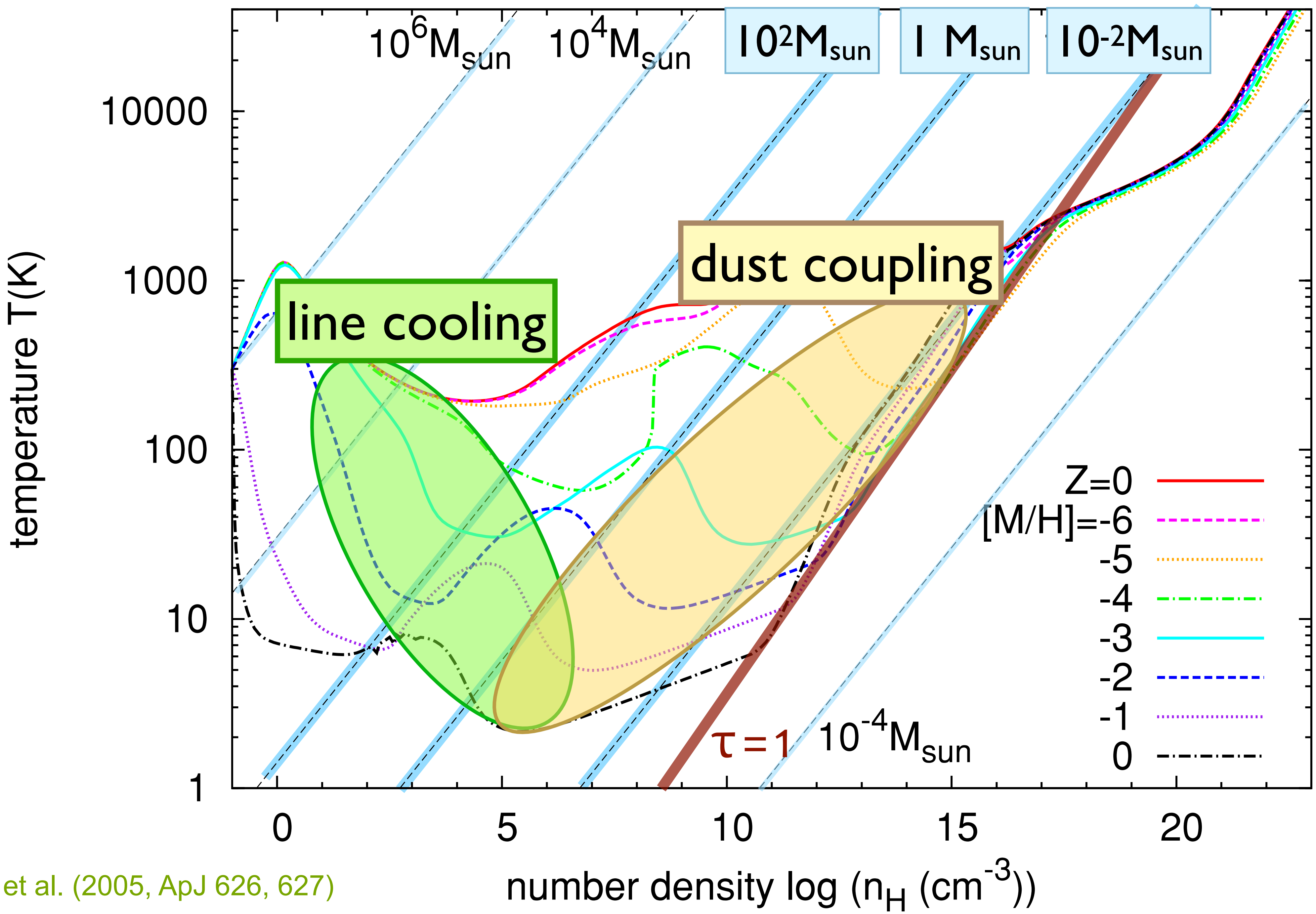


Omukai et al. (2005, ApJ 626, 627)

# transition from Pop III to Pop II star formation

UNIVERSITÄT HEIDELBERG
ZUKUNFT SEIT 1386

Pop II stars

at low metallicity, line cooling and dust coupling separate, and there is the question of what triggers transition from Pop III to Pop II star formation

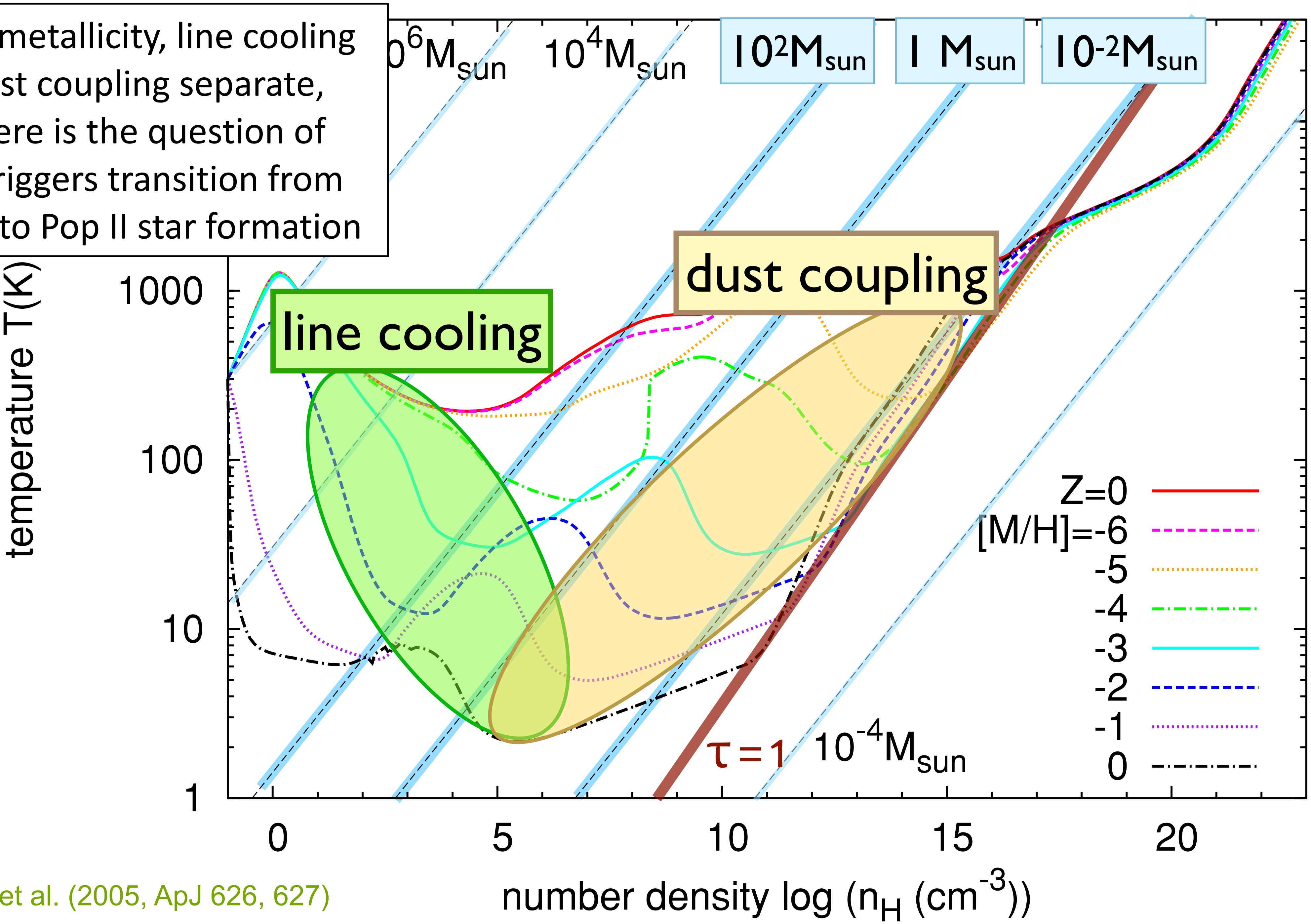


Omukai et al. (2005, ApJ 626, 627)

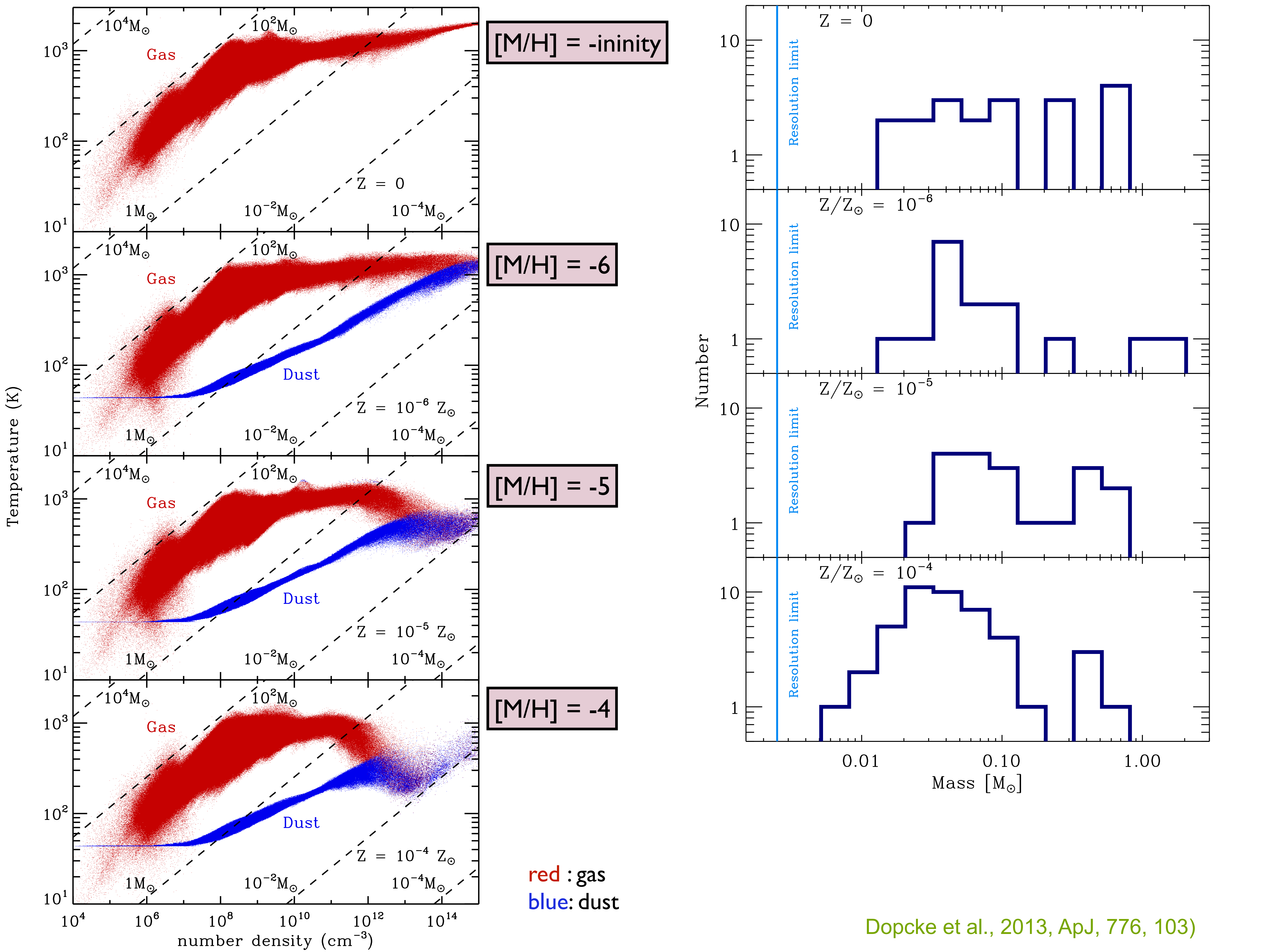


Dopcke et al., 2013, ApJ, 776, 103)

stellar mass spectrum

# transition from Pop III to Pop II star formation

UNIVERSITÄT HEIDELBERG
ZUKUNFT SEIT 1386

hints for changes in the mass spectrum in the metallicity range $10^{-4}$ — $10^{-5}$ $Z_{sun}$

driven by dust coupling

disk fragmentation mode

gravoturbulent fragmentation mode

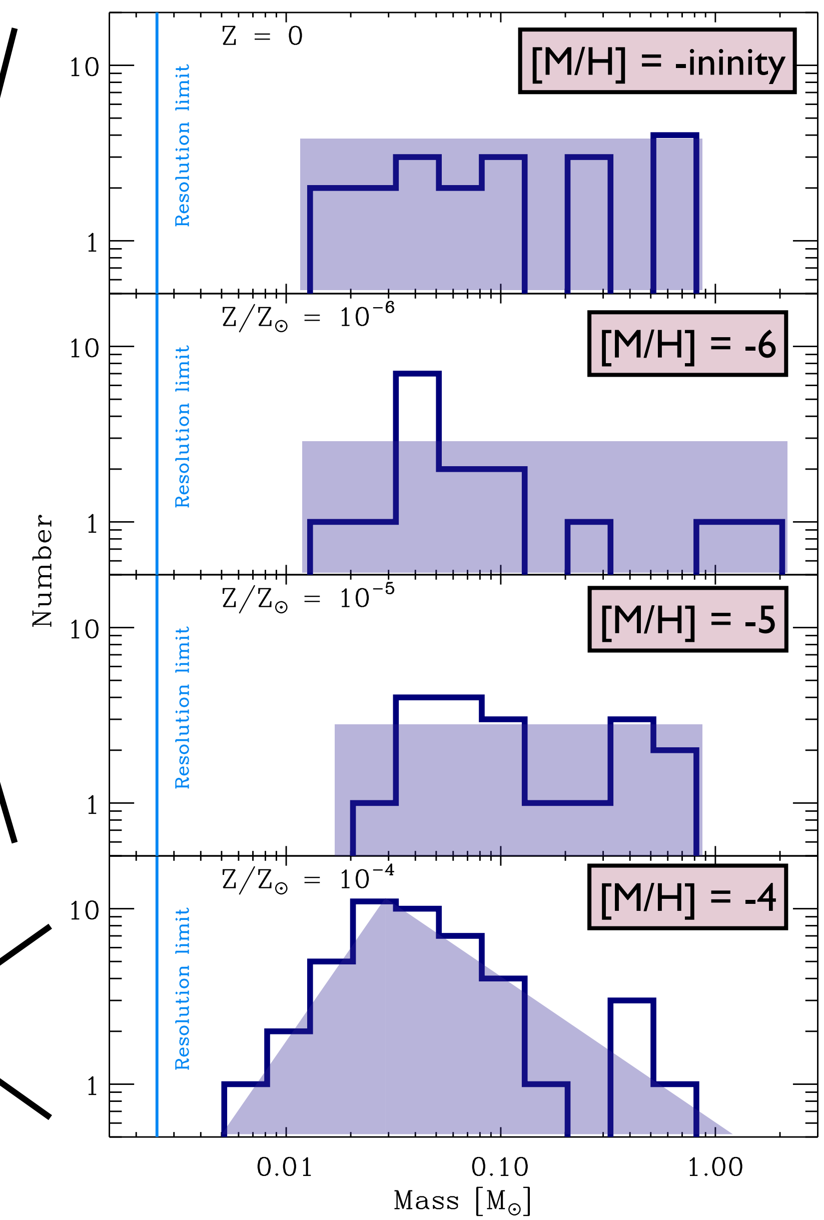


Caffau et al. (2011, Nature 477, 67), Schneider et al. (2006, MNRAS 369, 825), Schneider et al. (2012, MNRAS, 423, L60), Chiaki et al (2013, ApJ, 762, 50), Chiaki et al (2016, MNRAS, 463, 2781), Chon et al. (2021, MNRAS, 508, 4175)

Dopcke et al. (2013, ApJ, 776, 103)

# transition from Pop III to Pop II star formation

UNIVERSITÄT HEIDELBERG
ZUKUNFT SEIT 1386

hints for changes in the mass spectrum in the metallicity range $10^{-4}$ — $10^{-5}$ $Z_{sun}$

driven by dust coupling

BUT: depending on features you look at you may place transition to different Z

also stellar dynamical aspects and run-away collisions are important

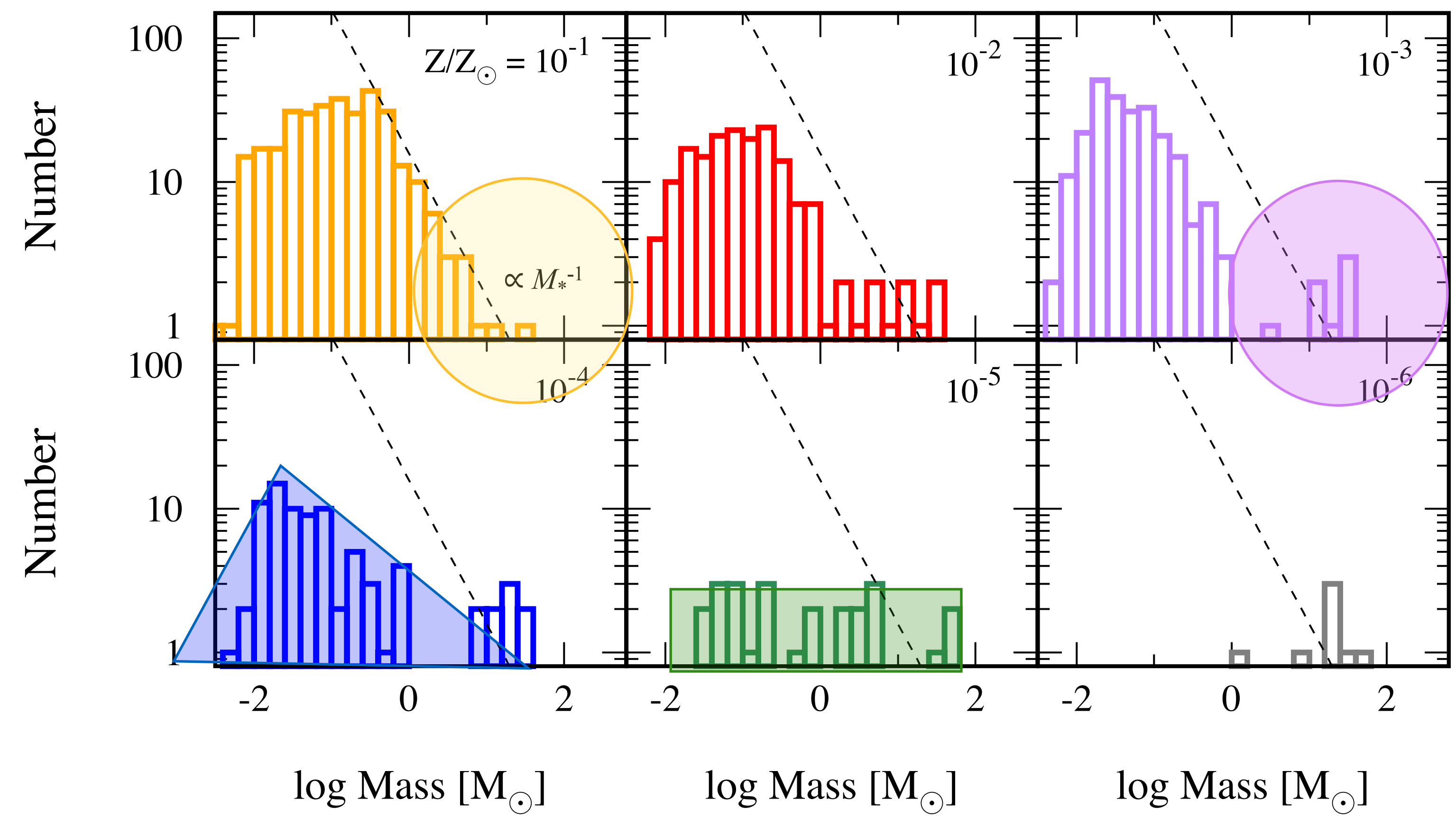


Caffau et al. (2011, Nature 477, 67), Schneider et al. (2006, MNRAS 369, 825), Schneider et al. (2012, MNRAS, 423, L60), Chiaki et al (2013, ApJ, 762, 50), Dopcke et al., 2013, ApJ, 776, 103), Chiaki et al (2016, MNRAS, 463, 2781)

Chon et al. (2021, MNRAS, 508, 4175)

stellar mass spectrum

# transition from Pop III to Pop II star formation

UNIVERSITÄT HEIDELBERG ZUKUNFT SEIT 1386

hints for changes in the mass spectrum in the metallicity range $10^{-4}$ — $10^{-5}$ $Z_{sun}$

driven by dust coupling

also stellar dynamical aspects and run-away collisions are important

- mass spectrum peaks *below 1* $M_{sun}$
- cluster VERY dense $n_{stars} = 2.5 \times 10^{9}\ pc^{-3}$
- fragmentation at density $n_{gas} = 10^{12} - 10^{13}\ cm^{-3}$

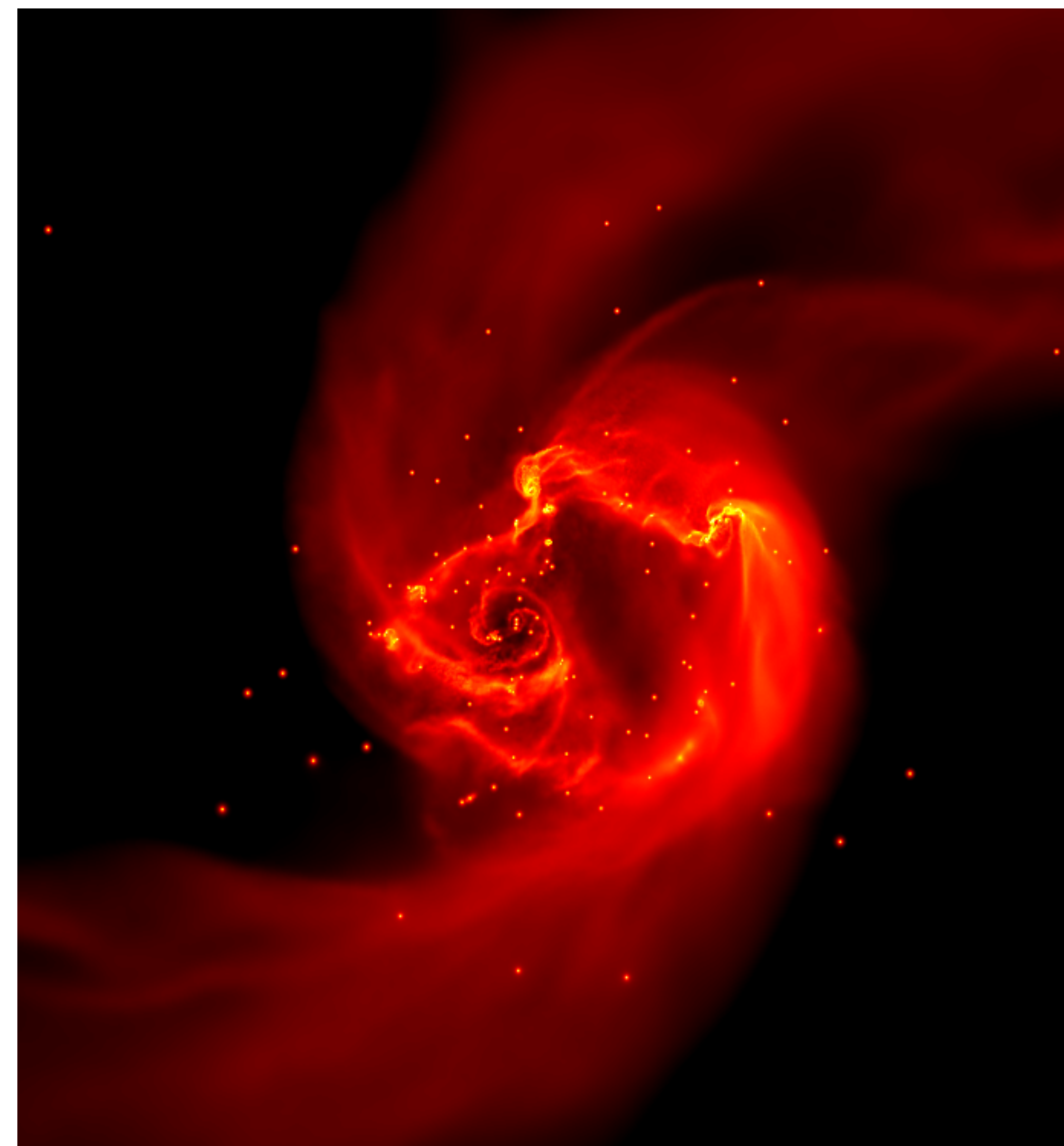

Clark et al. (2008, ApJ 672, 757)

# supermassive stars

Deutsche Forschungsgemeinschaft
DFG

ECOGAL
ERC Synergy Grant

erc
European Research Council

STRUCTURES
CLUSTER OF EXCELLENCE

UNIVERSITÄT HEIDELBERG
ZUKUNFT SEIT 1386

# critical halo mass for star formation

UNIVERSITÄT HEIDELBERG ZUKUNFT SEIT 1386

criteria for collapse and star formation

- look at competition between gravity (density $\rho$) and gas pressure (sound speed $c_s$ or temperature $T$): **Jeans mass**
- critical mass:

$$M_J = \frac{\pi^{5/2}}{6}\left(\frac{1}{G}\right)^{3/2}\rho^{-1/2}c_s^3 = \frac{\pi^{5/2}}{6}\left(\frac{k}{G}\right)^{3/2}\left(\frac{1}{\mu m_H}\right)^2 n^{-1/2}T^{3/2}$$

- $M_J$ goes up if T ↗ or ϱ ↘
  —> ***larger mass reservoir available in atomic cooling halos (as needed for SMS)***

- note: can be extended by considering effective sound speed
  $c_{s,eff}^2 = c_s^2 + \sigma^2$ with $\sigma = \sigma_{turb}$ or $\sigma = v_{Alfven}$
  —> ***higher masses favored in magnetized halos and in presence of high streaming velocity***

Jeans (1902, PTRS A, 199,1), Barkana & Loeb (2001, Phys. Rep. 349, 125), Glover (2013, ASSL, 396, 103), Klessen & Glover (2023, ARAA, 61, 65)

# atomic cooling halos

UNIVERSITÄT HEIDELBERG ZUKUNFT SEIT 1386

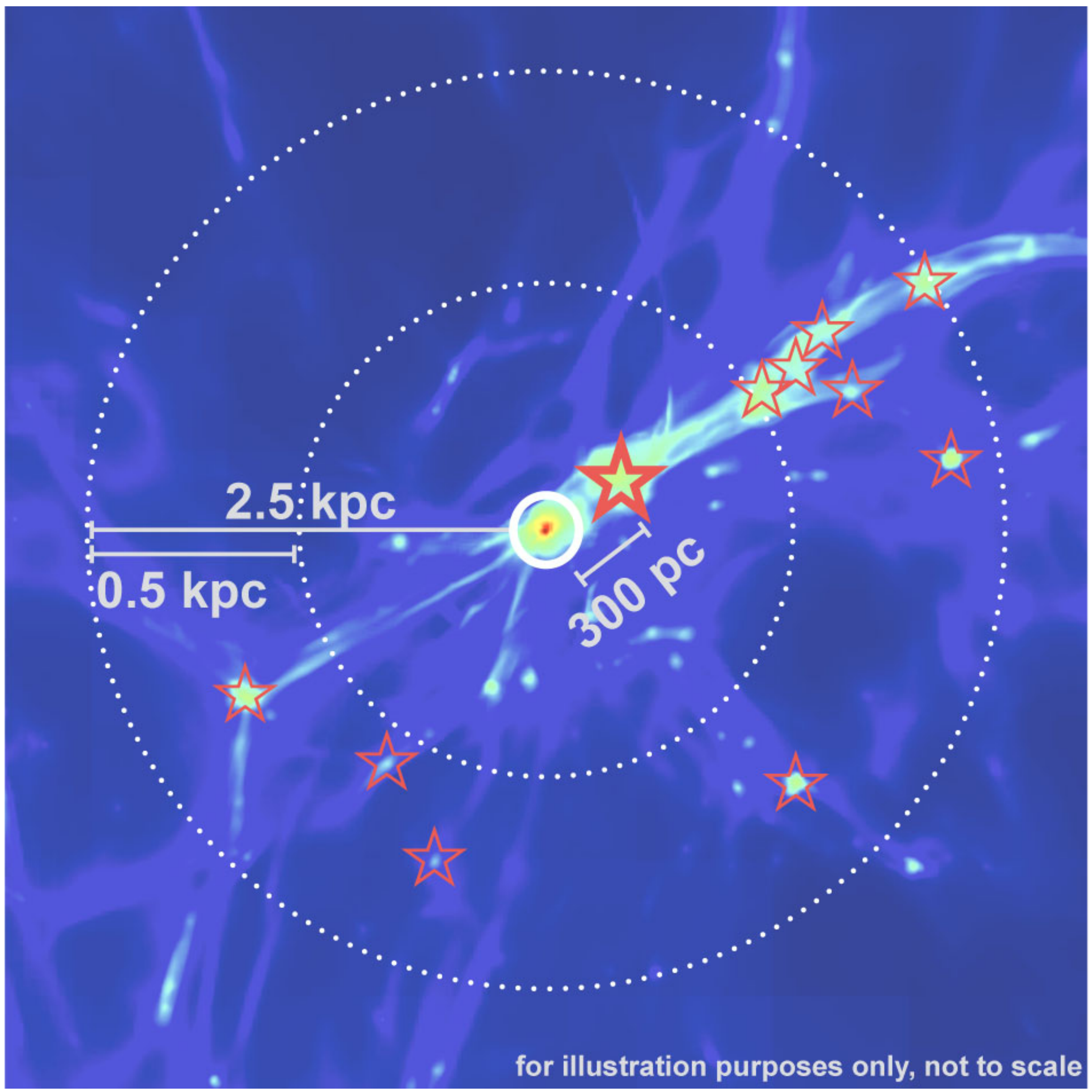


- halos come in groups
- some form Pop III stars earlier
- their LW/UV radiation prevents keeps neighboring halos in atomic phase —> ***not, no SF***
- need well tunes conditions: "*goldilock*" scenario
- these sit there and accumulate mass until they collapse in atomic phase —> ***SF***
- talks by John Regan, John Wise, Lewis Prole

Agarwal et al. (2016, MNRAS 470, 4034)

# impact of streaming velocity and LW background



UNIVERSITÄT HEIDELBERG
ZUKUNFT SEIT 1386

- streaming velocity and LW background can be included in early galaxy formation simulations

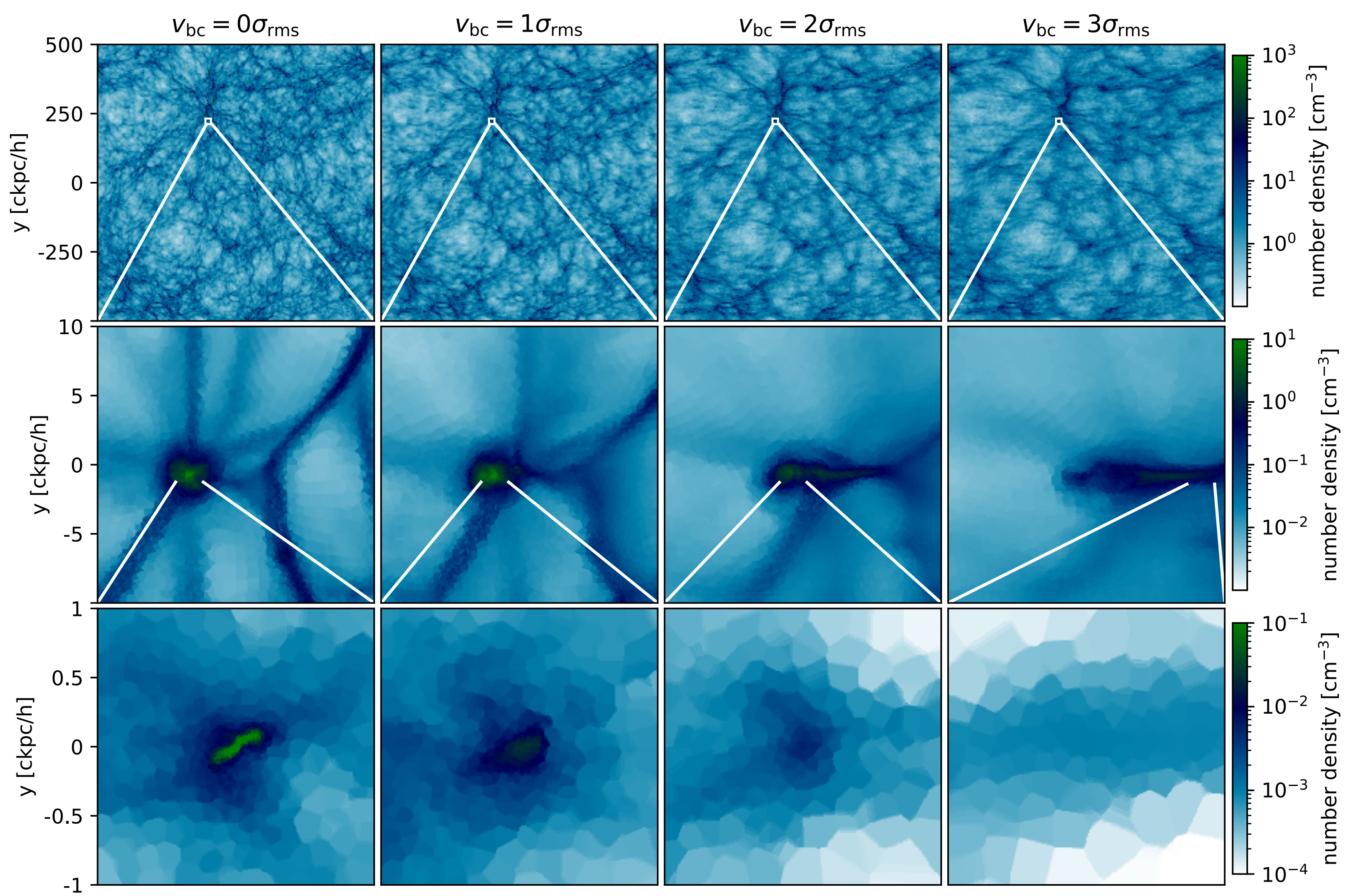


changing strength of streaming velocity

Schauer et al. (2021, MNRAS, 507, 1775)

# impact of streaming velocity and LW background

UNIVERSITÄT HEIDELBERG ZUKUNFT SEIT 1386

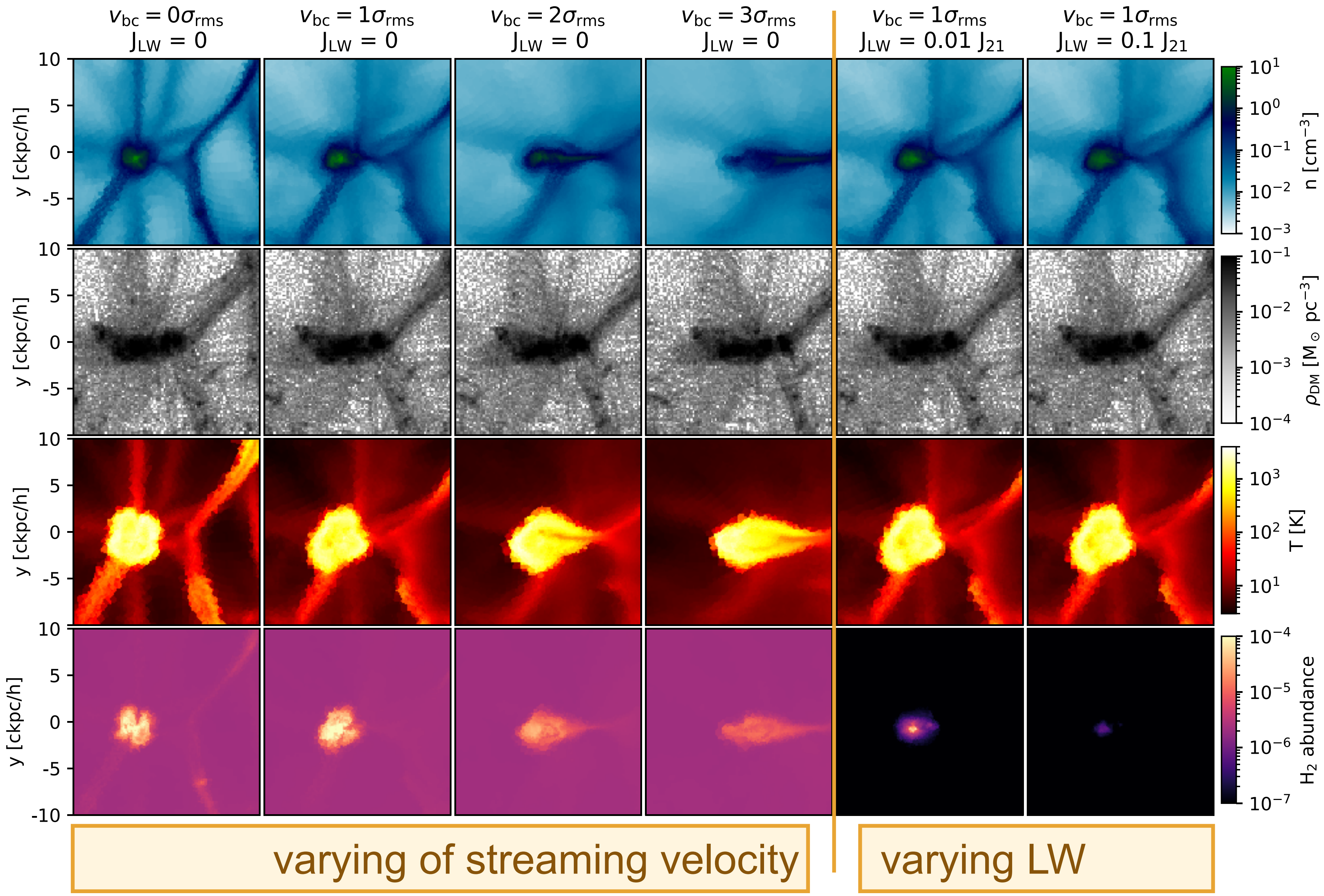


Schauer et al. (2021, MNRAS, 507, 1775)

# impact of streaming velocity and LW background

UNIVERSITÄT HEIDELBERG
ZUKUNFT SEIT 1386

- streaming velocity and LW background change critical mass for collapse

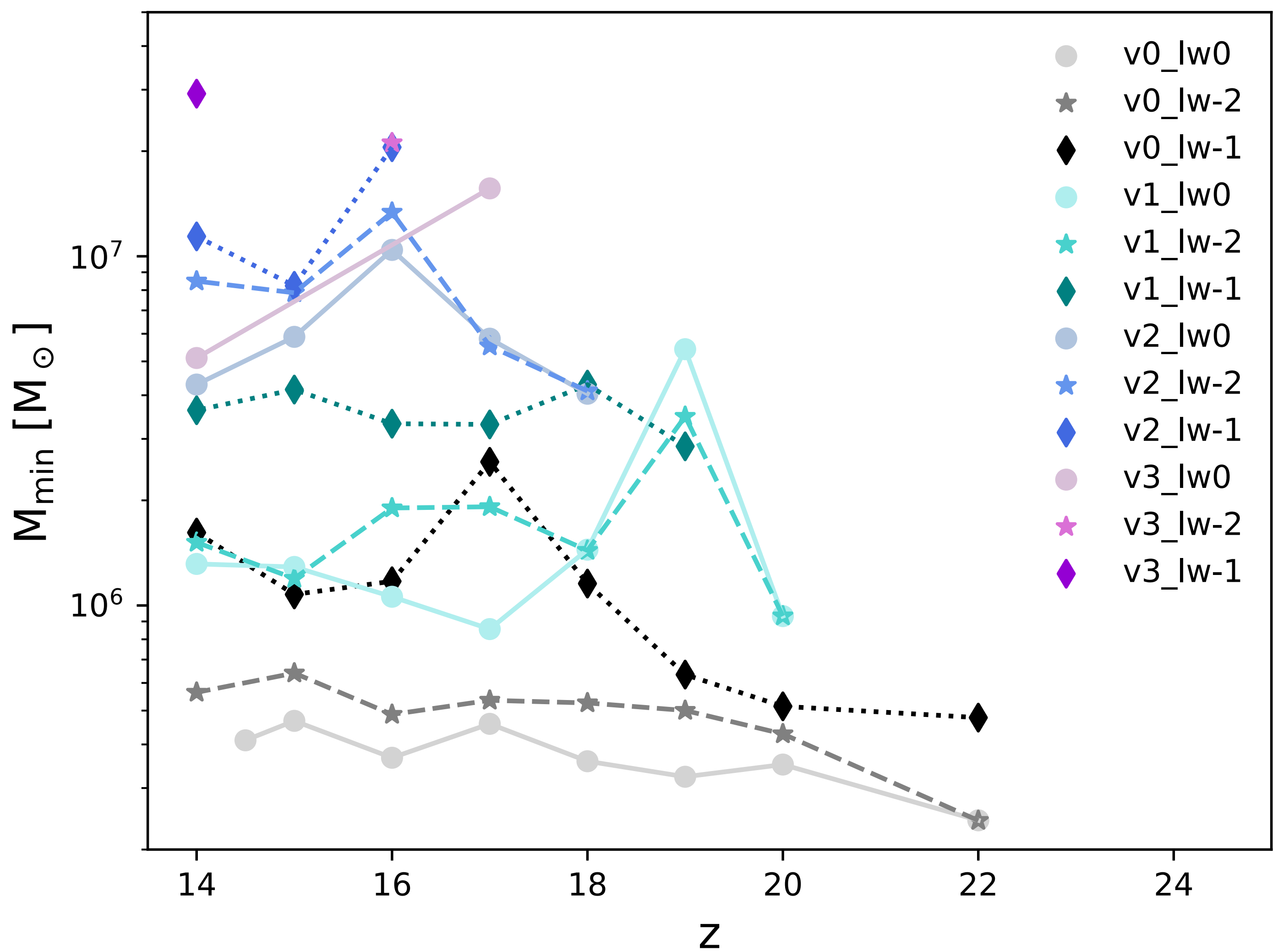


more streaming
higher $M_{crit}$

more LW
higher $M_{crit}$

minimum halo mass of star-forming halos at a given redshift depends on streaming and LW

Schauer et al. (2021, MNRAS, 507, 1775)

# impact of streaming velocity and LW background

UNIVERSITÄT HEIDELBERG
ZUKUNFT SEIT 1386

- analytic fit formula for $M_{crit}$ as function of sigma and $J_{21}$

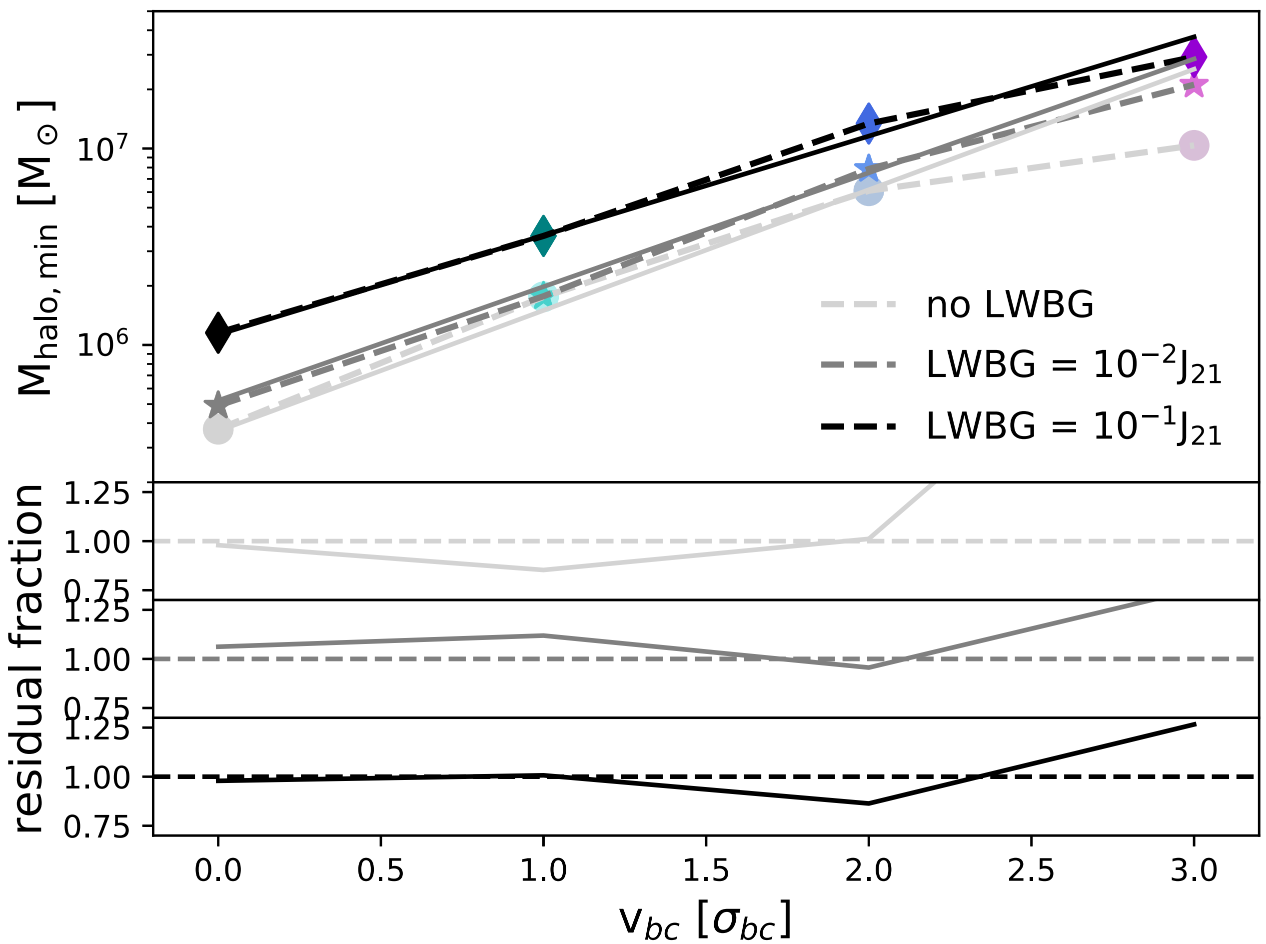


fit formula:

$$\log_{10} M_{\rm min} = \log_{10} M_0 + s \times \frac{v_{\rm bc}}{\sigma_{\rm rms}},$$

with

$$\log_{10} M_0 = 5.562 \times \left(1 + 0.279 \times \sqrt{J_{21}}\right),$$

and

$$s = 0.614 \times \left(1 - 0.560 \times \sqrt{J_{21}}\right).$$

this can be included as sub-grid estimate in numerical simulations or semi-analytic models

Schauer et al. (2021, MNRAS, 507, 1775)

# what is most likely streaming velocity?

UNIVERSITÄT HEIDELBERG
ZUKUNFT SEIT 1386

- distribution of streaming velocities

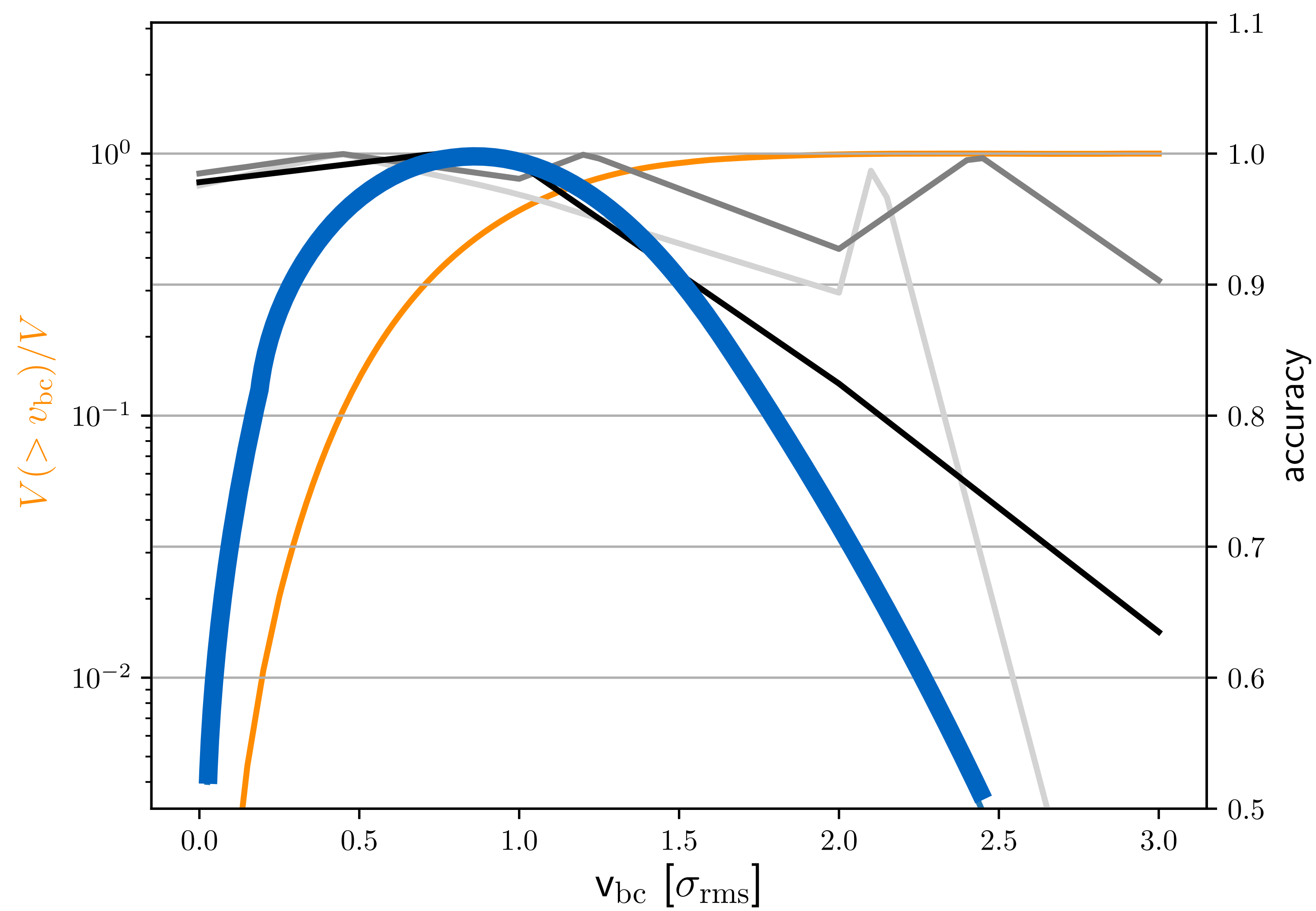


most likely streaming velocity is 0.8 $\sigma_{\rm rms}$

blue: differential

orange: cummulative

Schauer et al. (2021, MNRAS, 507, 1775)

# atomic cooling halos —> fragmentation!

fragmentation

UNIVERSITÄT HEIDELBERG
ZUKUNFT SEIT 1386

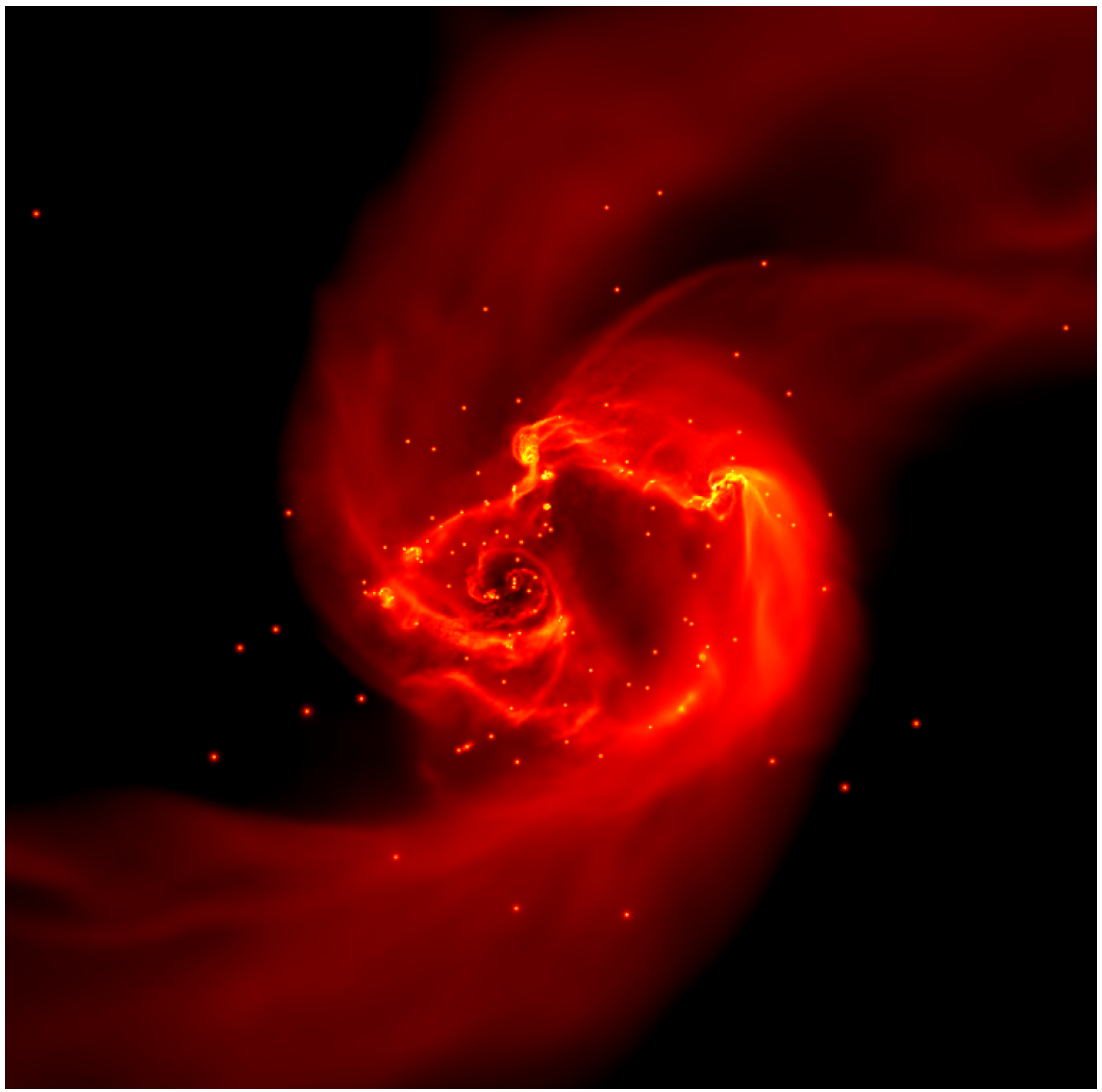

- halos come in groups
- some form Pop III stars earlier
- their LW/UV radiation prevents keeps neighboring halos in atomic phase —> ***not, no SF***
- these sit there and accumulate mass until they collapse in atomic phase —> ***SF***
- BUT: now rapid $H_2$ formation, and lots of fragmentation —> ***cluster of stars***
- again not good environment for direct collapse BH

Clark et al. (2008, ApJ 672, 757), Clark et al. (2011, ApJ, 727, 110)

# atomic cooling halos —> fragmentation!

UNIVERSITÄT HEIDELBERG
ZUKUNFT SEIT 1386

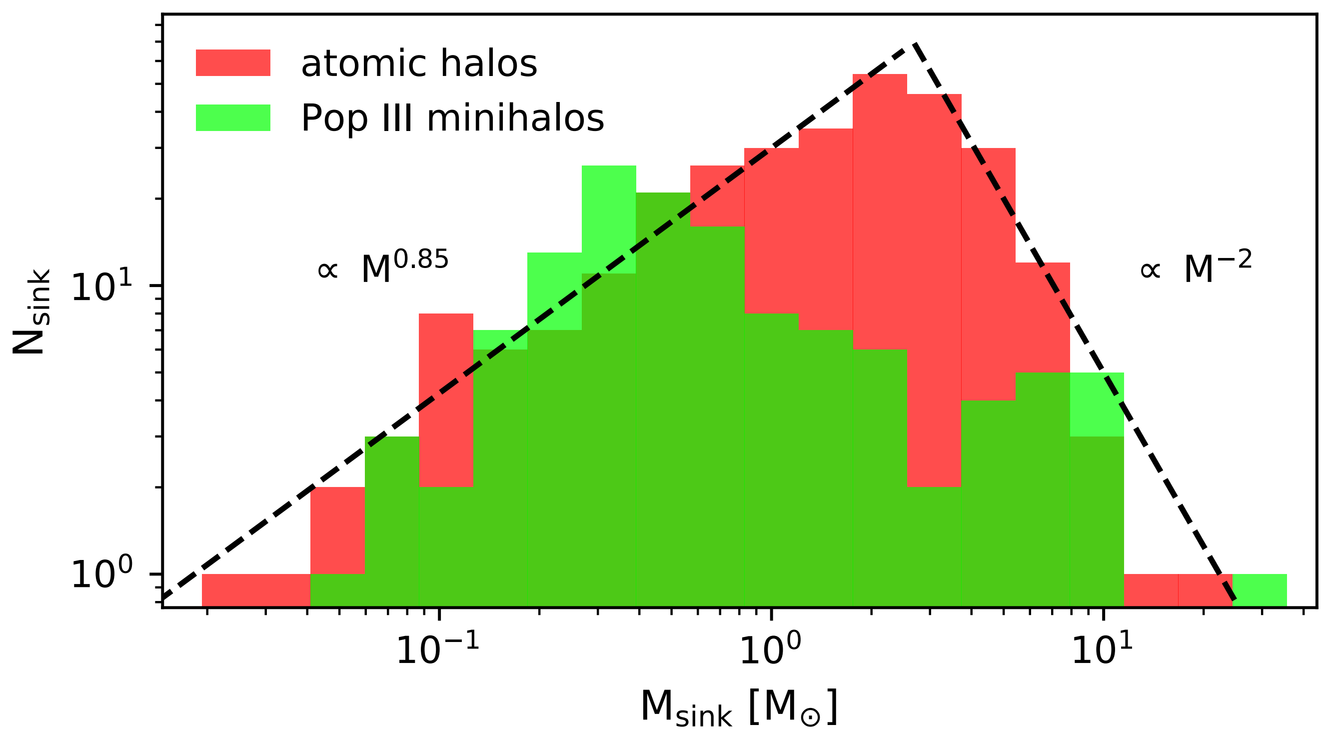


Fig. 9: Comparison of the sink particle mass function from the 3 atomic cooling halos at ~100 yr versus the 15 $H_2$ cooling minihalos from LP23 at ~300 yr. Power laws of $M^{0.85}$ and $M^{-2}$ are superimposed to give the reader an idea of the slopes involved.

- halos come in groups
- some form Pop III stars earlier
- their LW/UV radiation prevents keeps neighboring halos in atomic phase —> ***not, no SF***
- these sit there and accumulate mass until they collapse in atomic phase —> ***SF***
- BUT: now rapid $H_2$ formation, and lots of fragmentation —> ***cluster of stars***
- again not good environment for direct collapse BH

Clark et al. (2008, ApJ 672, 757), Clark et al. (2011, ApJ, 727, 110), Prole et al. (2024, in press)

# not just large mass reservoir, SMS also need dM/dt

UNIVERSITÄT
HEIDELBERG
ZUKUNFT
SEIT 1386

some theory

what is the resulting accretion rate?

- simple isothermal models give $\dot{M} = m_0\, c_s^3 / G$ (see e.g. Shu 1977)
- ***so again*** $\dot{M}$ ***↗ if T ↗***

- BUT: recall there is also the *multiplication factor* $m_0 \propto A^{3/2}$ with $A \propto N_J^{2/3}$ so that $m_0 \propto N_J$ with $N_J$ number of Jeans masses (Girichidis et al. 2011)

- ***also:*** $\dot{M}$ ***↗ in collisions of two halos or two proto-galaxies*** (e.g. Mayer et al. 2010, Lorenz Zwick's talk)

- again high degree of turbulence will lead to ***fragmentation***

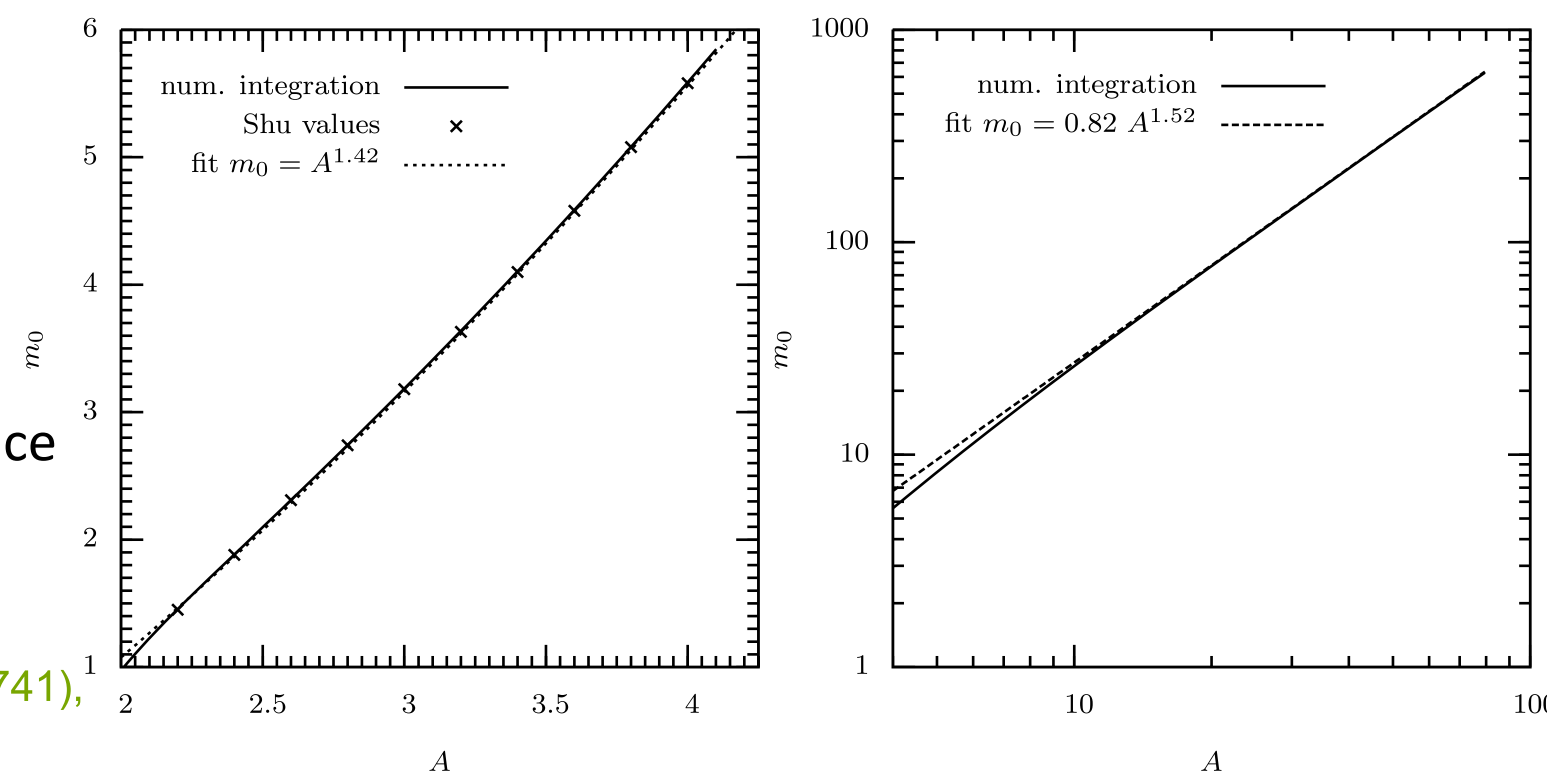



Shu (1977, ApJ, 214, 488),
Girichidis et al. (2011, MNRAS, 413, 2741),
Mayer et al. (2010, Nature, 466, 108)

# stellar evolution with different dM/dt

UNIVERSITÄT HEIDELBERG
ZUKUNFT SEIT 1386

How do stars evolve for different accretion rates?

- for $\dot{M} \geq 0.1 \mathrm{M}_{\odot}/\mathrm{yr}$ stars evolve with bloated radii
- see also Devesh Nandal's talk!

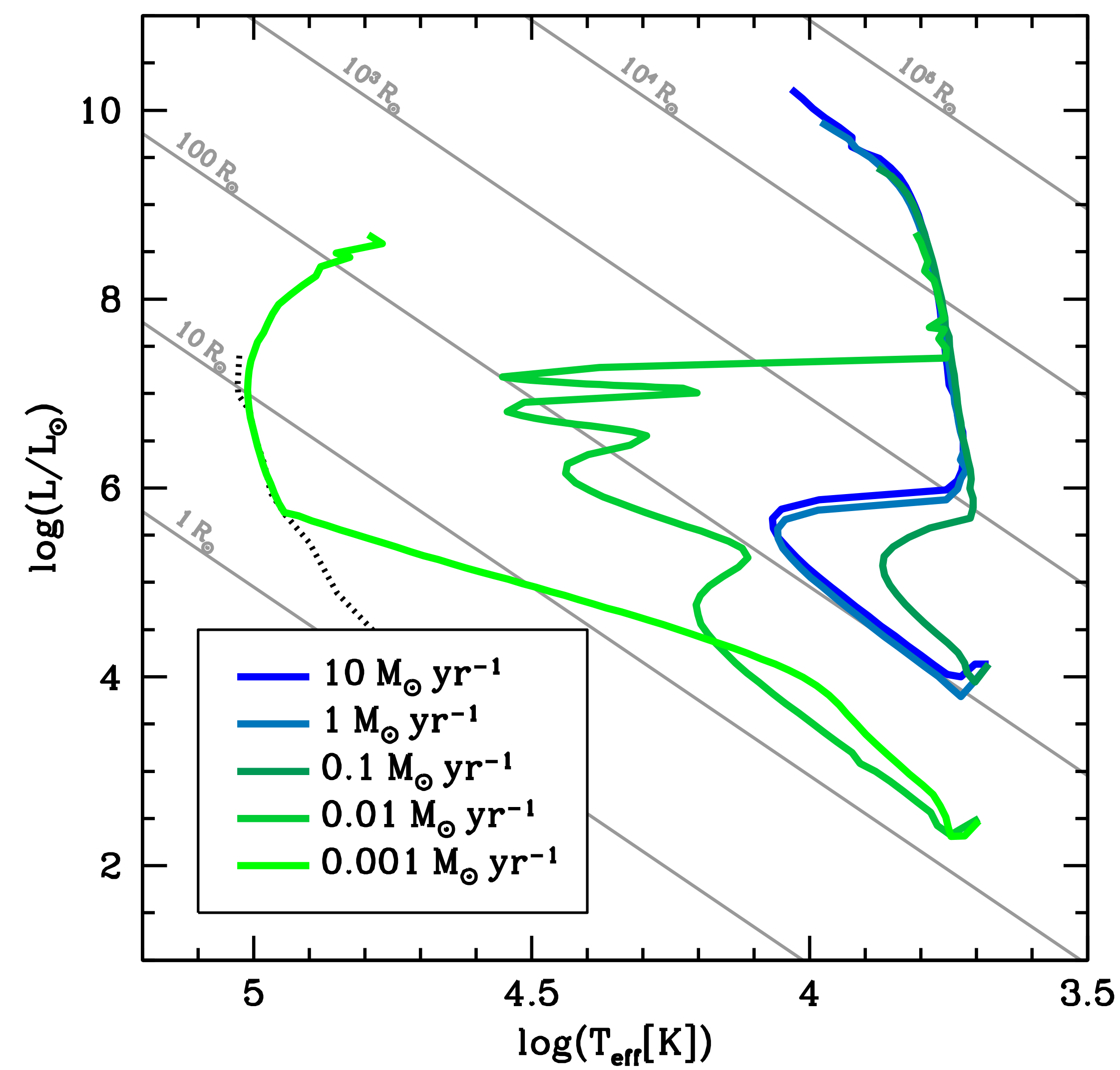


**Figure 1.** Evolutionary tracks on the HR diagram for the models at the indicated accretion rates. The grey straight lines indicate the stellar radius, and the black dotted curve is the ZAMS of Schaerer (2002).

Haemmerlé et al. (2018, MNRAS 474, 2757)
see also Hosokawa et al. (2012, ApJ, 756, 93),

some further theory

# stellar evolution with different dM/dt

UNIVERSITÄT HEIDELBERG ZUKUNFT SEIT 1386

How do stars evolve for different accretion rates?

- for $\dot{M} \geq 0.1 \mathrm{M}_{\odot}/\mathrm{yr}$ stars evolve with bloated radii

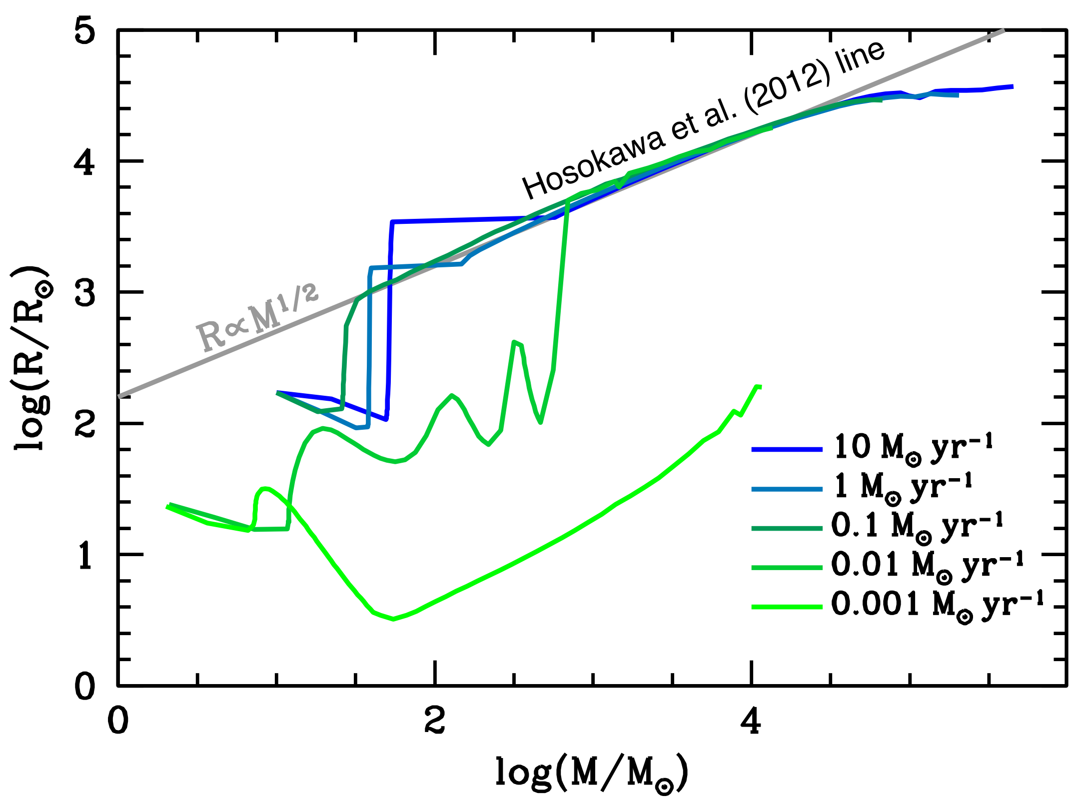


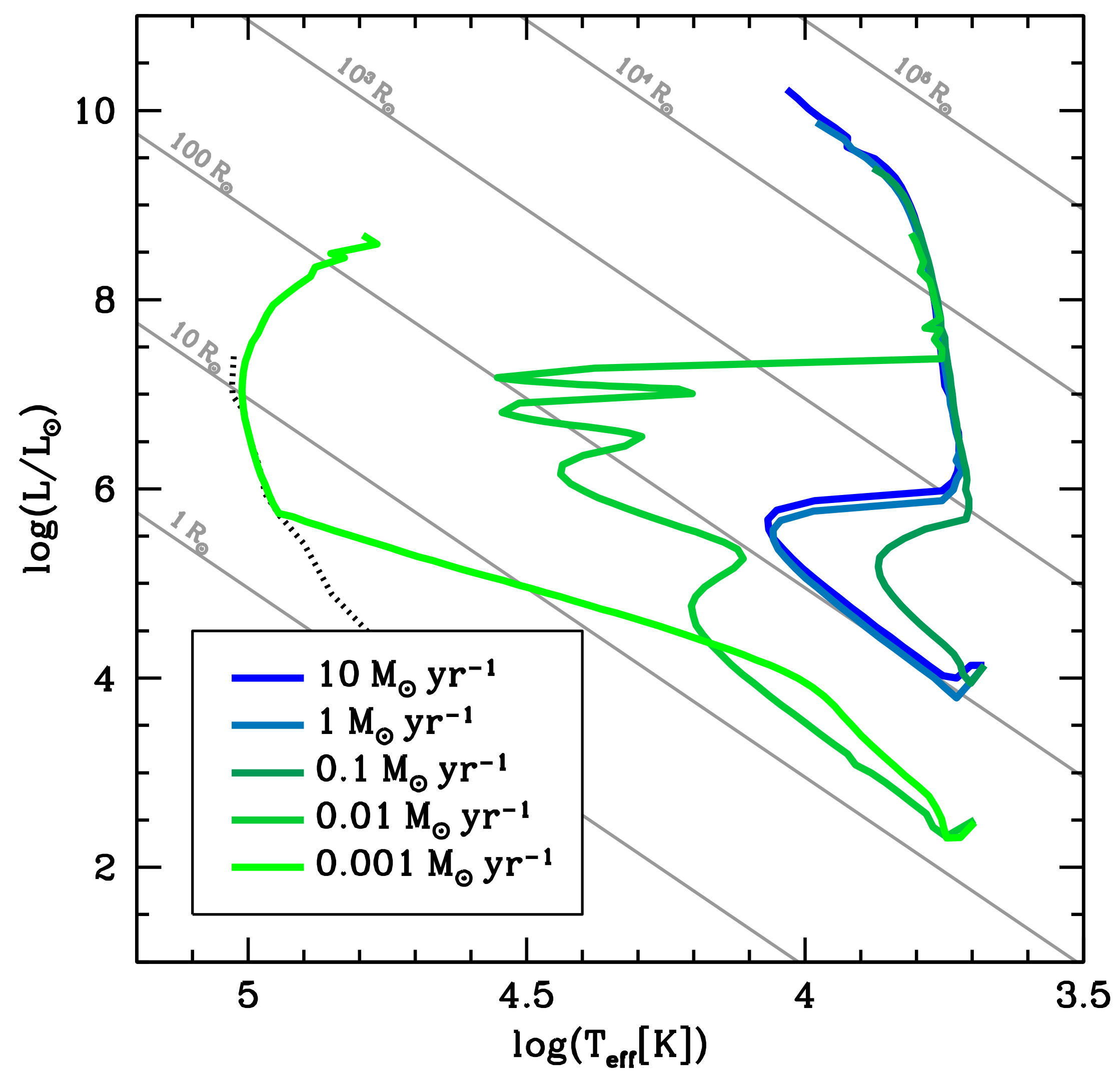


Haemmerlé et al. (2018, MNRAS 474, 2757)
see also Hosokawa et al. (2012, ApJ, 756, 93),

**Figure 1.** Evolutionary tracks on the HR diagram for the models at the indicated accretion rates. The grey straight lines indicate the stellar radius, and the black dotted curve is the ZAMS of Schaerer (2002).

some further theory

# stellar evolution with different dM/dt

How do stars evolve for different accretion rates?

- for $\dot{M} \geq 0.1 \mathrm{M}_{\odot}/\mathrm{yr}$ stars evolve with bloated radii
- different stellar structure for different $\dot{M}$

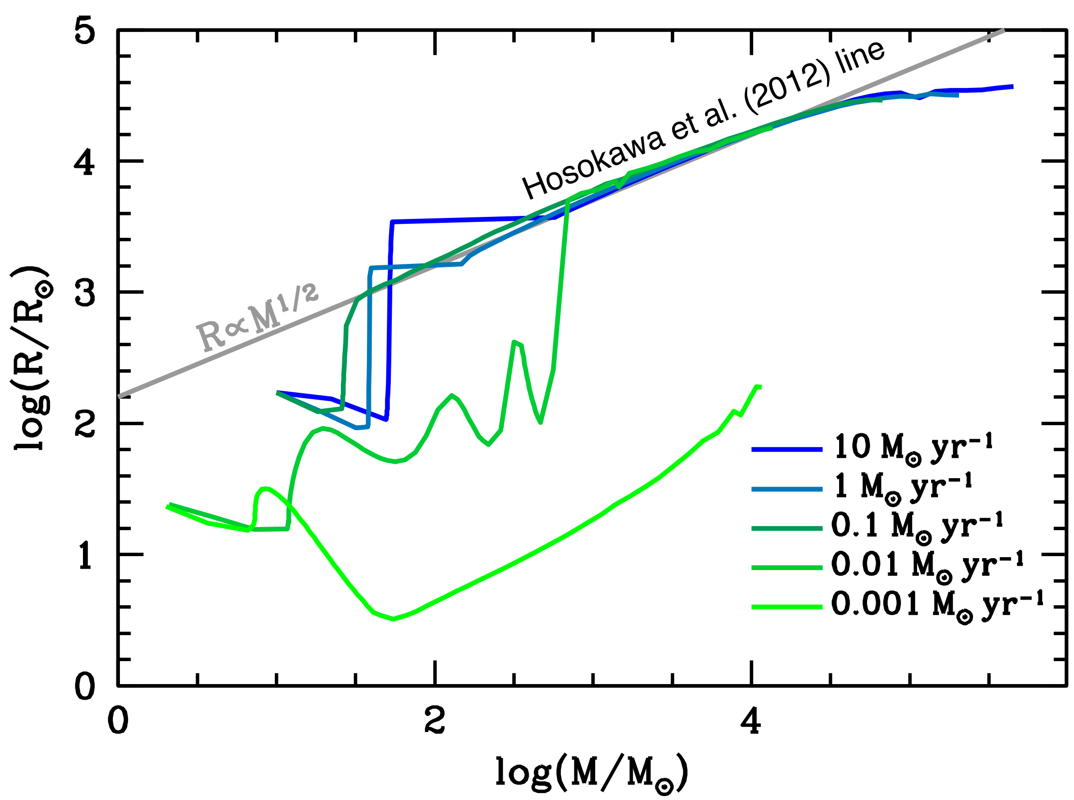


Haemmerlé et al. (2018, MNRAS 474, 2757)
see also Hosokawa et al. (2012, ApJ, 756, 93),

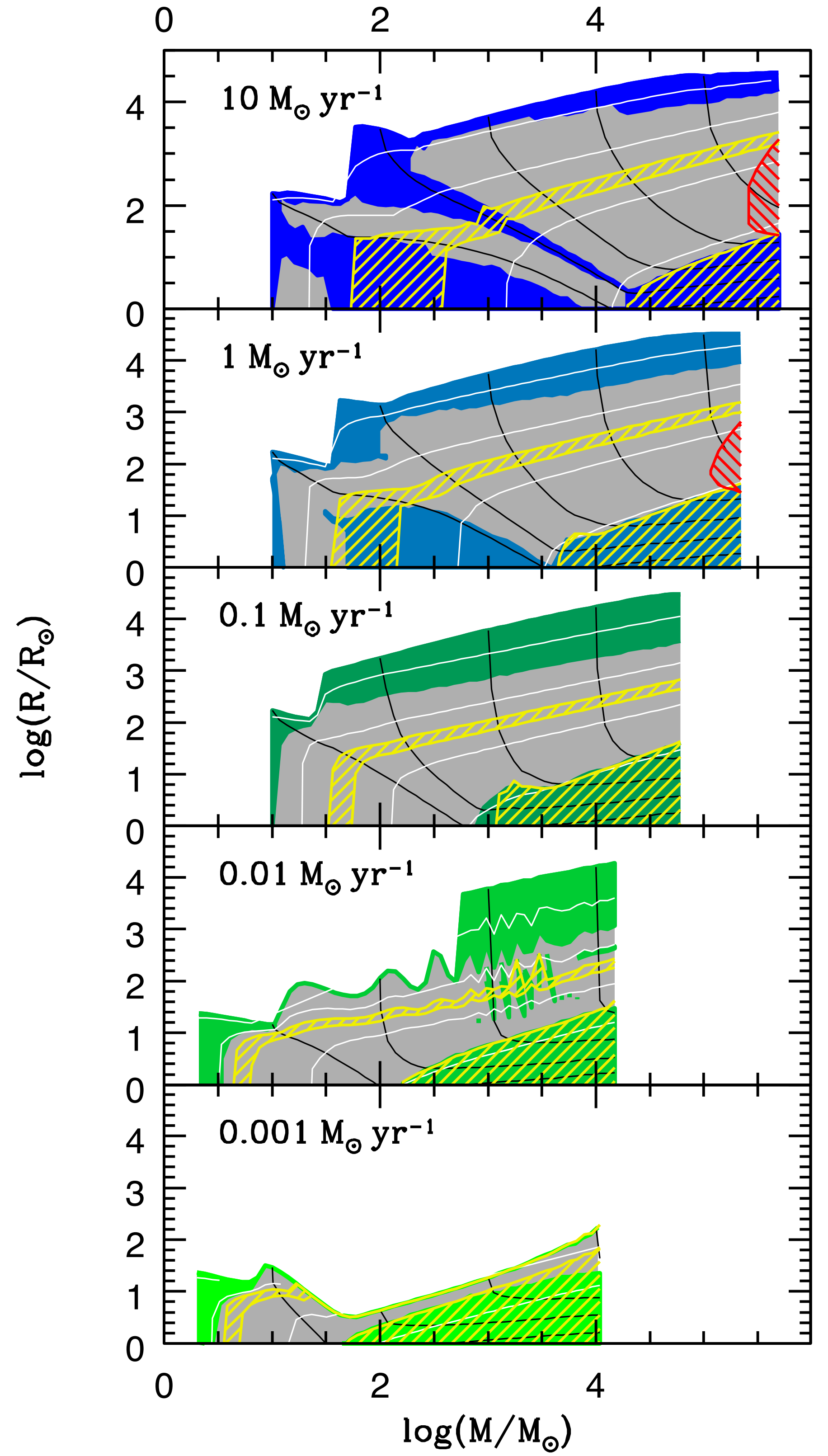


**Figure 2.** Internal structures of the models for the indicated accretion rates. In each panel, the upper curve is the stellar radius, the blue and green areas indicate convective zones, and the grey areas indicate radiative transport. The yellow hatched areas correspond to D- and H-burning, and the red hatched areas indicate the GR instability according to the polytropic criterion of equation (7) with $n = 3$. The black curves indicate the Lagrangian layers of $\log(M_r/\mathrm{M}_{\odot}) = 1, 2, 3, 4$ and 5, and the white ones are isotherms of $\log(T\,[\mathrm{K}]) = 5, 6, 7$ and 8.

some further theory

# stellar evolution with different dM/dt

How do stars evolve for different accretion rates?

- for $\dot{M} \geq 0.1 \mathrm{M}_\odot/\mathrm{yr}$ stars evolve with bloated radii
- different stellar structure for different $\dot{M}$
- for large $\dot{M}$ starts evolve until GR instability sets in

pathway to supermassive stars!

Haemmerlé et al. (2018, MNRAS 474, 2757)
see also Hosokawa et al. (2012, ApJ, 756, 93),

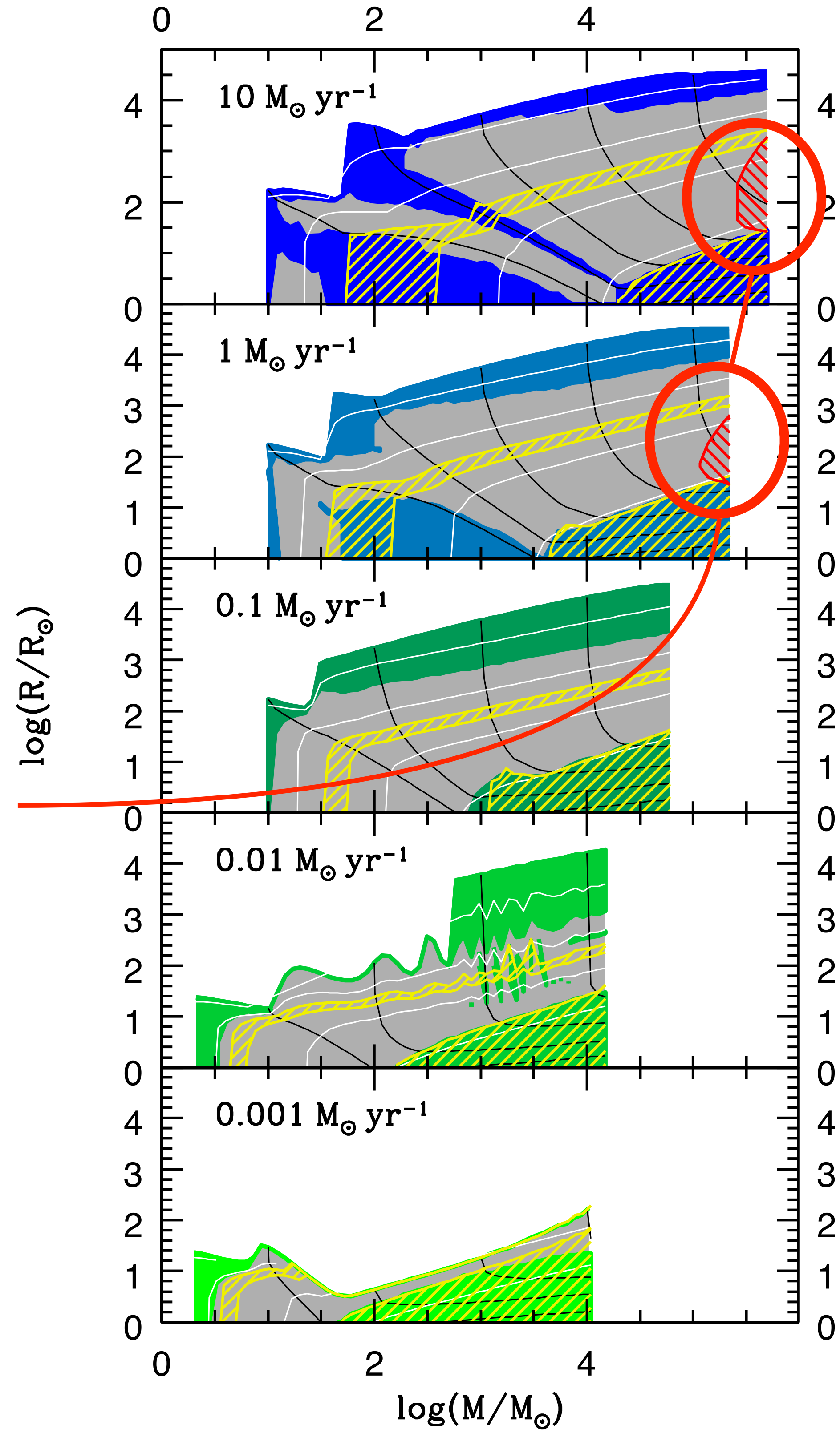


**Figure 2.** Internal structures of the models for the indicated accretion rates. In each panel, the upper curve is the stellar radius, the blue and green areas indicate convective zones, and the grey areas indicate radiative transport. The yellow hatched areas correspond to D- and H-burning, and the red hatched areas indicate the GR instability according to the polytropic criterion of equation (7) with $n = 3$. The black curves indicate the Lagrangian layers of $\log(M_r/\mathrm{M}_\odot) = 1, 2, 3, 4$ and 5, and the white ones are isotherms of $\log(T\,[\mathrm{K}]) = 5, 6, 7$ and 8.

some further theory

UNIVERSITÄT HEIDELBERG
ZUKUNFT SEIT 1386

# stellar evolution with different dM/dt

How do stars evolve for different accretion rates?

- for $\dot{M} \geq 0.1 \mathrm{M}_{\odot}/\mathrm{yr}$ stars evolve with bloated radii
- different stellar structure for different $\dot{M}$
- for large $\dot{M}$ starts evolve until GR instability sets in

pathway to supermassive stars!

- BUT: results *depend very strongly* on *numerical details* (example here: mass/resolution of outermost layer)

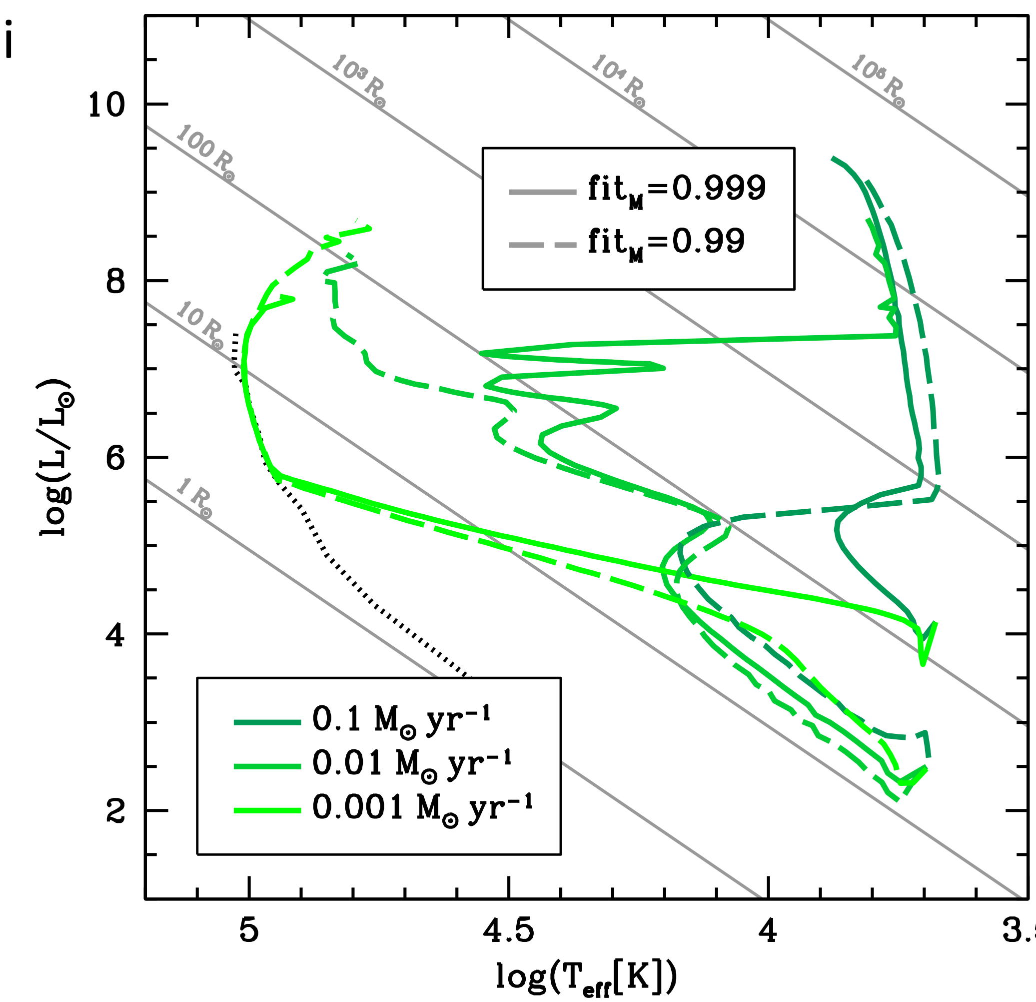


**Figure 9.** Evolutionary tracks of the models for the indicated accretion rates, for $\mathrm{fit}_M = 0.999$ (solid lines) and 0.99 (dashed lines). The grey straight lines indicate the stellar radius, and the black dotted curve is the ZAMS of Schaerer (2002).

Haemmerlé et al. (2018, MNRAS 474, 2757)
see also Hosokawa et al. (2012, ApJ, 756, 93),

supermassive stars

# what is the maximum stellar mass possible?

UNIVERSITÄT HEIDELBERG
ZUKUNFT SEIT 1386

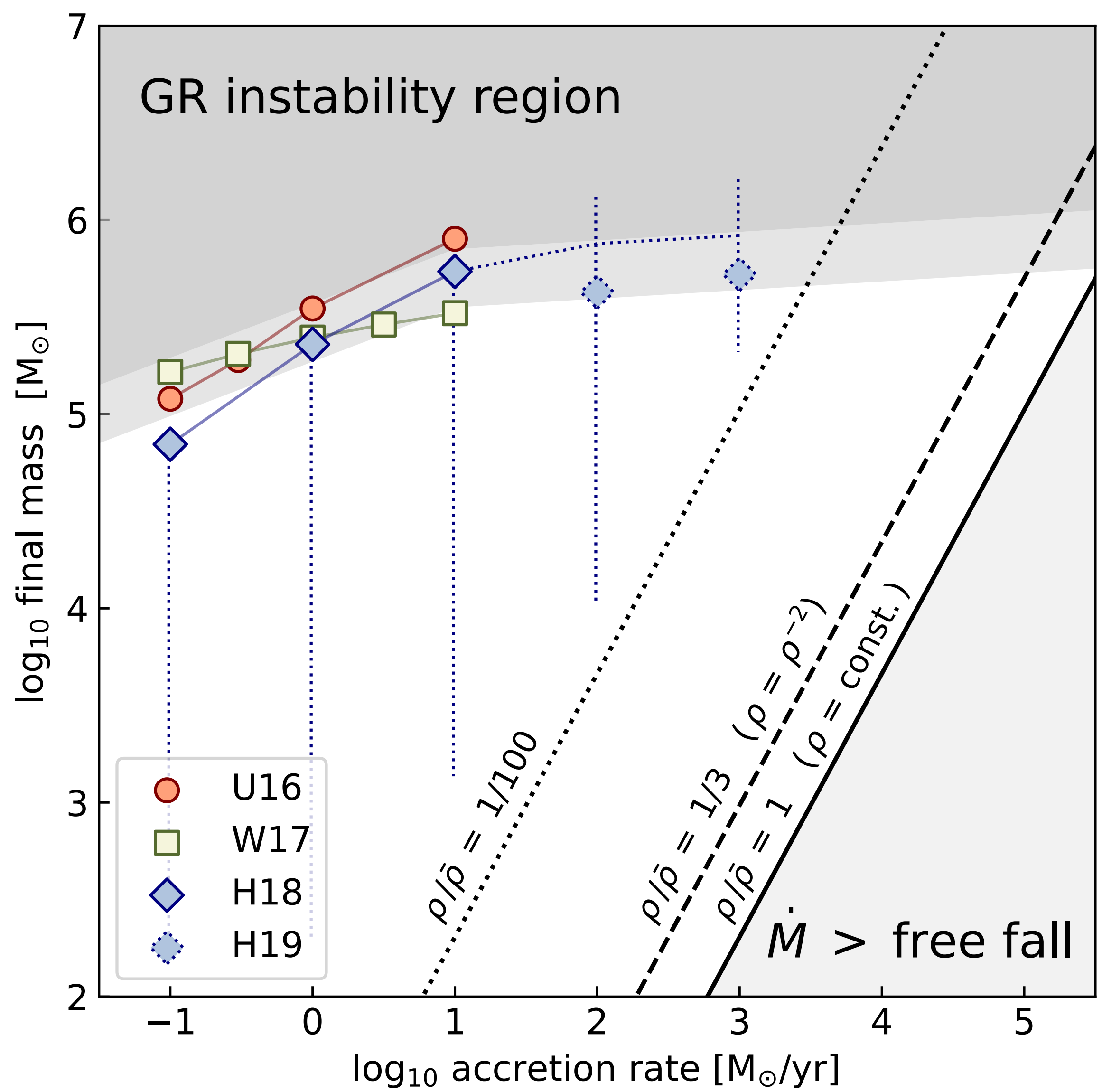


- for accretion rate above 0.1 M☉/yr, stars can easily reach several $10^5$ M☉ before GR instability kicks in
- then they collapse directly into a black hole of the same mass
- while accreting the stars are extremely puffed up and cold (3000 - 4000 K)
- no ionizing radiation: hard to see, little impact

Haemmerlé (2020, A&A 644, A154)
Haemmerlé (2021a. A&A 647, A83)
Haemmerlé (2021b. A&A 650, A204)

Umeda et al. (2016, ApJ, 830, L34),
Woods et al. (2017. ApJ, 842, L6),
Haemmerlé et al. (2018. MNRAS, 474, 2757)

image from Klessen, & Glover (2023, ARAA, 61, 65)

# we face a dilemma!

UNIVERSITÄT HEIDELBERG ZUKUNFT SEIT 1386

to form SMS, we need

***(1)*** a sufficiently large mass reservoir ($M_{\rm gas} \sim 10^6 {\rm M}_\odot$)

***(2)*** maintain $\dot{M} \geq 0.1 {\rm M}_\odot/{\rm yr}$ for a sufficiently long time

then can reach masses above $10^5 {\rm M}_\odot$ before the GR instability kicks in an they collapse into a BH…

BUT:

***(3)*** gas under this conditions will fragment!

***WHAT IS THE WAY OUT?***

image from Klessen, & Glover (2023, ARAA, 61, 65)

dilemma

# (proto)stellar clusters !!

solution

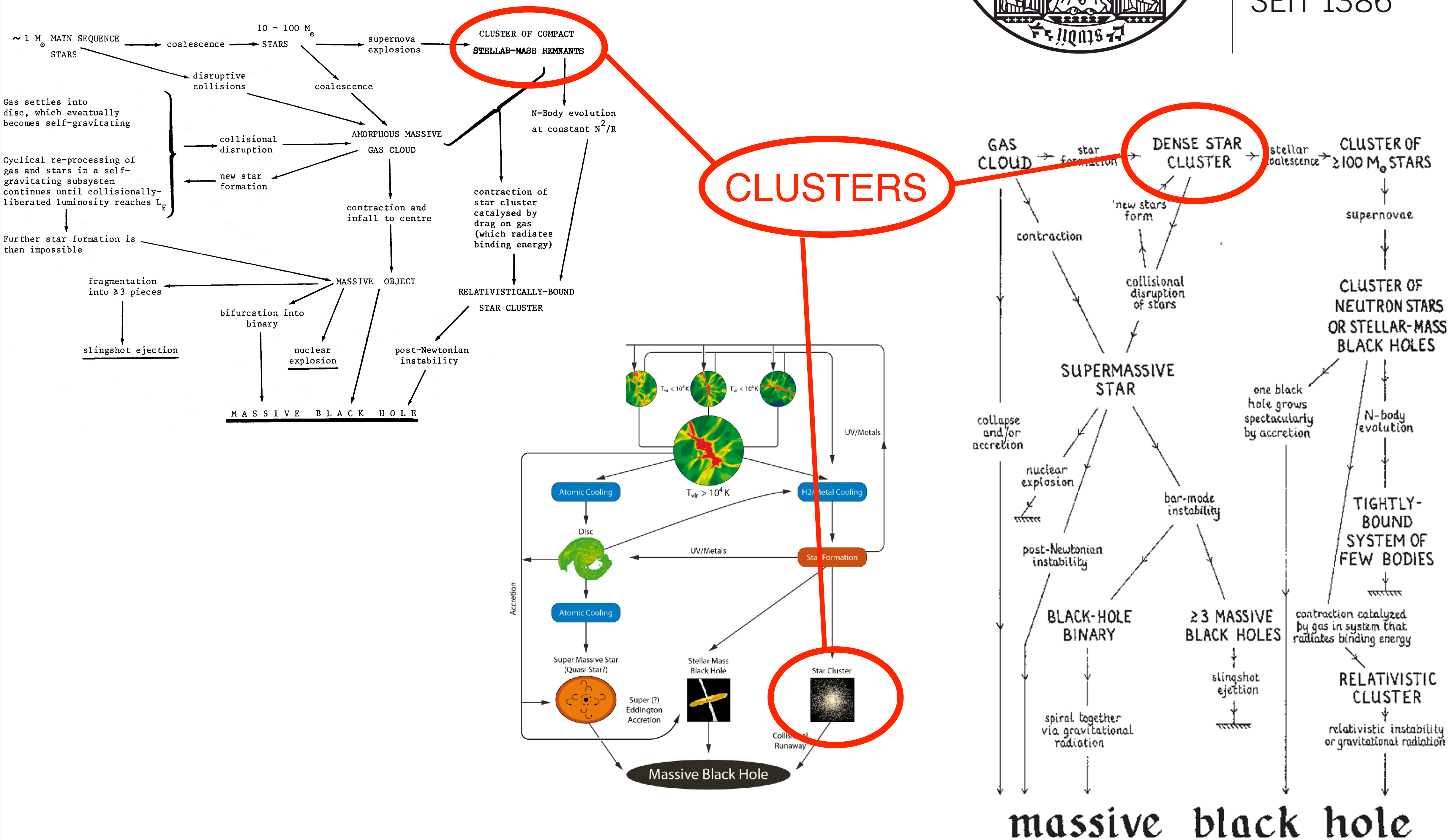


Begelman & Rees (1978, MNRAS, 185, 847), Rees (1984, ARA&A, 22, 471),
Regan & Haehnelt (2009, MNRAS, 396, 343), Woods et al. (2019, PASA, 36, e027)

supermassive stars

# how to form seeds of supermassive BHs?

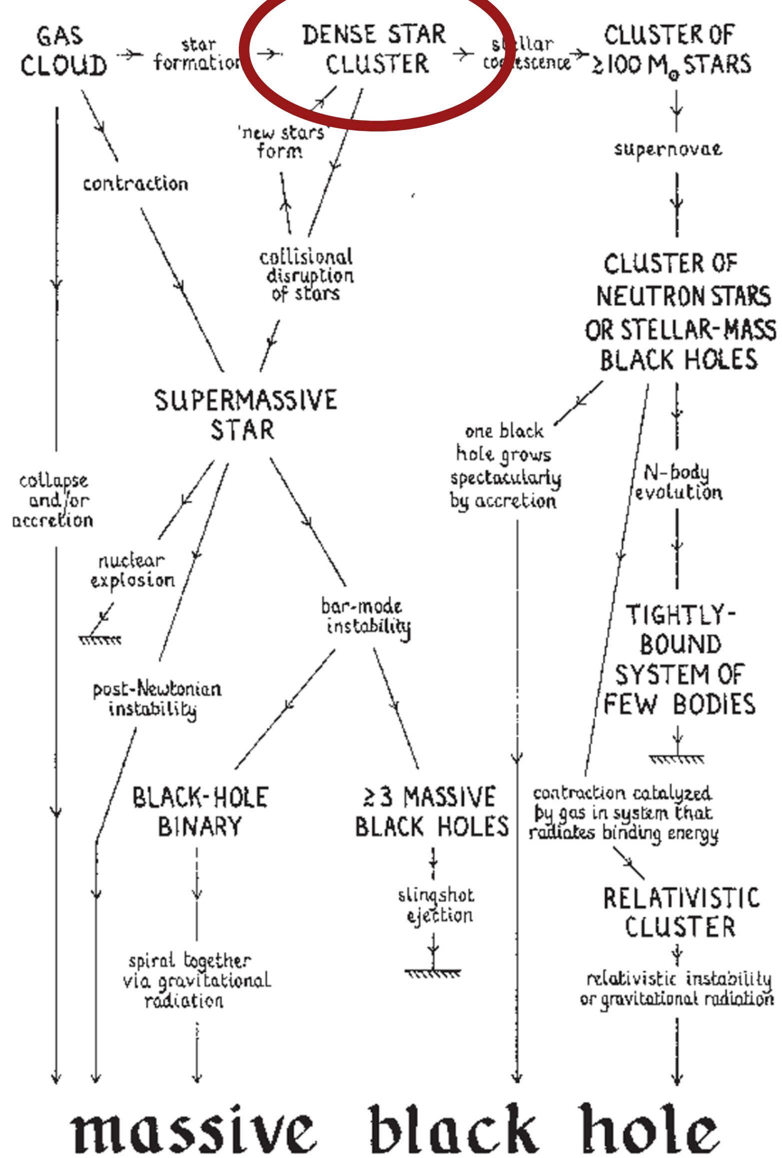


**Figure 1.** Original diagram from Rees (1978, 1984), outlining the possible formation pathways for supermassive black holes. In this review, as in the conference, our focus is on the left side of the diagram.

importance of run-away collisions and mergers in dense clusters

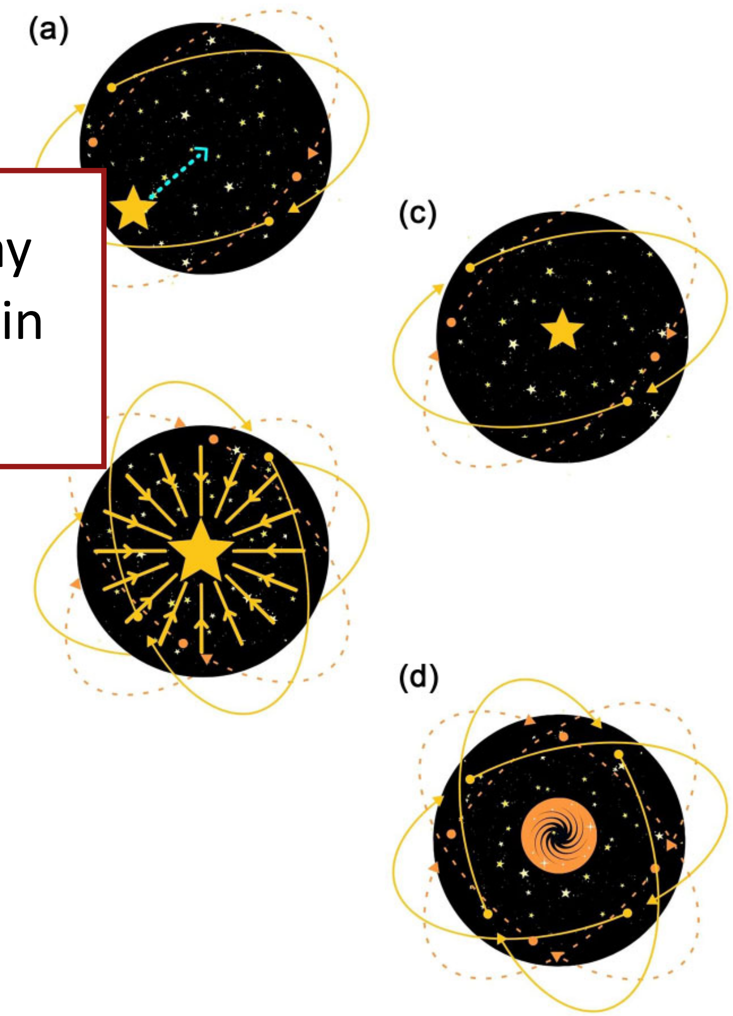


**Figure 1.** A sketch of the expected evolution of the stellar cluster and its central massive object. (a–b) The most massive star falls to the centre as a result of dynamical friction. (c) The most massive star in the centre accretes material through stellar collisions and from the gas. (d) The supermassive star collapses into a very massive black hole.

Rees (1984, ARA&A, 22, 471)
Woods et al. (2019, PASA, 36, e027)

Schleicher et al. (2022, MNRAS, 512, 6192)

# how to form seeds of supermassive BHs?

UNIVERSITÄT
HEIDELBERG
ZUKUNFT
SEIT 1386

clusters that form in massive and very dense gas clouds have

***(1)*** a sufficiently large mass reservoir ($M_{\rm gas} \sim 10^6 {\rm M}_\odot$)

***(2)*** individual stars have high accretion rates and evolve along large-R tracks

result is

***(3)*** combination of high stellar density and large stellar radii results in large collision rates

***(4)*** together this results in ***run-away mass growth*** of 1 or 2 objects to build SMS

Reinoso et al. (2018, A&A, 614, A14), Boekhold et al. (2018, MNRAS, 476, 366), Alister Seguel et al. (2020, MNRAS, 493, 2352), Reinoso et al. (2020, A&A, 639, A92), Vergara et al. (2021, A&A, 649, A160), Schleicher et al. (2022, MNRAS, 512, 6192), Reinoso et al. (2023, MNRAS, 521, 3553), Schleicher et al. (2023, MNRAS, 521, 3972)

run-away collisions

# how to form seeds of supermassive BHs?

UNIVERSITÄT
HEIDELBERG
ZUKUNFT
SEIT 1386

example of $10^4 M_\odot$ cloud

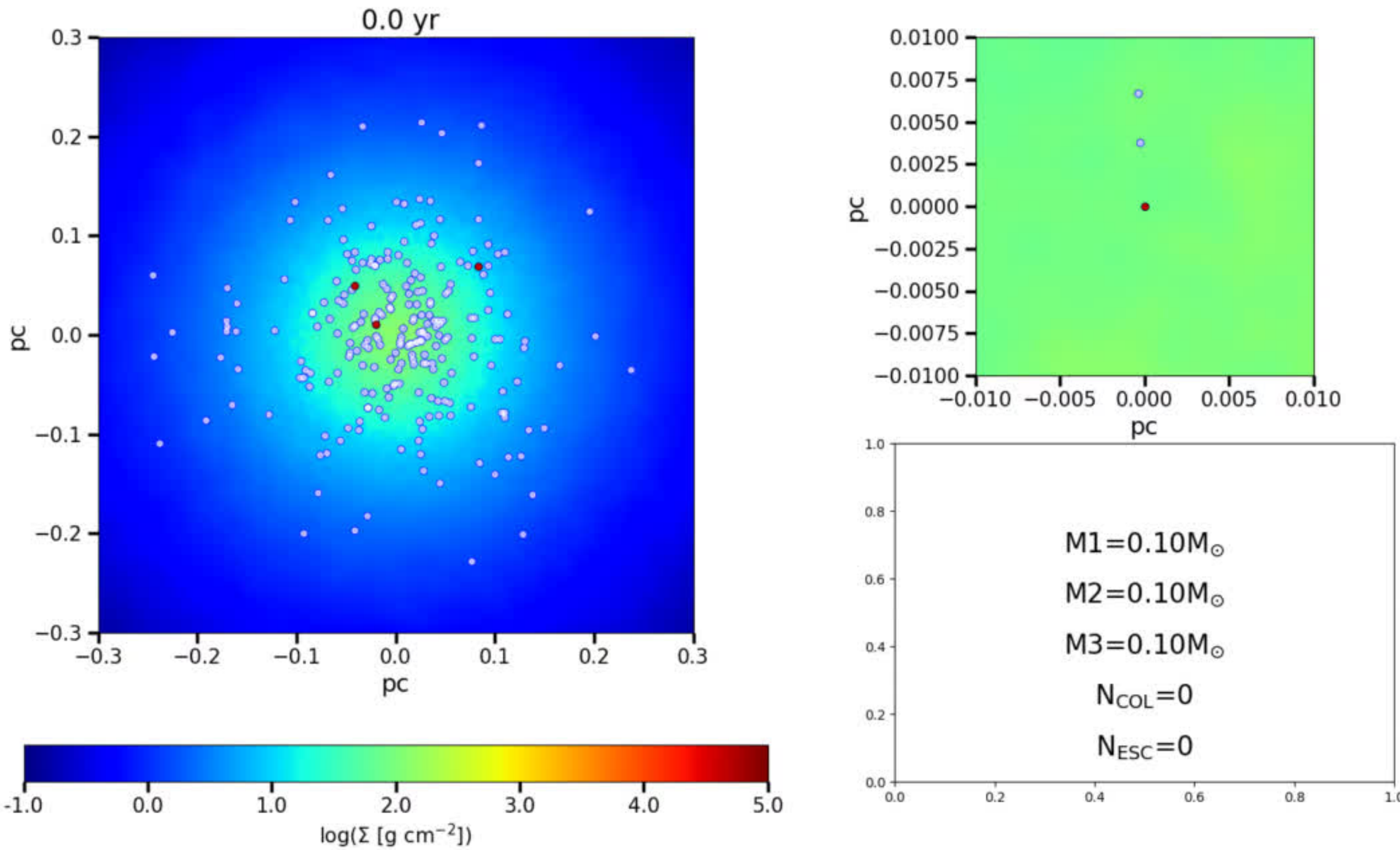


Reinoso et al. (2018, A&A, 614, A14), Boekhold et al. (2018, MNRAS, 476, 366), Alister Seguel et al. (2020, MNRAS, 493, 2352), Reinoso et al. (2020, A&A, 639, A92), Vergara et al. (2021, A&A, 649, A160), Schleicher et al. (2022, MNRAS, 512, 6192), Reinoso et al. (2023, MNRAS, 521, 3553), Schleicher et al. (2023, MNRAS, 521, 3972)

# run-away collisions

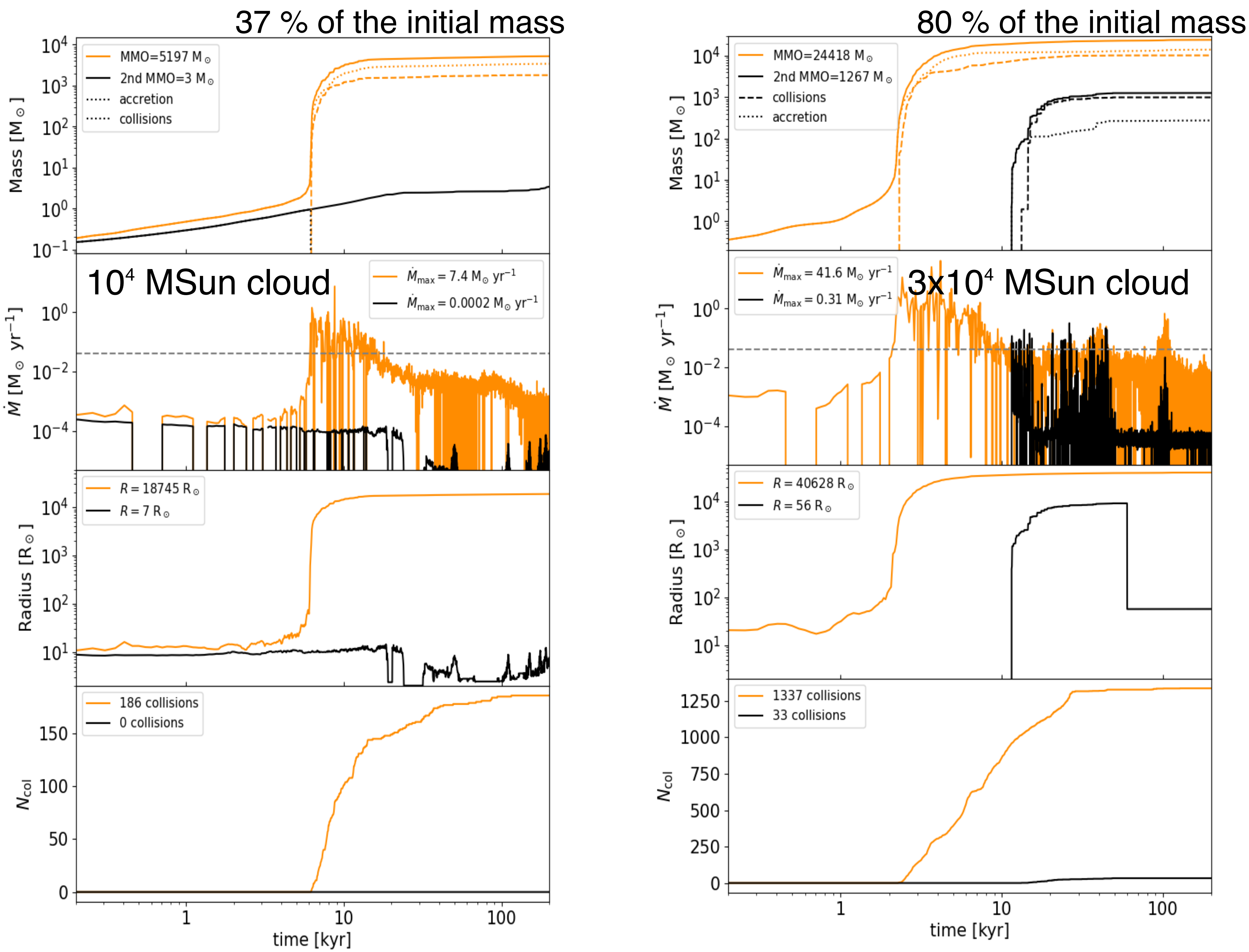


Reinoso et al. (2018, A&A, 614, A14), Boekholt et al. (2018, MNRAS, 476, 366), Alister Seguel et al. (2020, MNRAS, 493, 2352), Reinoso et al. (2020, A&A, 639, A92), Vergara et al. (2021, A&A, 649, A160), Schleicher et al. (2022, MNRAS, 512, 6192), Reinoso et al. (2023, MNRAS, 521, 3553), Schleicher et al. (2023, MNRAS, 521, 3972)

run-away collisions

10$^4$ MSun cloud

3x10$^4$ MSun cloud

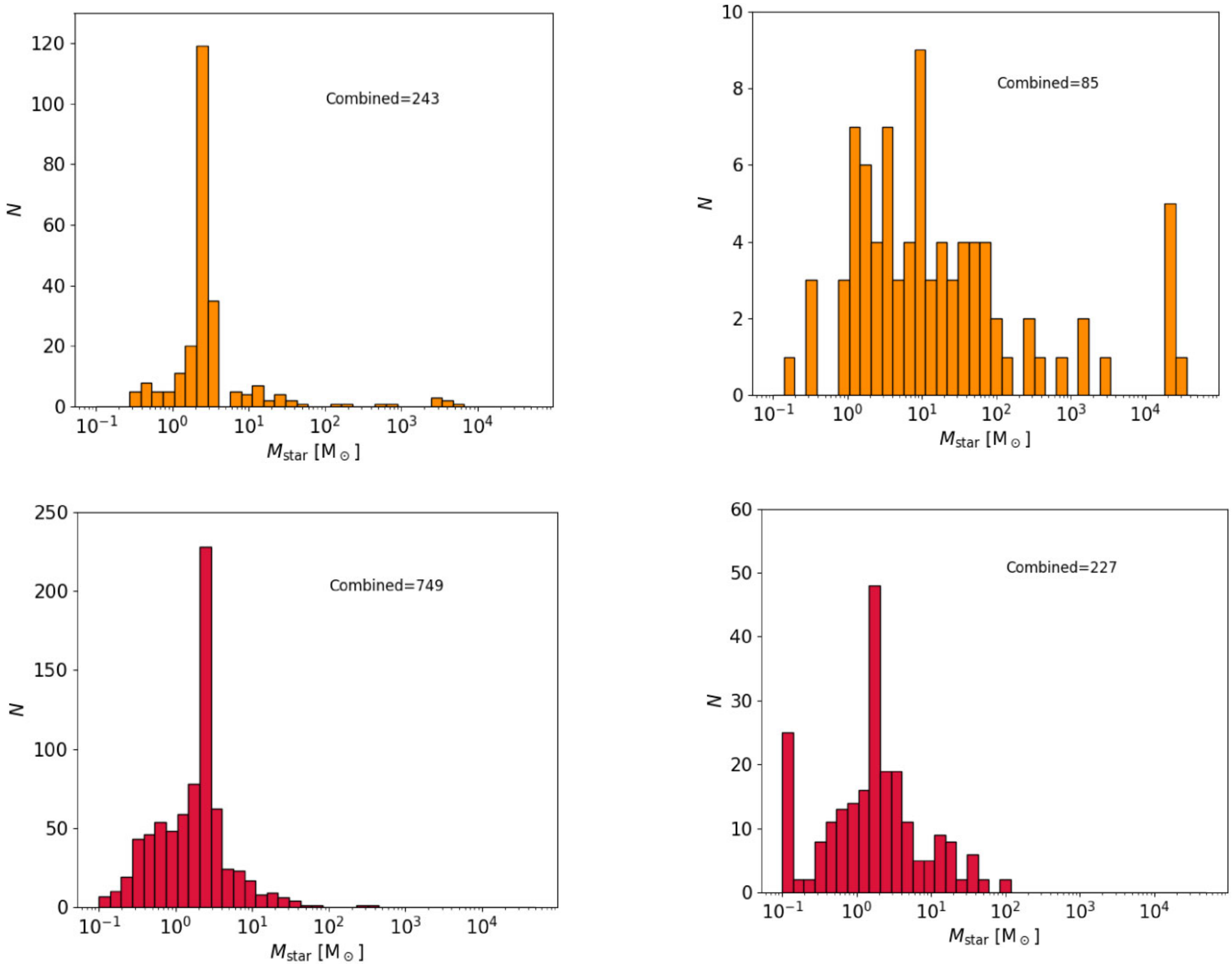


bound

ejected

all simulations combined


Reinoso et al. (2018, A&A, 614, A14), Boekhold et al. (2018, MNRAS, 476, 366), Alister Seguel et al. (2020, MNRAS, 493, 2352), Reinoso et al. (2020, A&A, 639, A92), Vergara et al. (2021, A&A, 649, A160), Schleicher et al. (2022, MNRAS, 512, 6192), Reinoso et al. (2023, MNRAS, 521, 3553), Schleicher et al. (2023, MNRAS, 521, 3972)

run-away collisions

**Table 1.** Summary of simulation outcomes. We present for each simulation the initial gas mass, the final time, the quiescent time adopted for contraction to the main sequence for supermassive stars, the simulation outcome, the total accreted mass, the final stellar mass bound to the mo[st] massive object, the mass of the most massive object, the efficienc[y] of massive object formation, the total mass in ejected stars, the number of stars b[ound to] the MMO, the number of ejections and the number of colli[sions].

| Simulation | $M_{\rm gas}$ [$M_\odot$] | $t_{\rm end}$ [yr] | $t_{\rm KH,\,surf}$ [$t_{\rm KH}$] | multiplicity | $M_{\rm accreted}$ [$M_\odot$] | $M_{\rm stellar,\,bound}$ [$M_\odot$] | $M_{\rm MMO}$ [$M_\odot$] | $\epsilon$ | $M_{\rm ejected}$ [$M_\odot$] | $N_{\rm stars}$ | $N_{\rm ejections}$ | collision number |
|---|---|---|---|---|---|---|---|---|---|---|---|---|
| M1_t100_1 | $10^4$ | 200 015 | 100 | single | 5414 | 5305 | 5197 | 0.52 | 109 | 56 | 70 | 256 |
| M1_t100_2 | $10^4$ | 200 005 | 100 | single | 3815 | 3482 | 3311 | 0.33 | 333 | 62 | 112 | 288 |
| M1_t100_3 | $10^4$ | 200 043 | 100 | single | 4709 | 4539 | 3893 | 0.39 | 170 | 56 | 77 | 341 |
| M1_t100_4 | $10^4$ | 200 023 | 100 | single | 3730 | 3315 | 3048 | 0.30 | 415 | 48 | 153 | 291 |
| M1_t100_5 | $10^4$ | 200 017 | 100 | binary | 5854 | 4821 | 4096 | 0.41 | 1033 | 6 | 141 | 369 |
| M1_t100_6 | $10^4$ | 200 050 | 100 | binary | 4150 | 3326 | 2831 | 0.28 | 824 | 15 | 196 | 300 |
| M1_t10_1 | $10^4$ | 200 024 | 10 | single | 5397 | 4952 | 4326 | 0.43 | 445 | 66 | 83 | 343 |
| M1_t10_2 | $10^4$ | 120 045 | 10 | single | 4548 | 4377 | 4156 | 0.42 | 171 | 88 | 79 | 375 |
| M1_t10_3 | $10^4$ | 200 022 | 10 | binary | 6057 | 5297 | 4064 | 0.41 | 760 | 65 | 147 | 364 |
| M1_t10_4 | $10^4$ | 200 029 | 10 | binary | 5262 | 4468 | 2901 | 0.29 | 794 | 86 | 141 | 456 |
| M1_t10_5 | $10^4$ | 200 036 | 10 | single | 6804 | 6256 | 4858 | 0.49 | 548 | 89 | 53 | 412 |
| M1_t10_6 | $10^4$ | 112 701 | 10 | single | 4617 | 4255 | 4135 | 0.41 | 362 | 56 | 119 | 301 |
| M3_t100_1 | $3 \times 10^4$ | 200 021 | 100 | single | 26 108 | 25 808 | 24 418 | 0.81 | 300 | 13 | 42 | 1892 |
| M3_t100_2 | $3 \times 10^4$ | 200 043 | 100 | single | 26 939 | 26 898 | 26 890 | 0.90 | 41 | 10 | 19 | 1842 |
| M3_t100_3 | $3 \times 10^4$ | 200 009 | 100 | single | 26 388 | 26 211 | 24 577 | 0.82 | 177 | 11 | 34 | 2547 |
| M3_t100_4 | $3 \times 10^4$ | 200 038 | 100 | single | 23 312 | 22 850 | 20 365 | 0.68 | 462 | 36 | 53 | 1844 |
| M3_t100_5 | $3 \times 10^4$ | 200 034 | 100 | single | 23 070 | 22 973 | 22 618 | 0.75 | 97 | 12 | 50 | 2215 |
| M3_t100_6 | $3 \times 10^4$ | 200 035 | 100 | single | 26 966 | 26 851 | 24 375 | 0.81 | 115 | 3 | 29 | 2522 |
| M3_t10_1 | $3 \times 10^4$ | 200 008 | 10 | single | 20 981 | 20 831 | 20 435 | 0.68 | 150 | 13 | 70 | 2283 |
| M3_t10_2 | $3 \times 10^4$ | 200 026 | 10 | single | 23 451 | 23 063 | 20 776 | 0.69 | 388 | 32 | 61 | 1807 |
| M3_t10_3 | $3 \times 10^4$ | 200 048 | 10 | single | 25 871 | 25 413 | 22 267 | 0.74 | 458 | 6 | 50 | 2354 |
| M3_t10_4 | $3 \times 10^4$ | 200 014 | 10 | single | 22 585 | 21 889 | 21 733 | 0.72 | 696 | 10 | 89 | 2445 |
| M3_t10_5 | $3 \times 10^4$ | 200 039 | 10 | single | 20 778 | 20 481 | 20 368 | 0.68 | 297 | 6 | 96 | 2297 |
| M3_t10_6 | $3 \times 10^4$ | 200 011 | 10 | single | 27 051 | 26 846 | 26 746 | 0.89 | 205 | 7 | 42 | 3514 |

Reinoso et al. (2018, A&A, 614, A14), Boekhold et al. (2018, MNRAS, 476, 366), Alister Seguel et al. (2020, MNRAS, 493, 2352), Reinoso et al. (2020, A&A, 639, A92), Vergara et al. (2021, A&A, 649, A160), Schleicher et al. (2022, MNRAS, 512, 6192), Reinoso et al. (2023, MNRAS, 521, 3553), Schleicher et al. (2023, MNRAS, 521, 3972)

# combination of collisions and accretion

UNIVERSITÄT HEIDELBERG
ZUKUNFT SEIT 1386

## $10^4$ MSun cloud

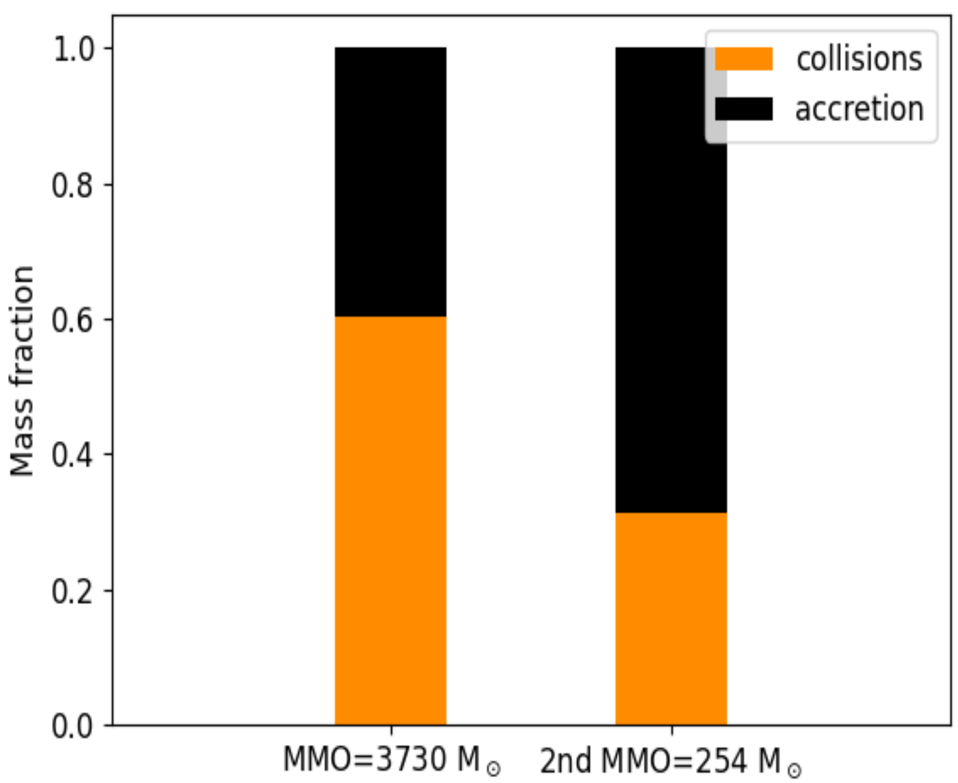


60% of the mass
comes from collisions

## $3x10^4$ MSun cloud

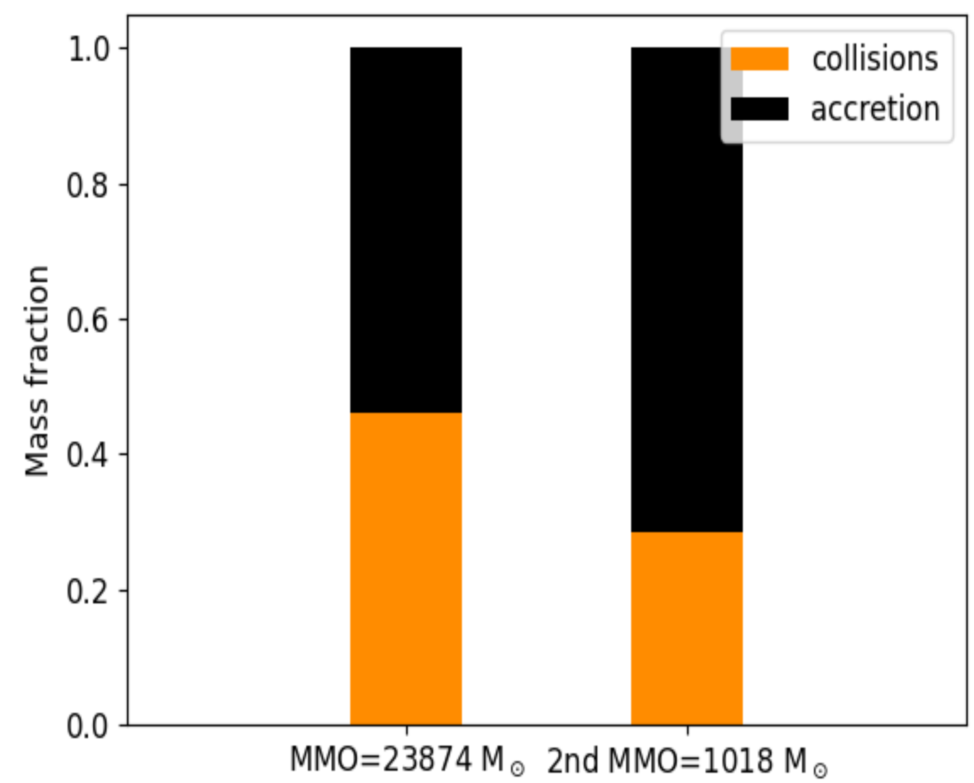


40% of the mass
comes from collisions

Reinoso et al. (2018, A&A, 614, A14), Boekhold et al. (2018, MNRAS, 476, 366), Alister Seguel et al. (2020, MNRAS, 493, 2352), Reinoso et al. (2020, A&A, 639, A92), Vergara et al. (2021, A&A, 649, A160), Schleicher et al. (2022, MNRAS, 512, 6192), Reinoso et al. (2023, MNRAS, 521, 3553), Schleicher et al. (2023, MNRAS, 521, 3972)


Deutsche Forschungsgemeinschaft
DFG
ECOGAL
ERC Synergy Grant
erc European Research Council
STRUCTURES CLUSTER OF EXCELLENCE
UNIVERSITÄT HEIDELBERG ZUKUNFT SEIT 1386

# observational constraints

UNIVERSITÄT HEIDELBERG ZUKUNFT SEIT 1386

- directly observing Pop III stars at high redshift is highly challenging
  - maybe SNe with JWST, but where to point
  - this may help to constrain the high-mass end of Pop III IMF
- more promising: Galactic archeology
  - maybe we find genuine low-mass Pop III stars (0.8 Msun should have survived until present day)
  - use detailed abundance pattern in EMP stars to high-mass end constrain high-mass end of IMF (no evidence of PISNe)
- very exciting: gravitational wave events
  - binary properties and high-mass end of Pop III IMF
- other testable expectation:
  - larger stellar density in clusters of lower metallicity, consequently: larger numbers of close binaries (and higher-order multiples)

(for further discussions, see Klessen, & Glover (2023, ARAA, 61, 65 -- arXiv.2303.12500)


Deutsche Forschungsgemeinschaft
DFG

ECOGAL
ERC Synergy Grant

European Research Council

STRUCTURES
CLUSTER OF
EXCELLENCE

UNIVERSITÄT
HEIDELBERG
ZUKUNFT
SEIT 1386

IMF of Pop III stars is not well understood
most likely log-flat and thus top heavy

transition to Pop II star formation at metallicities
log(Z/Zsun) ~ -5 due to dust

supermassive stars can easily reach
$10^5$ $M_\odot$ if subject to high accretion rates

best constraints to be expected from
Galactic archeology and gravitational waves

Deutsche Forschungsgemeinschaft
DFG
ECOGAL
ERC Synergy Grant
European Research Council
STRUCTURES
CLUSTER OF EXCELLENCE
UNIVERSITÄT HEIDELBERG
ZUKUNFT SEIT 1386

# thanks

IMF of Pop III stars is not well understood
most likely log-flat and thus top heavy

transition to Pop II star formation at metallicities
log(Z/Zsun) ~ -5 due to dust

supermassive stars can easily reach
$10^5$ $M_\odot$ if subject to high accretion rates

best constraints to be expected from
Galactic archeology and gravitational waves

Deutsche Forschungsgemeinschaft DFG

ECOGAL
ERC Synergy Grant

erc European Research Council

STRUCTURES CLUSTER OF EXCELLENCE

UNIVERSITÄT HEIDELBERG ZUKUNFT SEIT 1386